Studies on the yeast-hypha mediated virulence in *Candida* species

by

Anuja Paudyal

B.S., Purbanchal University, 2013
M.S., Fort Hays State University, 2017

AN ABSTRACT OF A DISSERTATION

submitted in partial fulfillment of the requirements for the degree

DOCTOR OF PHILOSOPHY

Division of Biology
College of Arts and Sciences

KANSAS STATE UNIVERSITY
Manhattan, Kansas

2022

Abstract

Candida albicans is a commensal and opportunistic fungal pathogen in humans. The transition of oval yeast form to filamentous hypha form is one among the several virulence factors in *C. albicans* causing its pathogenesis. Compounds known to inhibit this transition and hyphal growth have potential as antifungal agents and prevent tissue invasion of fungus, if they do not harm the host. Gymnemic acid (GAs) is a small molecule known to inhibit hyphal formation *in vitro* and in an invertebrate animal model under hypha inducing environment. However, the mechanism of GAs mediated hypha inhibition in poorly known.

Here, I present the work from four different but related studies on the morphology and pathogenesis of *Candida* species. The first two chapters describe studies aimed at understanding how *C. albicans* hyphal growth is inhibited by GAs at the molecular level. The chapters after that focus mainly on skin colonizing fungus *Candida auris*, its ability to form biofilms, identification of quorum sensing molecules, and the interaction of fungus with a skin resident bacterial pathogen, *Staphylococcus aureus*. The basic knowledge gained from the first two chapters helped us to decipher the pathogenesis mechanism of a newly emerged *Candida* species described in the latter chapters.

Our first study has highlighted GAs as a potential antifungal compound. We evaluated the efficacy of GAs in a mouse model of systemic candidiasis and demonstrated that GAs treatment rescued mice from *C. albicans*-mediated death while mice without treatment did not survive. The survival of infected mice in the presence of GAs corresponded with the strongly reduced fungal burden in the kidney tissues and is possibly due to GAs-mediated block of hyphal cells preventing the spread of fungus. In our second study, we investigated the mode of action of

GAs at molecular level. It is known that Nrg1 and Ume6 are negative and positive regulators of hyphal growth, respectively. Also, past and current studies from our laboratory showed GAs affect these genes. Therefore, we decided to identify proteins that associate with these regulators in the presence and absence of GAs. This will allow us to identify how GAs impact these regulatory pathways. For this we used a two-step tandem affinity purification approach followed by mass spectrometry. Addition of GAs to cells co-purified significantly more proteins as compared to controls without GAs. When these proteins were categorized using GO term analysis, majority of proteins were the proteins having DNA and RNA binding activity, proteins involved in hyphal growth and signaling, or ribosomal proteins. Our proteomics data suggested that GAs exposure to *C. albicans* recruit regulatory proteins at the transcriptional machinery that are known to promote budding and or suppress hyphal growth. The Ume6 copurified protein group have a relatively higher number of proteins having ligase activity involving synthesis of tRNA and amino acids when compared to Nrg1. We hypothesize there could be some cross talk between these regulatory proteins and the Hog1 pathway. In the third study, we investigated the Nrg1p in a recently emerged *Candida* species, *C. auris*, where the role of Nrg1p is unknown. *C. auris* primarily grows as yeast form. Based on immunofluorescence and proteomic methods, we found Nrg1p localized, surprisingly, on the cell surface of *C. auris* and was not directly involved in hyphal growth. Finally, the fourth study focused on *C. auris*' interaction with one of the skin colonizing bacterial pathogens. *C. auris* shares its habitat with several microbes, including *S. aureus*. Both *C. auris* and *S. aureus* being skin dwellers, salt tolerant, and drug-resistant, they were found to survive together in *in vitro* growth conditions that mimic the skin surface. They formed dual-species biofilms that had increased virulence (*e.g.* hemolytic activity of *S. aureus*). We surmised their synergistic biofilm growth and augmented bacterial virulence may involve

inter-kingdom quorum signaling. While much is known about quorum sensing (QS) signaling in *S. aureus,* nothing is known about it in *C. auris*. Extraction and analyses of QS molecules from *C. auris* growth medium revealed presence of novel QS molecules. To our knowledge, this is the first study to show that *C. auris* produces quorum sensing molecules different from farnesol secreted by *C. albicans* which inhibits filamentation in *C. albicans*.

Together, results from our studies added new insights into GAs-mediated hyphal inhibition in *C. albicans,* and GAs may be developed as novel antifungal agents to prevent hyphae-related fungal infections. Further, the synergistic interaction of *C. auris* and *S. aureus* in skin mimicking conditions with increased virulence highlight the potential risk to human health. Understanding their virulence mechanism better may help us to manage these pathogens effectively.

Studies on the yeast-hypha mediated virulence in *Candida* species

by

Anuja Paudyal

B.S., Purbanchal University, 2013
M.S., Fort Hays State University, 2017

A DISSERTATION

submitted in partial fulfillment of the requirements for the degree

DOCTOR OF PHILOSOPHY

Division of Biology
College of Arts and Sciences

KANSAS STATE UNIVERSITY
Manhattan, Kansas

2022

Approved by:

Major Professor
Govindsamy Vediyappan, PhD

Copyright

Abstract

Candida albicans is a commensal and opportunistic fungal pathogen in humans. The transition of oval yeast form to filamentous hypha form is one among the several virulence factors in *C. albicans* causing its pathogenesis. Compounds known to inhibit this transition and hyphal growth have potential as antifungal agents and prevent tissue invasion of fungus, if they do not harm the host. Gymnemic acid (GAs) is a small molecule known to inhibit hyphal formation *in vitro* and in an invertebrate animal model under hypha inducing environment. However, the mechanism of GAs mediated hypha inhibition in poorly known.

Here, I present the work from four different but related studies on the morphology and pathogenesis of *Candida* species. The first two chapters describe studies aimed at understanding how *C. albicans* hyphal growth is inhibited by GAs at the molecular level. The chapters after that focus mainly on skin colonizing fungus *Candida auris*, its ability to form biofilms, identification of quorum sensing molecules, and the interaction of fungus with a skin resident bacterial pathogen, *Staphylococcus aureus*. The basic knowledge gained from the first two chapters helped us to decipher the pathogenesis mechanism of a newly emerged *Candida* species described in the latter chapters.

Our first study has highlighted GAs as a potential antifungal compound. We evaluated the efficacy of GAs in a mouse model of systemic candidiasis and demonstrated that GAs treatment rescued mice from *C. albicans*-mediated death while mice without treatment did not survive. The survival of infected mice in the presence of GAs corresponded with the strongly reduced fungal burden in the kidney tissues and is possibly due to GAs-mediated block of hyphal cells preventing the spread of fungus. In our second study, we investigated the mode of action of

GAs at molecular level. It is known that Nrg1 and Ume6 are negative and positive regulators of hyphal growth, respectively. Also, past and current studies from our laboratory showed GAs affect these genes. Therefore, we decided to identify proteins that associate with these regulators in the presence and absence of GAs. This will allow us to identify how GAs impact these regulatory pathways. For this we used a two-step tandem affinity purification approach followed by mass spectrometry. Addition of GAs to cells co-purified significantly more proteins as compared to controls without GAs. When these proteins were categorized using GO term analysis, majority of proteins were the proteins having DNA and RNA binding activity, proteins involved in hyphal growth and signaling, or ribosomal proteins. Our proteomics data suggested that GAs exposure to *C. albicans* recruit regulatory proteins at the transcriptional machinery that are known to promote budding and or suppress hyphal growth. The Ume6 copurified protein group have a relatively higher number of proteins having ligase activity involving synthesis of tRNA and amino acids when compared to Nrg1. We hypothesize there could be some cross talk between these regulatory proteins and the Hog1 pathway. In the third study, we investigated the Nrg1p in a recently emerged *Candida* species, *C. auris*, where the role of Nrg1p is unknown. *C. auris* primarily grows as yeast form. Based on immunofluorescence and proteomic methods, we found Nrg1p localized, surprisingly, on the cell surface of *C. auris* and was not directly involved in hyphal growth. Finally, the fourth study focused on *C. auris*' interaction with one of the skin colonizing bacterial pathogens. *C. auris* shares its habitat with several microbes, including *S. aureus*. Both *C. auris* and *S. aureus* being skin dwellers, salt tolerant, and drug-resistant, they were found to survive together in *in vitro* growth conditions that mimic the skin surface. They formed dual-species biofilms that had increased virulence (*e.g.* hemolytic activity of *S. aureus*). We surmised their synergistic biofilm growth and augmented bacterial virulence may involve

inter-kingdom quorum signaling. While much is known about quorum sensing (QS) signaling in *S. aureus,* nothing is known about it in *C. auris*. Extraction and analyses of QS molecules from *C. auris* growth medium revealed presence of novel QS molecules. To our knowledge, this is the first study to show that *C. auris* produces quorum sensing molecules different from farnesol secreted by *C. albicans* which inhibits filamentation in *C. albicans*.

Together, results from our studies added new insights into GAs-mediated hyphal inhibition in *C. albicans,* and GAs may be developed as novel antifungal agents to prevent hyphae-related fungal infections. Further, the synergistic interaction of *C. auris* and *S. aureus* in skin mimicking conditions with increased virulence highlight the potential risk to human health. Understanding their virulence mechanism better may help us to manage these pathogens effectively.

Table of Contents

List of Figures

List of Tables

Acknowledgements

I would like to thank my major advisor, Dr. Govind Vediyappan, for his guidance and support. It would be impossible to complete my doctoral study without his encouragement. Thank you for always being so kind and understanding. I would also like to thank my supervisory committee members Dr. Michael Kanost, Dr. Ari Jumpponen, and Dr. Jeroen Roelofs for their constructive feedbacks and motivation. Committee meetings over the years have helped me a lot to do better every time.

I would like to thank Division of Biology for accepting me as a graduate student and providing me the opportunity to be trained by wonderful scientists in the Division. I want to extend my thanks to my BGSA friends and all the staffs in the Division who helped me to have a smooth PhD journey.

I would like to thank my family members especially my father Mr. Romhari Paudel for being pillar of our family, and my mother Mrs. Rama Devi Paudel for all their trust and love towards me. They always trusted my capabilities even when I did not. Though my mother was not privileged to receive formal education, she is an ocean of knowledge, and I am still learning from her. My lovely elder sister Indira Paudel and my dearest younger sister Ashna Paudel have been there in all my highs and lows. They support me in every step I take without a second thought and always prioritize my happiness amidst everything else. I am grateful to have my brother-in laws Sahadev Acharya and Binay Gautam in our family. My nephew Evan Acharya has been my muse throughout my PhD journey. I am grateful to the sister I met here in Kansas, Dr. Rashmi Thapa, who is a wonderful human being, so kind and full of love. I would also like to acknowledge my brother Sangam Chhatkuli and all the friends here in Manhattan.

I am beyond grateful to Tej Man Tamang, my dearest husband for coming to my life and adding joyous sparks into it. The fortune of having you by my side is surreal. Thank you for always being there for me.

Dedication

This dissertation is dedicated to my family.

Chapter 1 - Introduction

1.1 Introduction to *Candida* species and Candidiasis

There are about 600 fungal species capable of causing infections in humans, including *Candida* species [1]. From the 150 species of *Candida*, *Candida albicans* is considered a major human pathogen. It is a commensal in immunocompetent, however it can become pathogenic in immunocompromised individuals leading to a disease called candidiasis. Several non-*albicans* species of *Candida* such as *Candida glabrata*, *Candida tropicalis*, *Candida dubliniensis*, *Candida krusei*, and *Candida parapsilosis* are other species of *Candida* that can cause infections in humans [2,3]. A recently emerged *Candida* species, *Candida auris* is multidrug resistant and is of huge concern globally [4]. *Candida* species related fungal infections and diseases cost approximately 3 billion dollars every year in the United States [5] with 40% mortality rate [6]. So, the study of *Candida* spp. and candidiasis is important from both health and economic prospective.

In this chapter, I will review the literature on *Candida albicans*, its pathogenicity, and virulence factors involved with major focus on morphology and morphological switch inhibitors. I will also review on another skin colonizing *Candida* species, *Candida auris* and its interaction with a skin colonizing bacterium, *Staphylococcus aureus*.

1.2 *Candida albicans*

Candida albicans lives as a commensal in our mouth, throat, gut, vagina, and skin but can become pathogenic in immunocompromised individuals [7,8]. It can cause superficial infections that can eventually lead to invasive candidiasis by entering bloodstream and internal organs such as kidney, heart, and brain (CDC fact sheet) **(Figure 1.1)**. Most *C. albicans*

mediated systemic infections are due to already existing health conditions and its pathogenesis also depends on the site of colonization. *C. albicans* residing on our oral cavity are usually commensal unless immune system is weakened whereas, those in the genital tract causing vulvovaginal candidiasis involve hyperactive immune response leading damage to the host [9,10]. Few cases of *C. albicans* travelling across blood-brain barrier have also been observed in newly born children, causing brain infection [11–13].

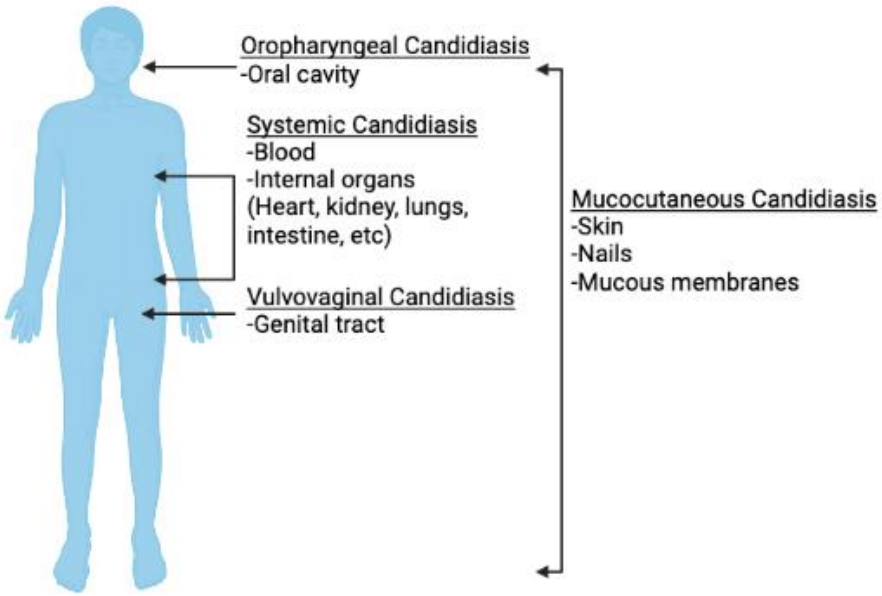

Figure 1.1. Different types of candidiasis and their sites of infection.

C. albicans can cause candidiasis in different body parts such as oropharyngeal candidiasis in mouth, vulvovaginal candidiasis in female genital tract, and mucocutaneous candidiasis on skin surface and nails. These infections might lead to systemic infection in bloodstream that spreads to internal organs such as heart, kidney, lungs, and others. Created in Biorender.com. Image modified from [10].

C. albicans has been commonly used as a model organism to understand fungal pathogenesis. It is a diploid organism containing approximately 6000 protein coding-genes with genome size of 14.3Mb [14]. Based on protein sequence homology, 774 out of 6000 ORFs are specific to *C. albicans* and not found in other highly studied fungi such as *Saccharomyces* spp. [15,16]. Experimental tools and techniques such as molecular, genetics, and proteomics used for studying *C. albicans* are derived from *S. cerevisiae* [17] .

1.3 Virulence factors in *C. albicans*

C. albicans possesses several virulence factors that enable the establishment and spread of infection. The transition between yeast and hyphal forms of *C. albicans* is considered one of the major virulence factors. Under favorable environmental conditions, *C. albicans* transitions from yeast growth form to invasive hyphal form and hence becomes more pathogenic. The hyphal form is invasive as it can penetrate into host epithelial layers [18,19]. *C. albicans* secretes a hypha-specific toxin called Candidalysin in its hyphal growth stage. This toxin can damage host cell membrane by creating pores and disrupting host cells [20–22]. Another virulence factor contributing to the pathogenicity is the expression of adhesion and invasion related proteins on hyphae. The agglutinin-like sequence (Als) family of proteins play important role during adhesion of *C. albicans* to the host [23]. Ability to form biofilm on host surfaces or body implants is another important characteristic of *C. albicans* resulting in pathogenesis [24]. Biofilms occur in three major steps: initiation, maturation, and dispersion. In initiation step, yeast cells adhere to the substrate and proliferate forming filamentous hyphal forms. In maturation step, along with yeast and hypha, extracellular polysaccharides accumulate resulting in the maturation of biofilms. Maturation is followed by dispersion step, where new yeast cells are

released from biofilms and repeat the cycle. The dispersion of cells systemically is of huge clinical importance as it can result fungemia. Further, the biofilm extracellular matrix (ECM) consists of mannan and beta-1,3 glucans, that contribute to the antifungal resistance by sequestering them [24–26]. Apart from these, secretion of hydrolytic enzymes such as secreted protease, lipase, phospholipase, and hemolysin are important virulence factor in *Candida* species. These enzymes facilitate them to attach and invade host tissues during disseminated candidiasis [27–31]. For example, they express hemolytic factor to acquire iron from the host. However, not all species of *Candida* are known to express hemolytic factor. *Candida* species such as *C. albicans, C. dubliniensis, C. krusei, C. glabrata, C. tropicalis*, and few others have been shown to exhibit hemolytic activity when grown on sheep blood agar with glucose in CO_2 rich environment, whereas species such as *C. parapsilosis*, *C. utilis*, and others did not show hemolytic activity under these conditions [29,32]. Out of all these virulence factors, morphogenetic switch will be discussed in detail in this review.

1.4 Morphogenetic switch in *C. albicans* and pathways involved

Candida albicans is a polymorphic fungus because it exists as an oval yeast cell, a short chain of elongated yeast cells without true septum called pseudohypha, and a tubular hypha with septum. Yeast cell multiplies via budding where nucleus divides at the junction between mother and daughter cells followed by cytokinesis resulting two physically detached progenies. In hypha, division of nucleus takes place within daughter cells and one progeny nucleus migrate back towards mother cells. Mother and daughter cells remain attached. However, in pseudohypha, nuclear division occurs in the junction between mother and daughter cells similar to that of yeast cells but after cytokinesis, mother and daughter cells remain attached similar to

that of hypha [18,33]. Based on the environmental conditions such as nutrient availability, pH, and temperature, *C. albicans* can change into different other phenotypes such as white, grey and opaque which are directly related to its virulence, non-virulence, mating kind, immune invasion, and adaptation to host environment [33–36]. *C. albicans* also exists as chlamydospores during starvation and low temperature [37]. In this study, yeast and hyphal forms and switch between them will be explained in detail.

Yeast to hypha conversion is induced by several environmental factors such as temperature (37 ^{o}C), presence of serum, pH greater than 7, N-acetylglucosamine, starvation, elevated CO_2, or low nitrogen [38]. Both yeast and hyphal form are required for virulence [33,39–41]. *C. albicans* in its yeast form helps in the dissemination of fungus whereas, hyphal form invades into the tissues during disease proliferation in the host [42]. The yeast to hypha transition involves wide range of changes in gene expression [38,39,43] and is regulated by multiple proteins and related pathways such as protein kinase A, Efg1, Cph1, Czf1, Hog1, and Nrg1 [44–46]. cAMP-PKA (cyclic adenosine monophosphate-protein kinase A) pathway regulates yeast to hypha transition that involves the activation of Ume6 via a transcription factor called Efg1 [47]. Similarly, several other proteins such as Cyr1, Ras1, Cap1, etc. trigger this pathway [48,49]. In both serum and temperature dependent yeast to hypha transition, cAMP-PKA pathway gets activated. When serum is added to the *C. albicans* growth media, Ras1 of cAMP-PKA pathway gets activated whereas, elevated temperature inhibits heat shock chaperone protein Hsp90 and trigger filamentation via same pathway [50–52]. Cell cycle inhibitors such hydroxyurea also promote filamentation via cAMP-PKA pathway [53,54]. MAPK (mitogen-activated protein kinase) pathway involves series of phosphotransfer steps in coordinating filamentation in *C. albicans*. It can be either cell wall integrity (PKC) and Cek1 related MAPK

pathway that response against cell wall damage or Hog1 MAPK pathway that gets activated under osmotic or oxidative stress. Hog1 pathway can affect filamentation and virulence of *C. albicans*. Apart from these, there are several negative regulators of hypha such as transcription factors Nrg1, Rfg1 and corepressor Tup1. These hyphal repressors downregulate hypha inducing genes [55–62] and the major regulatory pathways of morphogenesis are summarized in **Figure 1.2**.

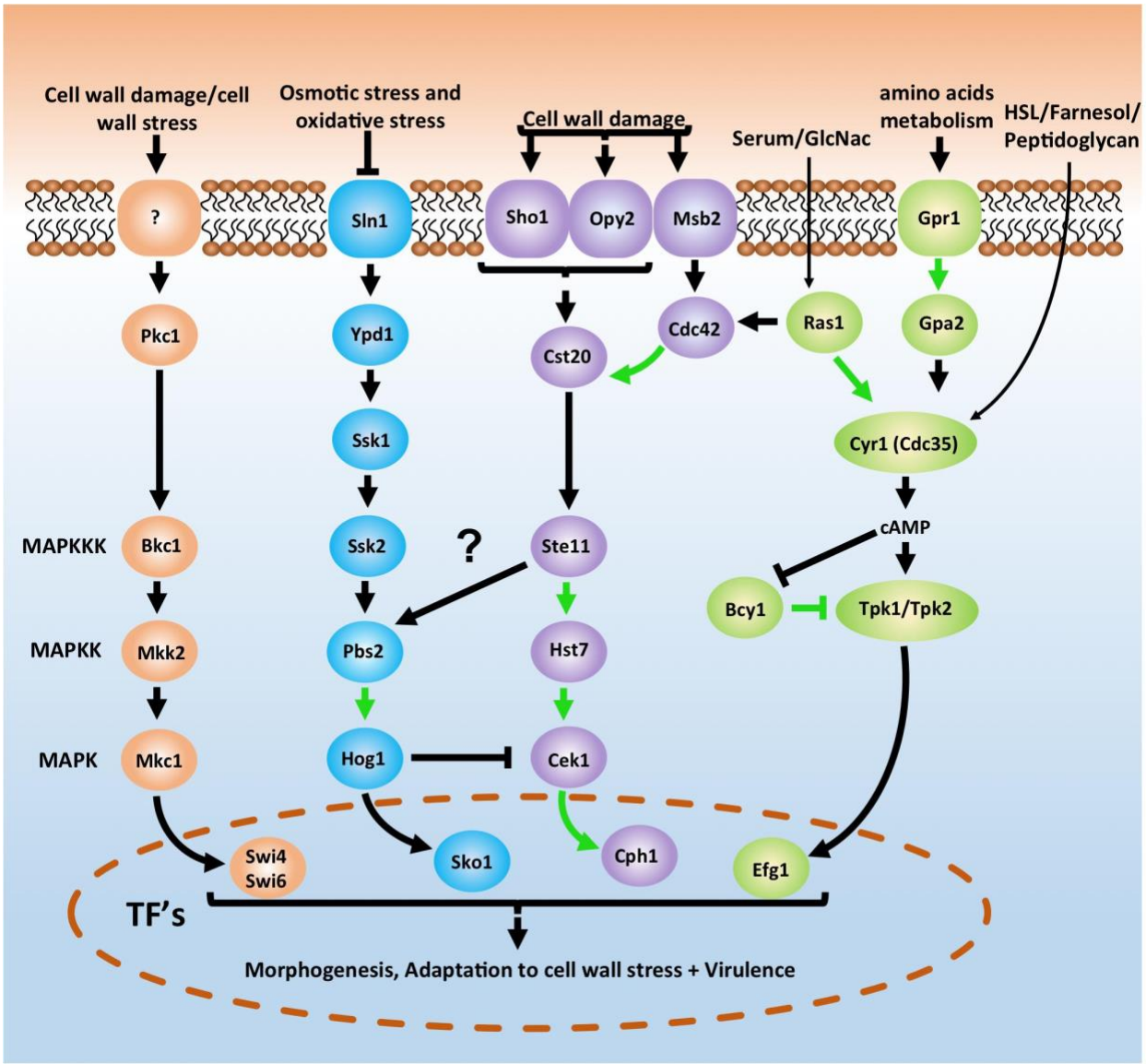

Figure 1.2. Schematics representing major pathways in regulation of morphogenesis and virulence in *C. albicans*.

The four most studied regulatory pathways are shown, and each color represents different pathway: cAMP-PKA pathway (green), CEK1 mediated pathway (purple), HOG pathway (blue), and PKC pathway (orange). Green arrows indicates that protein-protein interaction is already demonstrated in the earlier studies and black arrows represents the interactions between proteins not demonstrated yet. TF: Transcription factor. Image taken from [62].

1.4.1 Negative and positive hyphal regulators

As mentioned above, yeast to hypha transition is regulated by several genes and proteins from different pathways based on environmental cues. Below, I will review two transcription factors, Nrg1 and Ume6 that are known to play major role in regulating yeast-hyphal switch.

1.4.1.1 Nrg1

C. albicans Nrg1 is a transcriptional factor that contains a zinc finger domain at its C-terminus and is known to repress hyphal growth. Under hypha promoting growth conditions such as a temperature of 37 ^{o}C and media containing serum, expression of *NRG1* mRNA was shown to be reduced [59,63] and this reduction is required for hyphal development [64,65]. *Nrg1* mutant was grown as elongated pseudohypha in non-hyphal growth conditions and showed invasive growth in YPD agar [59]. However, pseudohyphae formation was not affected in the nitrogen-limiting synthetic low ammonia dextrose medium [66]. Nrg1 acts together with a corepressor, Tup1 and downregulates hyphal growth. However, Nrg1 also represses other genes that are independent of Tup1 [59]. They are shown to repress hypha-specific genes such as *ECE1*, *HWP1*, *HYR1*, *ALS8* by binding to the NRE (Nrg1 response element) region (A/C)(A/C/G)C_3T present in the promoter of these genes [59,63]. When two NREs were deleted from the promoter of *ALS8,* Nrg1 was no longer able to repress *ALS8* [59]. Strain expressing high levels of *NRG1* blocked the transition of yeast to hypha and when such *NRG1* expressing strain was used *in vivo* for disseminated candidiasis, survival rate of mice was 100 percent

[40,67]. However, when it is used as vaccine, only immunocompetent mice were protected but not immunodeficient mice [68]. Nrg1 has also been shown previously to repress the expression of Ume6 and these two genes act in a negative feedback loop to partly regulate morphogenesis in *C. albicans* [69]. Expression of *NRG1* repressed the formation of chlamydospore in *C. albicans* along with another non-*albicans* species, *C. dubliniensis* [70]. So, Nrg1 is an important regulator of morphological switch in *Candida*.

1.4.1.2 Ume6

Ume6 is a zinc finger DNA binding domain containing transcription factor. It is a positive hyphal regulator in *C. albicans*. Though *ume6* mutants were able to form hypha, they were unable to extend hypha both *in vitro* and *in vivo* experiments. When *UME6* was ectopically expressed, elongated hypha and germ tubes were observed [69,71]. In systematic candidiasis mouse model, *ume6* mutants were found to be avirulent [69]. *UME6* transcript is only expressed when cells are in hyphal form but not when cells are in the yeast form and this expression is known to be repressed by Nrg1-Tup1 complex. Along with Nrg1, *UME6* expression is also suppressed by another transcription factor, Rfg1 [61,71]. Overexpression of *UME6* resulted in dense filamentous biofilms [72]. Since hyphal growth is a major virulence factor in invasive candidiasis, agents that block hyphal initiation and growth are considered useful armamentarium to existing antifungals.

1.5 Hyphal inhibitors

Several new compounds have been identified over the years that inhibit filamentation such as copper oxide nanoparticle, 5-[3-substituted-4-(4-substituted benzyloxy)-benzylidene]-2-thioxo-thiazolidin-4-one derivatives [73,74]. Apart from these, farnesol is a quorum sensing

molecule secreted by *C. albicans* that is known block yeast to hypha transition [75]. Details on farnesol and its effect on *C. albicans* are described in section 1.12 below.

Antifungal drugs that are currently being used for treating fungal infections are categorized into four major classes: polyenes, azoles, echinocandins, and pyrimidine analogues. They target different components of fungi such as polyenes and azoles target cell membranes, echinocandins affect cell wall synthesis, and pyrimidine analogues block the synthesis of DNA [76,77]. Azole antifungal such as fluconazole is a broad spectrum antifungal effective against several fungi such as *Candida* spp., *Cryptococcus neoformans*, and others. Amphotericin B belongs to class polyenes which binds to ergosterol and disrupts cell membrane. It shows activity against *Candida* spp., *Arpergillus* spp., and other dimorphic fungi [78].

1.6 Gymnemic acids

Gymnemic acids (GAs) were isolated from a traditional medicinal plant called *Gymnema sylvestre,* a native plant from India and China. They are glycosides of triterpene that is known to suppress sweet sensation in human by binding to the human taste receptor T1R2 and T1R3 [79,80]. Besides sweet-suppressing effect, GAs poses other characteristics of medicinal value such as acting as antagonist of Liver X receptor in dislypidemic diseases and inhibiting uptake of glucose in the gastrointestinal tract [81,82]. A recent study has also shown that *G. sylvestre* administration lowered the body weight, body mass index and very low-density lipoprotein level in humans [83]. Various phytochemicals present in *G. sylvestre* and their parmacological properties were described in several recent reviews [84,85].

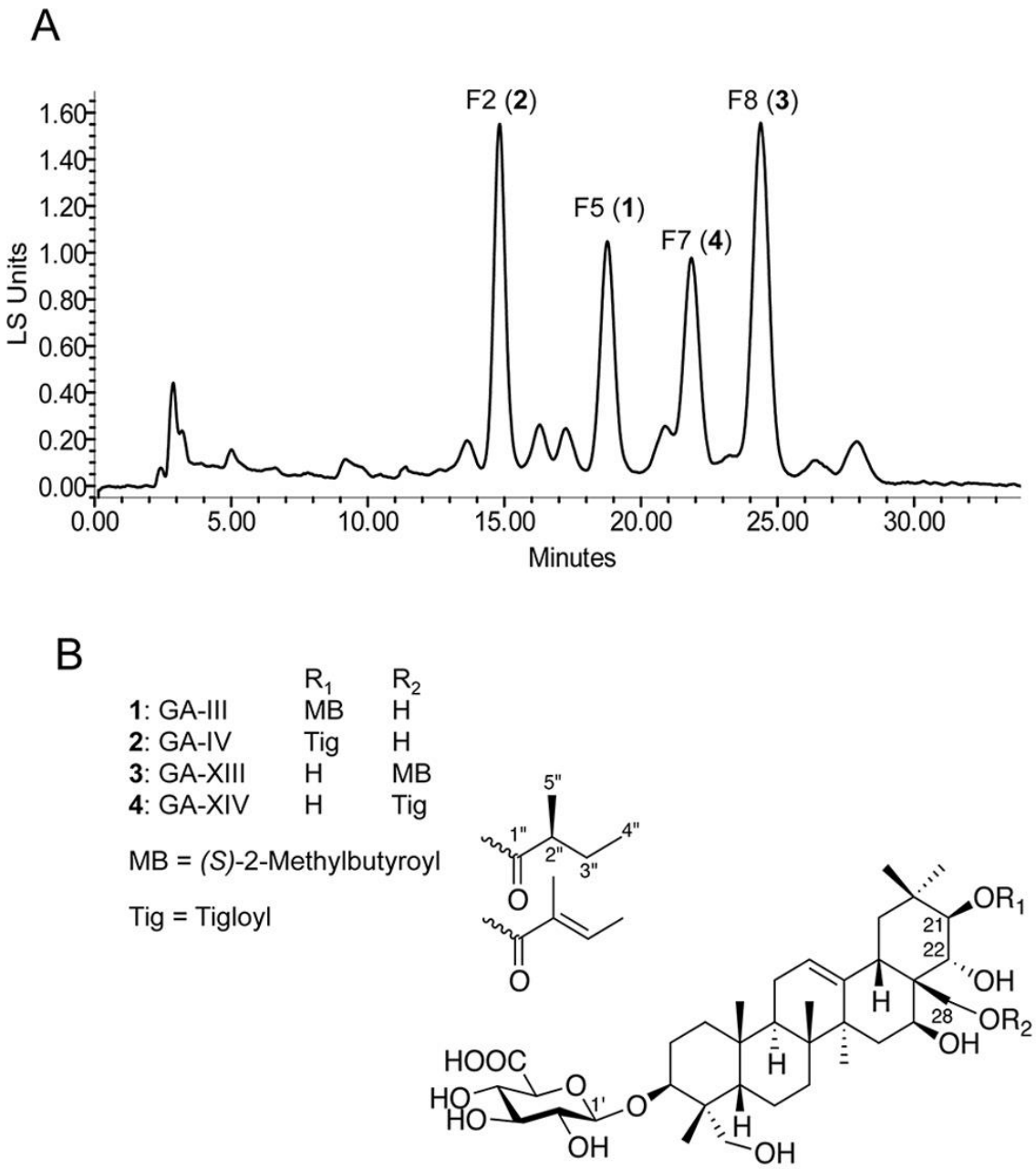

Figure 1.3. Gymnemic acids.

(A) Gymnemic acids were extracted from *G. sylvestre* plant leaves and fractionated using HPLC. Fractions from major peaks were collected individually and confirmed their activity of hyphal inhibition in *C. albicans*. **(B)** Four GAs and the general structure of GA are shown. Image taken from [86].

In *C. albicans*, GAs fraction extracted and separated using HPLC **(Figure 1.3)** inhibited the transition of yeast form to hyphal form and reverted pre-formed hyphae back to the yeast

cells *in vitro* **(Figure 1.4)** [86]. Also, in an *in vivo* model using *Caenorhabditis elegans*, GAs were able to rescue *C. albicans* infected worms from death. GAs also inhibited hyphal growth in another pathogenic fungus, *Aspergillus fumigat*us, and importantly, GAs were non-toxic to mammalian cells *in vitro* at the concentration of 40 μg/mL [86]. A recent study also showed that GAs inhibited mono- and dual-species biofilm formation by *C. albicans* and *Streptococcus gordonii* as well [87].

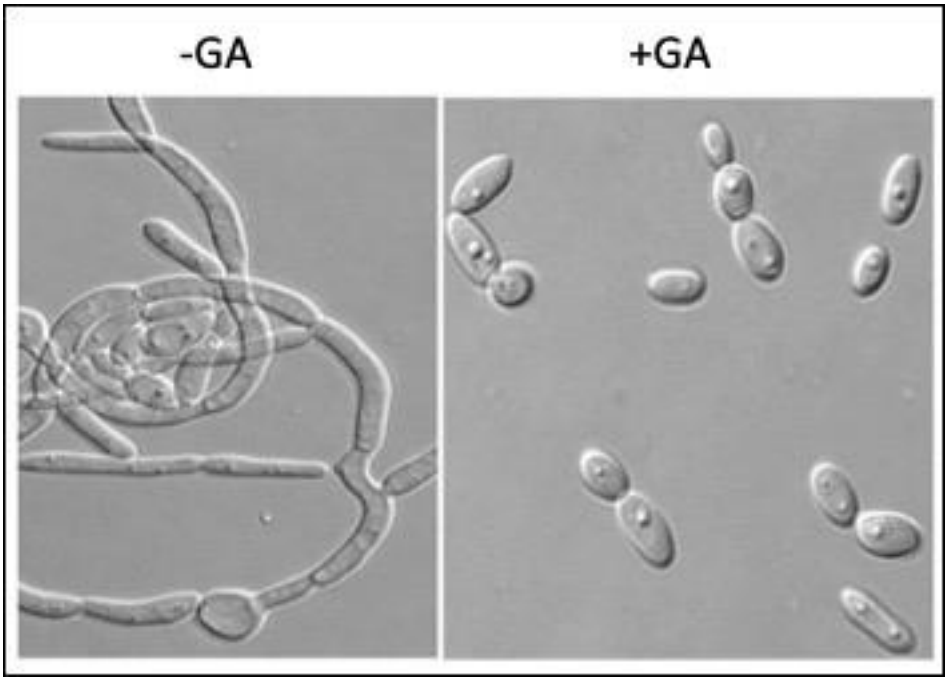

Figure 1.4. GAs inhibits filamentation in *C. albicans*.
C. albicans has grown in RPMI 1640 medium supplemented with 50 mM glucose at 37 ° C (hypha-inducing conditions) in the presence and absence of GAs. In the presence of GAs (+ GA) *C. albicans* fails to form hyphae, but it can produce yeast cells. Image taken from [86].

1.7 *C. auris* and its emergence

C. auris is a recently emerged opportunistic human fungal pathogen normally found on the skin and in the environment. It can cause skin and mucosal infection, and under favorable environmental conditions, it can cause bloodstream infection. It was identified 2009 in Japan

from the ear canal of a patient [88–90]. After that, *C. auris* has been isolated from different continents. Based on genetic variations and origin of isolation, *C. auris* has been categorized into five different clades namely: clade I (South Asia), clade II (East Asia), clade III (South Africa), clade IV (South America), and clade V (Iran) [91–93]. Several strains have already developed resistance against the three available antifungal groups (azoles, polyenes, and echinocandins). The mortality rate of *C. auris* mediated infections is above 50 %, and so CDC has listed *C. auris* as an urgent threat [91,94–96].

1.8 *C. auris* morphology

The morphological switch from yeast to hypha or pseudohypha is a key virulence factor in *C. albicans* and other fungi, not much is known about such a switch in *C. auris*. Environmental cues such as serum, temperature elevation, and nitrogen starvation that induce filamentation in *C. albicans* did not trigger filamentation in *C. auris* [97]. A *C. auris* strain obtained from a mouse was shown to undergo filamentation when grown at 25^{o} C [98]. However, such cases have not been reported later. Another study showed the ability of some *C. auris* strains undergo filamentation or pseudohyphal formation when treated with sublethal concentrations of genotoxins such as hydroxyurea, 5-fluorocytosine, and methyl methanosulfonate. The authors mentioned that this pseudohyphal growth was signaled through the S phase checkpoint during cell division [99].

1.9 *C. auris* biofilm in skin environment

C. auris, residing on our skin surfaces, are able to colonize and invade under favorable conditions. It has been linked to wound and bloodstream infections. A study has shown earlier

that *C. auris* are able to form biofilms by adhering to polymeric surfaces and this biofilm forming ability of *C. auris* contributes to its spread around healthcare facilities [100,101]. Along with biofilms on medical equipment such as catheters, a recent study has shown the ability of *C. auris* to form biofilms on human skin environment using synthetic medium that mimicked human sweat. Biofilm formed by *C. auris* using synthetic sweat medium was 10-folds denser than that of *C. albicans* biofilm. The same study further demonstrated this biofilm forming ability of *C. auris* using *ex vivo* porcine skin model [88]. Along with biofilm forming ability, *C. auris* can survive up to two weeks under dry environment whereas, *C. albicans* died within a week [88,102]. Such abilities of *C. auris* to survive in salty and dry environment for weeks might be the cause for the spread in hospital environments. Hence, thorough knowledge of *C. auris* mediated infection and pathogenesis, particularly its ability to form biofilm and spread on skin surfaces, are warranted.

1.10 *Candida auris* interaction with other skin residents

Candida auris resides on our skin surface which is home to several other skin inhabitants including other fungi, viruses, and bacteria **(Figure 1.5)**. Fungi such as *Malassezia* along with other *Candida* species such as *C. albicans*, *C. tropicalis*, and *C. parapsilosis* are commonly found on our skin. Recently, *C. auris* was isolated from COVID-10 patients that developed candidiasis [103,104]. Similarly, there are several bacteria residing on our skin including *S. aureus*, *S. epidermidis*, *P aeruginosa*, and more.

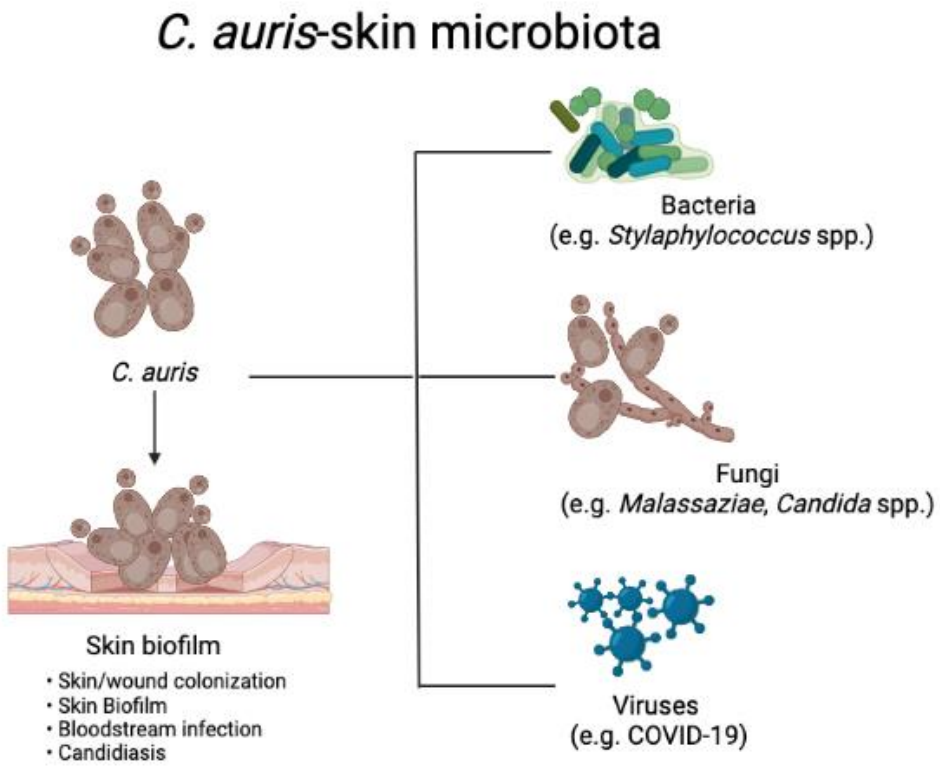

Figure 1.5. *C. auris*-skin microbiota.

C. auris forms biofilm on skin surface which is habitat for several other microbes such as bacteria, fungi, and viruses. Common habitat leads to possible microbial interaction as several bacteria and other fungi have been isolated together with *C. auris* including COVID-19 virus. Created in Biorender.com.

1.11 *Staphylococcus aureus* and biofilm

Staphylococcus aureus is a gram-positive bacterium and is an opportunistic pathogen colonizing on nasal and skin environment. It is capable of causing disease such as pneumonia, toxic shock syndrome, and bacteremia [105–108]. Emergence of antibiotic resistant *S. aureus* such as methicillin resistant *S. aureus*, has been a serious issue [109]. It possesses various virulence factors including hemolysin, proteases, toxins, leukocidins, and immune modulatory factors [108,110–112].

The ability to form biofilm is an important virulence factor in *S. aureus*. Extracellular polymeric substance (EPS) secreted during biofilm formation consists of extracellular DNA, proteins, and polysaccharides, making *S. aureus* biofilm resistant against existing antibiotics [113–115].

1.12 Quorum sensing activity

Quorum sensing (QS) allows bacteria or fungi to coordinate their growth strategies based on cell density and the surrounding environment. It is one of the strategies microbes use to survive in a competitive environment. Here, QS molecules secreted by *S. aureus* and *Candida* spp. are briefly discussed.

1.12.1 QS molecules in *S. aureus*

QS plays is an important virulence factor of *S. aureus* during infection and biofilm formation in host tissues. QS in *S. aureus* mainly involves Agr (accessory gene regulator) system which results in the secretion of several toxins and exoenzymes during high cell density. The Agr operon consists of *agrA, agrB, agrC,* and *agrD* genes that regulate the QS peptide, auto inducing peptide (AIP) which eventually controls Agr system activation or inhibition [116–118]. Agr system controls the expression of alpha-hemolysin or toxin (Hla) in *S. aureus*, which causes lysis of the blood cells leading to severe skin lesions [119,120]. Besides the Agr system, Hla expression is also controlled by other regulators such as Sae, and Sar regulatory system [121]. One study has shown that *C. albicans* induces hemolytic activity of *S. aureus* by increasing toxin production, when grown together [122]. So, evaluating the production and role of *S. aureus* QS molecule when grown together with *C. auris* will help understand its virulence if they colonize together.

1.12.2 QS molecules in *Candida*

The fact that fungal species can produce QS molecules was known for the first time after the discovery of farnesol secreted by *C. albicans* [75]. Farnesol inhibits conversion of yeast to hypha whereas another QS molecule secreted by *C. albicans* called tyrosol, stimulates filamentation under low cell density [75,123]. Other QS molecules secreted by *C. albicans* are phenylethyl alcohol, tryptophol, and morphogenic autoregulatory substance [124–126]. Other *Candida* species such as *C. glabrata*, *C. krusei*, *C. parapsilosis*, and others were previously shown to secrete farnesol [127]. However, *C. auris* secreting QS molecule has not been reported yet.

1.12.2.1 Farnesol

Farnesol **(Figure 1.6),** a known QS molecule produced by *C. albicans*, is one of the virulence factors in *C. albicans* [41,75], that inhibits yeast to hyphal transition along with the inhibition of biofilm formation by *C. albicans* [128]. Filamentation plays an important role in farnesol secretion as for example, *nrg1* or *tup1* homozygous mutants that exist in the constitutive filamentous form, did not respond to farnesol at all. In fact, *nrg1* and *tup1* mutants secreted more than 17 folds or more farnesol than wild type *C. albicans* [129]. Several pathways are involved in farnesol mediated response in *C. albicans* such as cAMP pathway, two-component signal pathway, and MAPK pathway [130–132]. Ras1, a protein of cAMP pathway is directly inhibited by farnesol.

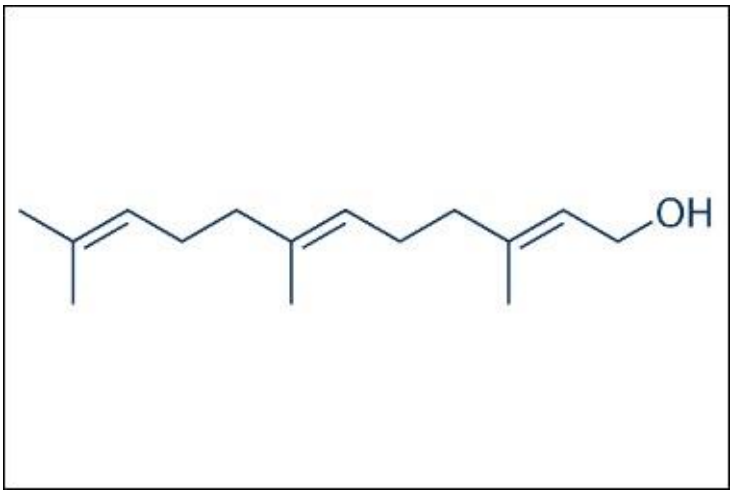

Figure 1.6. Chemical structure of farnesol.

Farnesol is a dodeca-2,6,10-triene substituted by a hydroxyl group at position 1 and 3 methyl groups at positions 3, 7, and 11. Image taken from PubChem.

After knowing *C. albicans* secretes farnesol, a study was done to check farnesol secretion in several other *Candida* species and it was found that *C. albicans* produces approximately 35 uM of farnesol which is significantly higher than that of other *Candida* species such as *C. glabrata*, *C. krusei*, *C. parapsilosis*, and others with less than 1 μM of farnesol production [127]. *DPP1* is a gene encoding phosphatase that converts farnesyl pyrophosphate into farnesol in *S. cerevisiae*. *C. albicans* contains *DPP3*, which is an ortholog of *DPP1* and *DPP3* mutant in *C. albicans* leads to six times less farnesol production as compared to the wild type *C. albicans* [133,134]. In the same study of systemic candidiasis in mice model, *DPP3* mutant that was injected intravenously via tail vein, was 4.4 times less virulent as compared to wild type strain. However, mice receiving *C. albicans* intravenously and exogenous farnesol orally, showed increased mortality as compared to the mice that only received *C. albicans* but not exogenous farnesol [134]. Effect of farnesol has been tested on several other fungi and bacteria, suggesting interspecies communication among microbes. In another filamentous *Candida* species, *C. dubliniensis*, farnesol inhibited filament formation as well as biofilms similar to that of *C.*

albicans [135–137]. Similarly, farnesol inhibits growth of *S. cerevisiae* by affecting cell cycle and increased reactive oxygen species (ROS) [138,139]. Besides fungi, growth of several bacteria such as *S. aureus, S. epidermidis,* and *S. mutans* is inhibited by different concentrations of farnesol [137,140,141]. To our knowledge, no farnesol or farnesol like compounds have been identified in *C. auris* so far.

1.13 Aims of this study:

Candida albicans is responsible for causing infection on several body parts that might lead to invasive systemic infection mostly by its hyphae. It is important to identify compounds that can inhibit the hypha-mediated spread of infections and understand their mode of action. Hence, one of the aims of this study is to determine the efficacy of hyphal inhibitory compounds, gymnemic acids, in systemic candidiasis mice model **(Chapter 2)**. My second goal was to identify protein complexes associated with GAs and investigate mechanisms involved in GAs-mediated hyphal inhibition **(Chapter 3)**.

Another emerging fungal pathogen, *C. auris*, remains mostly in yeast form but is reported to from pseudohypha under certain conditions. However, much less is known about the genes involved. In **Chapter 4**, the expression and function of a transcription factor called Nrg1 in *C. auris* that is previously known to impact morphology in *C. albicans,* is presented.

As *C. auris* can form biofilm on skin surface, there is high probability of it colonizing with other skin residents. So, the last aim of the study **(Chapter 5)** is to determine if *Candida auris* and *Staphylococcus aureus* can form dual-species biofilm on skin surface with increased virulence.

1.14 References

1. Mora, C.; Tittensor, D.P.; Adl, S.; Simpson, A.G.B.; Worm, B. How Many Species Are There on Earth and in the Ocean? *PLoS Biol* **2011**, *9*, e1001127, doi:10.1371/journal.pbio.1001127.

2. Friedman, D.Z.P.; Schwartz, I.S. Emerging Fungal Infections: New Patients, New Patterns, and New Pathogens. *J Fungi (Basel)* **2019**, *5*, 67, doi:10.3390/jof5030067.

3. Candidiasis (Invasive) - Infectious Diseases Available online: https://www.merckmanuals.com/professional/infectious-diseases/fungi/candidiasis-invasive (accessed on 11 August 2022).

4. Forsberg, K.; Woodworth, K.; Walters, M.; Berkow, E.L.; Jackson, B.; Chiller, T.; Vallabhaneni, S. *Candida auris*: The Recent Emergence of a Multidrug-Resistant Fungal Pathogen. *Medical Mycology* **2019**, *57*, 1–12, doi:10.1093/mmy/myy054.

5. Benedict, K.; Jackson, B.R.; Chiller, T.; Beer, K.D. Estimation of Direct Healthcare Costs of Fungal Diseases in the United States. *Clin Infect Dis* **2019**, *68*, 1791–1797, doi:10.1093/cid/ciy776.

6. *World of Microbiology and Immunology*; Lerner, K.L., Lerner, B.W., Eds.; Gale: Detroit, 2003; ISBN 978-0-7876-6540-1.

7. Findley, K.; Oh, J.; Yang, J.; Conlan, S.; Deming, C.; Meyer, J.A.; Schoenfeld, D.; Nomicos, E.; Park, M.; Kong, H.H.; et al. Topographic Diversity of Fungal and Bacterial Communities in Human Skin. *Nature* **2013**, *498*, 367–370, doi:10.1038/nature12171.

8. Nash, A.K.; Auchtung, T.A.; Wong, M.C.; Smith, D.P.; Gesell, J.R.; Ross, M.C.; Stewart, C.J.; Metcalf, G.A.; Muzny, D.M.; Gibbs, R.A.; et al. The Gut Mycobiome of the Human Microbiome Project Healthy Cohort. *Microbiome* **2017**, *5*, 153, doi:10.1186/s40168-017-0373-4.

9. Fidel, P.L.; Yano, J.; Esher, S.K.; Noverr, M.C. Applying the Host-Microbe Damage Response Framework to *Candida* Pathogenesis: Current and Prospective Strategies to Reduce Damage. *J Fungi (Basel)* **2020**, *6*, 35, doi:10.3390/jof6010035.

10. d'Enfert, C.; Kaune, A.-K.; Alaban, L.-R.; Chakraborty, S.; Cole, N.; Delavy, M.; Kosmala, D.; Marsaux, B.; Fróis-Martins, R.; Morelli, M.; et al. The Impact of the Fungus-Host-Microbiota Interplay upon *Candida albicans* Infections: Current Knowledge and New Perspectives. *FEMS Microbiol Rev* **2020**, *45*, fuaa060, doi:10.1093/femsre/fuaa060.

11. Ancalle, I.M.; Rivera, J.A.; García, I.; García, L.; Valcárcel, M. *Candida albicans* Meningitis and Brain Abscesses in a Neonate: A Case Report. *Bol Asoc Med P R* **2010**, *102*, 45–48.

12. Black, J.T. Cerebral Candidiasis: Case Report of Brain Abscess Secondary to *Candida albicans*, and Review of Literature. *J Neurol Neurosurg Psychiatry* **1970**, *33*, 864–870.

13. Tweddle, D.A.; Graham, J.C.; Shankland, G.S.; Kernahan, J. Cerebral Candidiasis in a Child 1 Year after Leukaemia. *British Journal of Haematology* **1998**, *103*, 795–797, doi:10.1046/j.1365-2141.1998.01023.x.

14. Butler, G.; Rasmussen, M.D.; Lin, M.F.; Santos, M.A.S.; Sakthikumar, S.; Munro, C.A.; Rheinbay, E.; Grabherr, M.; Forche, A.; Reedy, J.L.; et al. Evolution of Pathogenicity and Sexual Reproduction in Eight *Candida* Genomes. *Nature* **2009**, *459*, 657–662, doi:10.1038/nature08064.

15. Jones, T.; Federspiel, N.A.; Chibana, H.; Dungan, J.; Kalman, S.; Magee, B.B.; Newport, G.; Thorstenson, Y.R.; Agabian, N.; Magee, P.T.; et al. The Diploid Genome Sequence of *Candida albican*s. *Proceedings of the National Academy of Sciences* **2004**, *101*, 7329–7334, doi:10.1073/pnas.0401648101.

16. Kabir, M.A.; Hussain, M.A. Human Fungal Pathogen *Candida albicans* in the Postgenomic Era: An Overview. *Expert Review of Anti-infective Therapy* **2009**, *7*, 121–134, doi:10.1586/14787210.7.1.121.

17. Kabir, M.A.; Hussain, M.A.; Ahmad, Z. *Candida albicans*: A Model Organism for Studying Fungal Pathogens. *ISRN Microbiol* **2012**, *2012*, 538694, doi:10.5402/2012/538694.

18. Noble, S.M.; Gianetti, B.A.; Witchley, J.N. *Candida albicans* Cell Type Switches and Functional Plasticity in the Mammalian Host. *Nat Rev Microbiol* **2017**, *15*, 96–108, doi:10.1038/nrmicro.2016.157.

19. Maza, P.K.; Bonfim-Melo, A.; Padovan, A.C.B.; Mortara, R.A.; Orikaza, C.M.; Ramos, L.M.D.; Moura, T.R.; Soriani, F.M.; Almeida, R.S.; Suzuki, E.; et al. *Candida albicans*: The Ability to Invade Epithelial Cells and Survive under Oxidative Stress Is Unlinked to Hyphal Length. *Front Microbiol* **2017**, *8*, 1235, doi:10.3389/fmicb.2017.01235.

20. Moyes, D.L.; Wilson, D.; Richardson, J.P.; Mogavero, S.; Tang, S.X.; Wernecke, J.; Höfs, S.; Gratacap, R.L.; Robbins, J.; Runglall, M.; et al. Candidalysin Is a Fungal Peptide Toxin Critical for Mucosal Infection. *Nature* **2016**, *532*, 64–68, doi:10.1038/nature17625.

21. Kasper, L.; König, A.; Koenig, P.-A.; Gresnigt, M.S.; Westman, J.; Drummond, R.A.; Lionakis, M.S.; Groß, O.; Ruland, J.; Naglik, J.R.; et al. The Fungal Peptide Toxin Candidalysin Activates the NLRP3 Inflammasome and Causes Cytolysis in Mononuclear Phagocytes. *Nat Commun* **2018**, *9*, 4260, doi:10.1038/s41467-018-06607-1.

22. König, A.; Hube, B.; Kasper, L. The Dual Function of the Fungal Toxin Candidalysin during *Candida albicans*—Macrophage Interaction and Virulence. *Toxins* **2020**, *12*, 469, doi:10.3390/toxins12080469.

23. Virulence Traits Contributing to Pathogenicity of *Candida* Species. **2017**, *Volume 5*, doi:10.15406/jmen.2017.05.00140.

24. Tsui, C.; Kong, E.F.; Jabra-Rizk, M.A. Pathogenesis of *Candida albicans* Biofilm. *Pathog Dis* **2016**, *74*, ftw018, doi:10.1093/femspd/ftw018.

25. Priya, A.; Pandian, S.K. Piperine Impedes Biofilm Formation and Hyphal Morphogenesis of *Candida albicans*. *Front Microbiol* **2020**, *11*, 756, doi:10.3389/fmicb.2020.00756.

26. Karygianni, L.; Ren, Z.; Koo, H.; Thurnheer, T. Biofilm Matrixome: Extracellular Components in Structured Microbial Communities. *Trends in Microbiology* **2020**, *28*, 668–681, doi:10.1016/j.tim.2020.03.016.

27. Wibawa, T. The Role of Virulence Factors In *Candida albicans* pathogenicity. *JMedScie* **2016**, *48*, 58–68, doi:10.19106/JMedSci004801201606.

28. Takahashi, M.; Banno, Y.; Nozawa, Y. Secreted *Candida albicans* Phospholipases: Purification and Characterization of Two Forms of Lysophospholipase-Transacylase. *J Med Vet Mycol* **1991**, *29*, 193–204.

29. Manns, J.M.; Mosser, D.M.; Buckley, H.R. Production of a Hemolytic Factor by *Candida albicans*. *Infect Immun* **1994**, *62*, 5154–5156, doi:10.1128/iai.62.11.5154-5156.1994.

30. B, H.; Cj, T.; Fc, O.; H, E.; Gj, B.; H, K.; R, R. [Identification, Cloning and Characterization of the Gene for the Secretory Aspartate Protease of *Candida albicans*]. *Mycoses* **1991**, *34 Suppl 1*.

31. Lee, G.-C.; Tang, S.-J.; Sun, K.-H.; Shaw, J.-F. Analysis of the Gene Family Encoding Lipases in *Candida rugosa* by Competitive Reverse Transcription-PCR. *Applied and Environmental Microbiology* **1999**, *65*, 3888, doi:10.1128/aem.65.9.3888-3895.1999.

32. Luo, G.; Samaranayake, L.P.; Yau, J.Y.Y. *Candida* Species Exhibit Differential In Vitro Hemolytic Activities. *Journal of Clinical Microbiology* **2001**, *39*, 2971–2974, doi:10.1128/JCM.39.8.2971-2974.2001.

33. Sudbery, P.; Gow, N.; Berman, J. The Distinct Morphogenic States of *Candida albicans*. *Trends in Microbiology* **2004**, *12*, 317–324, doi:10.1016/j.tim.2004.05.008.

34. Pande, K.; Chen, C.; Noble, S.M. Passage through the Mammalian Gut Triggers a Phenotypic Switch That Promotes *Candida albicans* Commensalism. *Nat Genet* **2013**, *45*, 1088–1091, doi:10.1038/ng.2710.

35. Miller, M.G.; Johnson, A.D. White-Opaque Switching in *Candida albicans* Is Controlled by Mating-Type Locus Homeodomain Proteins and Allows Efficient Mating. *Cell* **2002**, *110*, 293–302, doi:10.1016/S0092-8674(02)00837-1.

36. Xie, J.; Tao, L.; Nobile, C.J.; Tong, Y.; Guan, G.; Sun, Y.; Cao, C.; Hernday, A.D.; Johnson, A.D.; Zhang, L.; et al. White-Opaque Switching in Natural MTLa/α Isolates of

Candida albicans: Evolutionary Implications for Roles in Host Adaptation, Pathogenesis, and Sex. *PLoS Biol* **2013**, *11*, e1001525, doi:10.1371/journal.pbio.1001525.

37. Staib, P.; Morschhäuser, J. Chlamydospore Formation in *Candida albicans* and *Candida dubliniensis*– an Enigmatic Developmental Programme. *Mycoses* **2007**, *50*, 1–12, doi:10.1111/j.1439-0507.2006.01308.x.

38. Mayer, F.L.; Wilson, D.; Hube, B. *Candida albicans* Pathogenicity Mechanisms. *Virulence* **2013**, *4*, 119–128, doi:10.4161/viru.22913.

39. Jacobsen, I.D.; Wilson, D.; Wächtler, B.; Brunke, S.; Naglik, J.R.; Hube, B. *Candida albicans* Dimorphism as a Therapeutic Target. *Expert Review of Anti-infective Therapy* **2012**, *10*, 85–93, doi:10.1586/eri.11.152.

40. Saville, S.P.; Lazzell, A.L.; Monteagudo, C.; Lopez-Ribot, J.L. Engineered Control of Cell Morphology In Vivo Reveals Distinct Roles for Yeast and Filamentous Forms of *Candida albicans* during Infection. *Eukaryot Cell* **2003**, *2*, 1053–1060, doi:10.1128/EC.2.5.1053-1060.2003.

41. Lo, H.-J.; Köhler, J.R.; DiDomenico, B.; Loebenberg, D.; Cacciapuoti, A.; Fink, G.R. Nonfilamentous *C. albicans* Mutants Are Avirulent. *Cell* **1997**, *90*, 939–949, doi:10.1016/S0092-8674(00)80358-X.

42. Gow, N.A.R.; Brown, A.J.P.; Odds, F.C. Fungal Morphogenesis and Host Invasion. *Current Opinion in Microbiology* **2002**, *5*, 366–371, doi:10.1016/S1369-5274(02)00338-7.

43. Chen, H.; Zhou, X.; Ren, B.; Cheng, L. The Regulation of Hyphae Growth in *Candida albicans*. *Virulence* **2020**, *11*, 337–348, doi:10.1080/21505594.2020.1748930.

44. Basso, V.; d'Enfert, C.; Znaidi, S.; Bachellier-Bassi, S. From Genes to Networks: The Regulatory Circuitry Controlling *Candida albicans* Morphogenesis. In *Fungal Physiology and Immunopathogenesis*; Rodrigues, M.L., Ed.; Current Topics in Microbiology and Immunology; Springer International Publishing: Cham, 2019; pp. 61–99 ISBN 978-3-030-30237-5.

45. Kadosh, D. Regulatory Mechanisms Controlling Morphology and Pathogenesis in *Candida albicans*. *Curr Opin Microbiol* **2019**, *52*, 27–34, doi:10.1016/j.mib.2019.04.005.

46. Kornitzer, D. Regulation of *Candida albicans* Hyphal Morphogenesis by Endogenous Signals. *J Fungi (Basel)* **2019**, *5*, 21, doi:10.3390/jof5010021.

47. Hogan, D.A.; Sundstrom, P. The Ras/CAMP/PKA Signaling Pathway and Virulence in *Candida albicans*. *Future Microbiology* **2009**, *4*, 1263–1270, doi:10.2217/fmb.09.106.

48. RA Domain-mediated Interaction of Cdc35 with Ras1 Is Essential for Increasing Cellular CAMP Level for *Candida albicans* Hyphal Development - Fang - 2006 - Molecular Microbiology - Wiley Online Library Available online:

https://onlinelibrary.wiley.com/doi/10.1111/j.1365-2958.2006.05248.x (accessed on 8 August 2022).

49. Zou, H.; Fang, H.-M.; Zhu, Y.; Wang, Y. *Candida albicans* Cyr1, Cap1 and G-Actin Form a Sensor/Effector Apparatus for Activating CAMP Synthesis in Hyphal Growth. *Molecular Microbiology* **2010**, *75*, 579–591, doi:10.1111/j.1365-2958.2009.06980.x.

50. Feng, Q.; Summers, E.; Guo, B.; Fink, G. Ras Signaling Is Required for Serum-Induced Hyphal Differentiation in *Candida albicans*. *J Bacteriol* **1999**, *181*, 6339–6346.

51. Leberer, E.; Harcus, D.; Dignard, D.; Johnson, L.; Ushinsky, S.; Thomas, D.Y.; Schröppel, K. Ras Links Cellular Morphogenesis to Virulence by Regulation of the MAP Kinase and CAMP Signalling Pathways in the Pathogenic Fungus *Candida albicans*. *Molecular Microbiology* **2001**, *42*, 673–687, doi:10.1046/j.1365-2958.2001.02672.x.

52. Leach, M.D.; Farrer, R.A.; Tan, K.; Miao, Z.; Walker, L.A.; Cuomo, C.A.; Wheeler, R.T.; Brown, A.J.P.; Wong, K.H.; Cowen, L.E. Hsf1 and Hsp90 Orchestrate Temperature-Dependent Global Transcriptional Remodelling and Chromatin Architecture in *Candida albicans*. *Nat Commun* **2016**, *7*, 11704, doi:10.1038/ncomms11704.

53. Bachewich, C.; Whiteway, M. Cyclin Cln3p Links G1 Progression to Hyphal and Pseudohyphal Development in *Candida albicans*. *Eukaryot Cell* **2005**, *4*, 95–102, doi:10.1128/EC.4.1.95-102.2005.

54. Bachewich, C.; Nantel, A.; Whiteway, M. Cell Cycle Arrest during S or M Phase Generates Polarized Growth via Distinct Signals in *Candida albicans. Molecular Microbiology* **2005**, *57*, 942–959, doi:10.1111/j.1365-2958.2005.04727.x.

55. Monge, R.A.; Román, E.; Nombela, C.; Pla, J.Y. 2006 The MAP Kinase Signal Transduction Network in *Candida albicans*. *Microbiology 152*, 905–912, doi:10.1099/mic.0.28616-0.

56. Román, E.; Arana, D.M.; Nombela, C.; Alonso-Monge, R.; Pla, J. MAP Kinase Pathways as Regulators of Fungal Virulence. *Trends in Microbiology* **2007**, *15*, 181–190, doi:10.1016/j.tim.2007.02.001.

57. Biswas, K.; Morschhäuser, J. The Mep2p Ammonium Permease Controls Nitrogen Starvation-Induced Filamentous Growth in *Candida albicans*. *Molecular Microbiology* **2005**, *56*, 649–669, doi:10.1111/j.1365-2958.2005.04576.x.

58. Braun, B.R.; Johnson, A.D. Control of Filament Formation in *Candida albicans* by the Transcriptional Repressor TUP1. *Science* **1997**, *277*, 105–109, doi:10.1126/science.277.5322.105.

59. Murad, A.M.A.; Leng, P.; Straffon, M.; Wishart, J.; Macaskill, S.; MacCallum, D.; Schnell, N.; Talibi, D.; Marechal, D.; Tekaia, F.; et al. NRG1 Represses Yeast–Hypha Morphogenesis and Hypha-Specific Gene Expression in *Candida albicans*. *EMBO J* **2001**, *20*, 4742–4752, doi:10.1093/emboj/20.17.4742.

60. Kadosh, D.; Johnson, A.D. Rfg1, a Protein Related to the *Saccharomyces Cerevisiae* Hypoxic Regulator Rox1, Controls Filamentous Growth and Virulence in *Candida albicans*. *Molecular and Cellular Biology* **2001**, *21*, 2496–2505, doi:10.1128/MCB.21.7.2496-2505.2001.

61. Kadosh, D.; Johnson, A.D. Induction of the *Candida albicans* Filamentous Growth Program by Relief of Transcriptional Repression: A Genome-Wide Analysis. *Mol Biol Cell* **2005**, *16*, 2903–2912, doi:10.1091/mbc.E05-01-0073.

62. Schoeters, F.; Van Dijck, P. Protein-Protein Interactions in *Candida albicans*. *Frontiers in Microbiology*. **2019**, *10*, doi.org/10.3389/fmicb.2019.01792.

63. Braun, B.R.; Kadosh, D.; Johnson, A.D. NRG1, a Repressor of Filamentous Growth in *C.albicans*, Is down-Regulated during Filament Induction. *EMBO J* **2001**, *20*, 4753–4761, doi:10.1093/emboj/20.17.4753.

64. Lu, Y.; Su, C.; Wang, A.; Liu, H. Hyphal Development in *Candida albicans* Requires Two Temporally Linked Changes in Promoter Chromatin for Initiation and Maintenance. *PLOS Biology* **2011**, *9*, e1001105, doi:10.1371/journal.pbio.1001105.

65. Lu, Y.; Su, C.; Liu, H. A GATA Transcription Factor Recruits Hda1 in Response to Reduced Tor1 Signaling to Establish a Hyphal Chromatin State in *Candida albicans*. *PLOS Pathogens* **2012**, *8*, e1002663, doi:10.1371/journal.ppat.1002663.

66. Cleary, I.A.; Saville, S.P. An Analysis of the Impact of NRG1 Overexpression on the *Candida albicans* Response to Specific Environmental Stimuli. *Mycopathologia* **2010**, *170*, 1–10, doi:10.1007/s11046-010-9297-2.

67. Uppuluri, P.; Pierce, C.G.; Thomas, D.P.; Bubeck, S.S.; Saville, S.P.; Lopez-Ribot, J.L. The Transcriptional Regulator Nrg1p Controls *Candida albicans* Biofilm Formation and Dispersion. *Eukaryot Cell* **2010**, *9*, 1531–1537, doi:10.1128/EC.00111-10.

68. Saville, S.P.; Lazzell, A.L.; Chaturvedi, A.K.; Monteagudo, C.; Lopez-Ribot, J.L. Efficacy of a Genetically Engineered *Candida albicans* Tet-NRG1 Strain as an Experimental Live Attenuated Vaccine against Hematogenously Disseminated Candidiasis. *Clin Vaccine Immunol* **2009**, *16*, 430–432, doi:10.1128/CVI.00480-08.

69. Banerjee, M.; Thompson, D.S.; Lazzell, A.; Carlisle, P.L.; Pierce, C.; Monteagudo, C.; López-Ribot, J.L.; Kadosh, D. UME6, a Novel Filament-Specific Regulator of *Candida albicans* Hyphal Extension and Virulence. *Mol Biol Cell* **2008**, *19*, 1354–1365, doi:10.1091/mbc.E07-11-1110.

70. Staib, P.; Morschhäuser, J. Differential Expression of the NRG1 Repressor Controls Species-Specific Regulation of Chlamydospore Development in *Candida albicans* and *Candida dubliniensis*. *Molecular Microbiology* **2005**, *55*, 637–652, doi:10.1111/j.1365-2958.2004.04414.x.

71. Zeidler, U.; Lettner, T.; Lassnig, C.; Müller, M.; Lajko, R.; Hintner, H.; Breitenbach, M.; Bito, A. UME6 Is a Crucial Downstream Target of Other Transcriptional Regulators of True Hyphal Development in *Candida albicans*. *FEMS Yeast Research* **2009**, *9*, 126–142, doi:10.1111/j.1567-1364.2008.00459.x.

72. Uppuluri, P.; Chaturvedi, A.K.; Srinivasan, A.; Banerjee, M.; Ramasubramaniam, A.K.; Köhler, J.R.; Kadosh, D.; Lopez-Ribot, J.L. Dispersion as an Important Step in the *Candida albicans* Biofilm Developmental Cycle. *PLoS Pathog* **2010**, *6*, e1000828, doi:10.1371/journal.ppat.1000828.

73. Padmavathi, A.R.; P., S.M.; Das, A.; Priya, A.; Sushmitha, T.J.; Pandian, S.K.; Toleti, S.R. Impediment to Growth and Yeast-to-Hyphae Transition in *Candida albicans* by Copper Oxide Nanoparticles. *Biofouling* **2020**, *36*, 56–72, doi:10.1080/08927014.2020.1715371.

74. Hamdy, R.; Soliman, S.S.M.; Alsaadi, A.I.; Fayed, B.; Hamoda, A.M.; Elseginy, S.A.; Husseiny, M.I.; Ibrahim, A.S. Design and Synthesis of New Drugs Inhibitors of *Candida albicans* Hyphae and Biofilm Formation by Upregulating the Expression of TUP1 Transcription Repressor Gene. *Eur J Pharm Sci* **2020**, *148*, 105327, doi:10.1016/j.ejps.2020.105327.

75. Hornby, J.M.; Jensen, E.C.; Lisec, A.D.; Tasto, J.J.; Jahnke, B.; Shoemaker, R.; Dussault, P.; Nickerson, K.W. Quorum Sensing in the Dimorphic Fungus *Candida albicans* Is Mediated by Farnesol. *Appl Environ Microbiol* **2001**, *67*, 2982–2992, doi:10.1128/AEM.67.7.2982-2992.2001.

76. Alabama, J.N.O., PharmD Community Practitioner Bessemer, Alabama Jessica W. Skelley, PharmD Pharmacy Resident Jefferson County Health Department Samford University McWhorter School of Pharmacy Birmingham, Alabama Jeffrey A. Kyle, PharmD, BCPS Assistant Professor of Pharmacy Practice Samford University McWhorter School of Pharmacy Birmingham The Fungus Among Us: An Antifungal Review Available online: https://www.uspharmacist.com/article/the-fungus-among-us-an-antifungal-review (accessed on 9 August 2022).

77. Carmona, E.M.; Limper, A.H. Overview of Treatment Approaches for Fungal Infections. *Clinics in Chest Medicine* **2017**, *38*, 393–402, doi:10.1016/j.ccm.2017.04.003.

78. Gintjee, T.J.; Donnelley, M.A.; Thompson, G.R. Aspiring Antifungals: Review of Current Antifungal Pipeline Developments. *J Fungi (Basel)* **2020**, *6*, 28, doi:10.3390/jof6010028.

79. Yoshikawa, K.; Amimoto, K.; Arihara, S.; Matsuura, K. Structure Studies of New Antisweet Constituents from *Gymnema sylvestre. Tetrahedron Letters* **1989**, *30*, 1103–1106, doi:10.1016/S0040-4039(01)80371-3.

80. Sanematsu, K.; Kusakabe, Y.; Shigemura, N.; Hirokawa, T.; Nakamura, S.; Imoto, T.; Ninomiya, Y. Molecular Mechanisms for Sweet-Suppressing Effect of Gymnemic Acids. *J Biol Chem* **2014**, *289*, 25711–25720, doi:10.1074/jbc.M114.560409.

81. Renga, B.; Festa, C.; Marino, S.D.; Micco, S.D.; D'Auria, M.V.; Bifulco, G.; Fiorucci, S.; Zampella, A. Molecular Decodification of Gymnemic Acids from *Gymnema sylvestre*. Discovery of a New Class of Liver X Receptor Antagonists. *Steroids* **2015**, *96*, 121–131.

82. Wang, Y.; Dawid, C.; Kottra, G.; Daniel, H.; Hofmann, T. Gymnemic Acids Inhibit Sodium-Dependent Glucose Transporter 1. *J. Agric. Food Chem.* **2014**, *62*, 5925–5931, doi:10.1021/jf501766u.

83. Zuñiga, L.Y.; González-Ortiz, M.; Martínez-Abundis, E. Effect of *Gymnema sylvestre* Administration on Metabolic Syndrome, Insulin Sensitivity, and Insulin Secretion. *Journal of Medicinal Food* **2017**, *20*, 750–754, doi:10.1089/jmf.2017.0001.

84. Tiwari, P.; Mishra, B.N.; Sangwan, N.S. Phytochemical and Pharmacological Properties of *Gymnema sylvestre*: An Important Medicinal Plant. *BioMed Research International* **2014**, *2014*, doi:10.1155/2014/830285.

85. Khan, F.; Sarker, M.M.R.; Ming, L.C.; Mohamed, I.N.; Zhao, C.; Sheikh, B.Y.; Tsong, H.F.; Rashid, M.A. Comprehensive Review on Phytochemicals, Pharmacological and Clinical Potentials of *Gymnema sylvestre*. *Frontiers in Pharmacology* **2019**, *10*, doi:10.3389/fphar.2019.01223.

86. Vediyappan, G.; Dumontet, V.; Pelissier, F.; d'Enfert, C. Gymnemic Acids Inhibit Hyphal Growth and Virulence in *Candida albicans*. *PLoS One* **2013**, *8*, e74189, doi:10.1371/journal.pone.0074189.

87. Veerapandian, R.; Vediyappan, G. Gymnemic Acids Inhibit Adhesive Nanofibrillar Mediated *Streptococcus gordonii–Candida albicans* Mono-Species and Dual-Species Biofilms. *Front Microbiol* **2019**, *10*, 2328, doi:10.3389/fmicb.2019.02328.

88. Horton, M.V.; Johnson, C.J.; Kernien, J.F.; Patel, T.D.; Lam, B.C.; Cheong, J.Z.A.; Meudt, J.J.; Shanmuganayagam, D.; Kalan, L.R.; Nett, J.E. *Candida auris* Forms High-Burden Biofilms in Skin Niche Conditions and on Porcine Skin. **2020**, *5*, 8.

89. Du, H.; Bing, J.; Hu, T.; Ennis, C.L.; Nobile, C.J.; Huang, G. *Candida auris*: Epidemiology, Biology, Antifungal Resistance, and Virulence. *PLoS Pathog* **2020**, *16*, e1008921, doi:10.1371/journal.ppat.1008921.

90. Satoh, K.; Makimura, K.; Hasumi, Y.; Nishiyama, Y.; Uchida, K.; Yamaguchi, H. *Candida auris* Sp. Nov., a Novel Ascomycetous Yeast Isolated from the External Ear Canal of an Inpatient in a Japanese Hospital. *Microbiology and Immunology* **2009**, *53*, 41–44, doi:10.1111/j.1348-0421.2008.00083.x.

91. Lockhart, S.R.; Etienne, K.A.; Vallabhaneni, S.; Farooqi, J.; Chowdhary, A.; Govender, N.P.; Colombo, A.L.; Calvo, B.; Cuomo, C.A.; Desjardins, C.A.; et al. Simultaneous Emergence of Multidrug-Resistant *Candida auris* on 3 Continents Confirmed by Whole-Genome Sequencing and Epidemiological Analyses. *Clin Infect Dis* **2017**, *64*, 134–140, doi:10.1093/cid/ciw691.

92. Chow, N.A.; de Groot, T.; Badali, H.; Abastabar, M.; Chiller, T.M.; Meis, J.F. Potential Fifth Clade of *Candida auris*, Iran, 2018. *Emerg Infect Dis* **2019**, *25*, 1780–1781, doi:10.3201/eid2509.190686.

93. Muñoz, J.F.; Gade, L.; Chow, N.A.; Loparev, V.N.; Juieng, P.; Berkow, E.L.; Farrer, R.A.; Litvintseva, A.P.; Cuomo, C.A. Genomic Insights into Multidrug-Resistance, Mating and Virulence in *Candida auris* and Related Emerging Species. *Nat Commun* **2018**, *9*, 5346, doi:10.1038/s41467-018-07779-6.

94. Zhu, Y.; O'Brien, B.; Leach, L.; Clarke, A.; Bates, M.; Adams, E.; Ostrowsky, B.; Quinn, M.; Dufort, E.; Southwick, K.; et al. Laboratory Analysis of an Outbreak of *Candida auris* in New York from 2016 to 2018: Impact and Lessons Learned. *J Clin Microbiol* **2020**, *58*, e01503-19, doi:10.1128/JCM.01503-19.

95. Lee, W.G.; Shin, J.H.; Uh, Y.; Kang, M.G.; Kim, S.H.; Park, K.H.; Jang, H.-C. First Three Reported Cases of Nosocomial Fungemia Caused by *Candida auris* ▿. *J Clin Microbiol* **2011**, *49*, 3139–3142, doi:10.1128/JCM.00319-11.

96. Chowdhary, A.; Sharma, C.; Duggal, S.; Agarwal, K.; Prakash, A.; Singh, P.K.; Jain, S.; Kathuria, S.; Randhawa, H.S.; Hagen, F.; et al. New Clonal Strain of *Candida auris*, Delhi, India. *Emerg Infect Dis* **2013**, *19*, 1670–1673, doi:10.3201/eid1910.130393.

97. Wang, X.; Bing, J.; Zheng, Q.; Zhang, F.; Liu, J.; Yue, H.; Tao, L.; Du, H.; Wang, Y.; Wang, H.; et al. The First Isolate of *Candida auris* in China: Clinical and Biological Aspects. *Emerg Microbes Infect* **2018**, *7*, 93, doi:10.1038/s41426-018-0095-0.

98. Yue, H.; Bing, J.; Zheng, Q.; Zhang, Y.; Hu, T.; Du, H.; Wang, H.; Huang, G. Filamentation in *Candida auris*, an Emerging Fungal Pathogen of Humans: Passage through the Mammalian Body Induces a Heritable Phenotypic Switch. *Emerg Microbes Infect* **2018**, *7*, 188, doi:10.1038/s41426-018-0187-x.

99. Bravo Ruiz, G.; Ross, Z.K.; Gow, N.A.R.; Lorenz, A. Pseudohyphal Growth of the Emerging Pathogen *Candida auris* Is Triggered by Genotoxic Stress through the S Phase Checkpoint. *mSphere* **2020**, *5*, e00151-20, doi:10.1128/mSphere.00151-20.

100. Sherry, L.; Ramage, G.; Kean, R.; Borman, A.; Johnson, E.M.; Richardson, M.D.; Rautemaa-Richardson, R. Biofilm-Forming Capability of Highly Virulent, Multidrug-Resistant *Candida auris*. *Emerg Infect Dis* **2017**, *23*, 328–331, doi:10.3201/eid2302.161320.

101. Calvo, B.; Melo, A.S.A.; Perozo-Mena, A.; Hernandez, M.; Francisco, E.C.; Hagen, F.; Meis, J.F.; Colombo, A.L. First Report of *Candida auris* in America: Clinical and Microbiological Aspects of 18 Episodes of Candidemia. *Journal of Infection* **2016**, *73*, 369–374, doi:10.1016/j.jinf.2016.07.008.

102. Welsh, R.M.; Bentz, M.L.; Shams, A.; Houston, H.; Lyons, A.; Rose, L.J.; Litvintseva, A.P. Survival, Persistence, and Isolation of the Emerging Multidrug-Resistant Pathogenic

Yeast *Candida auris* on a Plastic Health Care Surface. *J Clin Microbiol* **2017**, *55*, 2996–3005, doi:10.1128/JCM.00921-17.

103. Goravey, W.; Ali, G.A.; Ali, M.; Ibrahim, E.B.; Al Maslamani, M.; Abdel Hadi, H. Ominous Combination: COVID-19 Disease and *Candida auris* Fungemia—Case Report and Review of the Literature. *Clin Case Rep* **2021**, *9*, e04827, doi:10.1002/ccr3.4827.

104. Chowdhary, A.; Tarai, B.; Singh, A.; Sharma, A. Multidrug-Resistant *Candida auris* Infections in Critically Ill Coronavirus Disease Patients, India, April–July 2020. *Emerg Infect Dis* **2020**, *26*, 2694–2696, doi:10.3201/eid2611.203504.

105. Williams, R.E.O. Healthy Carriage of *Staphylococcus aureus*: its prevalence and importance. *Bacteriol Rev* **1963**, *27*, 56–71.

106. Kloos, W.E.; Musselwhite, M.S. Distribution and Persistence of S*taphylococcus* and *Micrococcus* Species and Other Aerobic Bacteria on Human Skin1. *Appl Microbiol* **1975**, *30*, 381–395.

107. *Staphylococcus aureus* Infections | NEJM Available online: https://www.nejm.org/doi/10.1056/NEJM199808203390806?url_ver=Z39.88-2003&rfr_id=ori:rid:crossref.org&rfr_dat=cr_pub%20%200pubmed (accessed on 9 August 2022).

108. Foster, T.J. The *Staphylococcus aureus* "Superbug." *J Clin Invest* **2004**, *114*, 1693–1696, doi:10.1172/JCI200423825.

109. Grundmann, H.; Aires-de-Sousa, M.; Boyce, J.; Tiemersma, E. Emergence and Resurgence of Meticillin-Resistant *Staphylococcus aureus* as a Public-Health Threat. *The Lancet* **2006**, *368*, 874–885, doi:10.1016/S0140-6736(06)68853-3.

110. Foster, T.J. Immune Evasion by *Staphylococci. Nat Rev Microbiol* **2005**, *3*, 948–958, doi:10.1038/nrmicro1289.

111. Manders, S.M. Toxin-Mediated Streptococcal and Staphylococcal Disease. *Journal of the American Academy of Dermatology* **1998**, *39*, 383–398, doi:10.1016/S0190-9622(98)70314-7.

112. Rooijakkers, S.H.M.; Kessel, K.P.M. van; Strijp, J.A.G. van Staphylococcal Innate Immune Evasion. *Trends in Microbiology* **2005**, *13*, 596–601, doi:10.1016/j.tim.2005.10.002.

113. Kaplan, J.B.; Mlynek, K.D.; Hettiarachchi, H.; Alamneh, Y.A.; Biggemann, L.; Zurawski, D.V.; Black, C.C.; Bane, C.E.; Kim, R.K.; Granick, M.S. Extracellular Polymeric Substance (EPS)-Degrading Enzymes Reduce Staphylococcal Surface Attachment and Biocide Resistance on Pig Skin in Vivo. *PLoS One* **2018**, *13*, e0205526, doi:10.1371/journal.pone.0205526.

114. Donlan, R.M. Biofilms: Microbial Life on Surfaces. *Emerg Infect Dis* **2002**, *8*, 881–890, doi:10.3201/eid0809.020063.

115. Idrees, M.; Mohammad, A.R.; Karodia, N.; Rahman, A. Multimodal Role of Amino Acids in Microbial Control and Drug Development. *Antibiotics (Basel)* **2020**, *9*, 330, doi:10.3390/antibiotics9060330.

116. Ji, G.; Beavis, R.; Novick, R.P. Bacterial Interference Caused by Autoinducing Peptide Variants. *Science* **1997**, *276*, 2027–2030, doi:10.1126/science.276.5321.2027.

117. Otto, M.; Echner, H.; Voelter, W.; Götz, F. Pheromone Cross-Inhibition between *Staphylococcus aureus* and *Staphylococcus epidermidis*. *Infect Immun* **2001**, *69*, 1957–1960, doi:10.1128/IAI.69.3.1957-1960.2001.

118. Olson, M.E.; Todd, D.A.; Schaeffer, C.R.; Paharik, A.E.; Van Dyke, M.J.; Büttner, H.; Dunman, P.M.; Rohde, H.; Cech, N.B.; Fey, P.D.; et al. *Staphylococcus epidermidis* Agr Quorum-Sensing System: Signal Identification, Cross Talk, and Importance in Colonization. *J Bacteriol* **2014**, *196*, 3482–3493, doi:10.1128/JB.01882-14.

119. Novick, R.P.; Ross, H.F.; Projan, S.J.; Kornblum, J.; Kreiswirth, B.; Moghazeh, S. Synthesis of Staphylococcal Virulence Factors Is Controlled by a Regulatory RNA Molecule. *EMBO J* **1993**, *12*, 3967–3975.

120. Berube, B.J.; Bubeck Wardenburg, J. *Staphylococcus aureus* α-Toxin: Nearly a Century of Intrigue. *Toxins (Basel)* **2013**, *5*, 1140–1166, doi:10.3390/toxins5061140.

121. Xiong, Y.Q.; Willard, J.; Yeaman, M.R.; Cheung, A.L.; Bayer, A.S. Regulation of *Staphylococcus aureus* α-Toxin Gene (Hla) Expression by Agr, SarA and Sae In Vitro and in Experimental Infective Endocarditis. *The Journal of Infectious Diseases* **2006**, *194*, 1267–1275, doi:10.1086/508210.

122. Todd, O.A.; Fidel, P.L.; Harro, J.M.; Hilliard, J.J.; Tkaczyk, C.; Sellman, B.R.; Noverr, M.C.; Peters, B.M. *Candida albicans* Augments *Staphylococcus aureus* Virulence by Engaging the Staphylococcal Agr Quorum Sensing System. *mBio* **2019**, *10*, e00910-19, doi:10.1128/mBio.00910-19.

123. Chen, H.; Fujita, M.; Feng, Q.; Clardy, J.; Fink, G.R. Tyrosol Is a Quorum-Sensing Molecule in *Candida albicans*. *Proc Natl Acad Sci U S A* **2004**, *101*, 5048–5052, doi:10.1073/pnas.0401416101.

124. HAZEN, K.C.; CUTLER, J.E. Isolation and Purification of Morphogenic Autoregulatory Substance Produced by *Candida albicans*. *The Journal of Biochemistry* **1983**, *94*, 777–783, doi:10.1093/oxfordjournals.jbchem.a134419.

125. Ghosh, S.; Kebaara, B.W.; Atkin, A.L.; Nickerson, K.W. Regulation of Aromatic Alcohol Production in *Candida albicans*. *Applied and Environmental Microbiology* **2008**, *74*, 7211–7218, doi:10.1128/AEM.01614-08.

126. Chauhan, N.M.; Raut, J.S.; Karuppayil, S.M. A Morphogenetic Regulatory Role for Ethyl Alcohol in *Candida albicans*. *Mycoses* **2011**, *54*, e697–e703, doi:10.1111/j.1439-0507.2010.02002.x.

127. Weber, K.; Sohr, R.; Schulz, B.; Fleischhacker, M.; Ruhnke, M. Secretion of E,E-Farnesol and Biofilm Formation in Eight Different *Candida* Species. *Antimicrob Agents Chemother* **2008**, *52*, 1859–1861, doi:10.1128/AAC.01646-07.

128. Ramage, G.; Saville, S.P.; Wickes, B.L.; López-Ribot, J.L. Inhibition of *Candida albicans* Biofilm Formation by Farnesol, a Quorum-Sensing Molecule. *Appl Environ Microbiol* **2002**, *68*, 5459–5463, doi:10.1128/AEM.68.11.5459-5463.2002.

129. Kebaara, B.W.; Langford, M.L.; Navarathna, D.H.M.L.P.; Dumitru, R.; Nickerson, K.W.; Atkin, A.L. *Candida albicans* Tup1 Is Involved in Farnesol-Mediated Inhibition of Filamentous-Growth Induction. *Eukaryot Cell* **2008**, *7*, 980–987, doi:10.1128/EC.00357-07.

130. Davis-Hanna, A.; Piispanen, A.E.; Stateva, L.I.; Hogan, D.A. Farnesol and Dodecanol Effects on the *Candida albicans* Ras1-CAMP Signalling Pathway and the Regulation of Morphogenesis. *Mol Microbiol* **2008**, *67*, 47–62, doi:10.1111/j.1365-2958.2007.06013.x.

131. Kruppa, M.; Krom, B.P.; Chauhan, N.; Bambach, A.V.; Cihlar, R.L.; Calderone, R.A. The Two-Component Signal Transduction Protein Chk1p Regulates Quorum Sensing in *Candida albicans*. *Eukaryotic Cell* **2004**, *3*, 1062–1065, doi:10.1128/EC.3.4.1062-1065.2004.

132. Sato, T.; Watanabe, T.; Mikami, T.; Matsumoto, T. Farnesol, a Morphogenetic Autoregulatory Substance in the Dimorphic Fungus *Candida albicans*, Inhibits Hyphae Growth through Suppression of a Mitogen-Activated Protein Kinase Cascade. *Biological and Pharmaceutical Bulletin* **2004**, *27*, 751–752, doi:10.1248/bpb.27.751.

133. Toke, D.A.; Bennett, W.L.; Oshiro, J.; Wu, W.-I.; Voelker, D.R.; Carman, G.M. Isolation and Characterization of the *Saccharomyces Cerevisiae* LPP1 Gene Encoding a Mg2+-Independent Phosphatidate Phosphatase *. *Journal of Biological Chemistry* **1998**, *273*, 14331–14338, doi:10.1074/jbc.273.23.14331.

134. Navarathna, D.H.M.L.P.; Hornby, J.M.; Krishnan, N.; Parkhurst, A.; Duhamel, G.E.; Nickerson, K.W. Effect of Farnesol on a Mouse Model of Systemic Candidiasis, Determined by Use of a DPP3 Knockout Mutant of *Candida albicans*. *Infect Immun* **2007**, *75*, 1609–1618, doi:10.1128/IAI.01182-06.

135. Henriques, M.; Martins, M.; Azeredo, J.; Oliveira, R. Effect of Farnesol on *Candida dubliniensis* Morphogenesis. *Letters in Applied Microbiology* **2007**, *44*, 199–205, doi:10.1111/j.1472-765X.2006.02044.x.

136. Martins, M.; Henriques, M.; Azeredo, J.; Rocha, S.M.; Coimbra, M.A.; Oliveira, R. Morphogenesis Control in *Candida albicans* and *Candida dubliniensis* through Signaling

Molecules Produced by Planktonic and Biofilm Cells. *Eukaryotic Cell* **2007**, *6*, 2429–2436, doi:10.1128/EC.00252-07.

137. Jabra-Rizk, M.A.; Shirtliff, M.; James, C.; Meiller, T. Effect of Farnesol on *Candida dubliniensis* Biofilm Formation and Fluconazole Resistance. *FEMS Yeast Research* **2006**, *6*, 1063–1073, doi:10.1111/j.1567-1364.2006.00121.x.

138. Machida, K.; Tanaka, T.; Fujita, K.; Taniguchi, M. Farnesol-Induced Generation of Reactive Oxygen Species via Indirect Inhibition of the Mitochondrial Electron Transport Chain in the Yeast *Saccharomyces cerevisiae*. *J Bacteriol* **1998**, *180*, 4460–4465.

139. Machida, K.; Tanaka, T. Farnesol-Induced Generation of Reactive Oxygen Species Dependent on Mitochondrial Transmembrane Potential Hyperpolarization Mediated by F0F1-ATPase in Yeast. *FEBS Letters* **1999**, *462*, 108–112, doi:10.1016/S0014-5793(99)01506-9.

140. Gomes, F.I.A.; Teixeira, P.; Azeredo, J.; Oliveira, R. Effect of Farnesol on Planktonic and Biofilm Cells of *Staphylococcus epidermidis*. *Curr Microbiol* **2009**, *59*, 118–122, doi:10.1007/s00284-009-9408-9.

141. Koo, H.; Pearson, S.K.; Scott-Anne, K.; Abranches, J.; Cury, J.A.; Rosalen, P.L.; Park, Y.K.; Marquis, R.E.; Bowen, W.H. Effects of Apigenin and Tt-Farnesol on Glucosyltransferase Activity, Biofilm Viability and Caries Development in Rats. *Oral Microbiology and Immunology* **2002**, *17*, 337–343, doi:10.1034/j.1399-302X.2002.170602.x.

Chapter 2 - Determination of the hyphal inhibitory efficacy of GAs in *Candida albicans* using the mouse model of disseminated candidiasis

2.1 Abstract

Yeast to hypha transition is one among the several virulence factors in *C. albicans* causing pathogenesis in human. Compounds known to inhibit this transition are potential antifungal agents that do not allow the tissue invasion by the fungus. Gymnemic acid (GAs) is a small molecule known to inhibit hyphal formation in *in vitro* under hypha inducing environment. However, efficacy of GAs has not been tested in a mammalian *in vivo* model. Hence, we wanted to test the efficacy of GAs in a mouse model of systemic candidiasis. Since GAs was shown to be non-toxic to mammalian cell lines *in vitro* and worked effectively in *C. elegans* model, we hypothesized that treatment of *C. albicans* infected mice with GAs will rescue diseased mice or extend the survival time of infected mice without causing cytotoxic effect. For this study, we used intravenous route via tail vein to infect mice and treated them with GAs via intraperitoneal route. We used female mice for our experiments as vulvovaginal candidiasis is common in women. Interestingly, we observed that GAs treatment rescued diseased mice while mice without treatment died. The survival of infected mice in the presence of GAs corresponded with clearance of fungal burden in kidney tissues and is possibly due to GAs mediated block of hyphal cells preventing the spread of fungus.

2.2 Introduction

Candida infection in blood is often misdiagnosed as bacteremia resulting in delayed diagnosis and hence leading to higher mortality rates as delayed diagnosis along with antifungal resistance worsen the situation [1–3]. So, it is important to establish a model system to understand candidiasis infection, its prognosis, establishment, and dissemination into host body. Such understanding will be useful in identifying early diagnosis and developing effective therapeutic measures to prevent the occurrence and spread of *Candida*. Animal models have been used as a powerful tool in biological research for studying infections and diseases. Several non-mammalian mini-host models such as flies and worms have been used for studying fungal pathogenesis [4]. However, the mammalian hosts are genetically close to humans and provide a better understanding of the disease. Compared to large mammals such as pigs and rabbits, small mammal like mice is widely used because of their cost-effectiveness, ease to handle, and availability. Mice models have been extensively used and well established for candidiasis such as disseminated, oropharyngeal, vaginal, and cutaneous [5–8].

C. albicans, being the lead cause of systemic candidiasis, has been used to establish candidiasis disease in a mouse model. As *C. albicans* usually colonize on immunosuppressed individuals, candidiasis models have been established in both immunocompetent and immunosuppressed mice models [5]. The intravenous infection model is a widely used model where *Candida* cells are injected into the mouse bloodstream via the lateral tail vein. Fungal cells then go to the kidney, brain, and other body parts resulting in sepsis followed by death. This model represents dissemination of *Candida* through wounds, gut, or implants, into the blood which further spreads to other body parts [9–12].

Currently available antifungals such as fluconazole and Amphotericin B are widely used to treat candidiasis [13,14]. These antifungals are often combined with compounds with potential synergistic effects to increase their antifungal efficacy [15,16]. However, antifungal resistance has been a huge issue lately and the need of developing new antifungals is of huge necessity.

Morphogenetic switch from yeast to hypha and hyphal growth is one of the major virulence factors in *C. albicans* which results in the invasive candidiasis affecting vital body parts when the host immune system is compromised. Inhibition of this morphogenetic switch attenuates virulence in mice models [17,18]. Gymnemic acid (GAs), a triterpene compound known to inhibit hyphal formation, is a potential antifungal compound. Efficacy of GAs has been tested earlier using the non-mammalian host *Caenorhabditis elegans*. *C. albicans* fed larvae grown with and without GAs showed that GAs rescued *C. elegans* infected with *C. albicans* by inhibiting hypha formation [19]. However, the efficacy of GAs has not been studied using a mammalian host model. In this study, we determine the effect of GAs in a mouse model of invasive candidiasis.

2.3 Materials and methods

2.3.1 Ethics statement

Animal experiments were performed at the Comparative Medicine Group animal facility of the Kansas State University with prior approval from Institutional Animal Care and Use Committee (IACUC) of Kansas State University (IACUC Protocol Number: 3888.1). Animals were placed in cages with enough water and mouse chow. Animals showing disease symptoms such as hunched posture, reduced activity, and weight loss more than 20%, were euthanized using deep isoflurane anesthesia followed by cervical dislocation.

2.3.2 Strain, growth conditions, and GAs

C. albicans SC5314 strain (genome sequenced) was routinely maintained in Yeast Peptone Dextrose (YPD) agar. A single colony of *C. albicans* was inoculated into YPD broth and grown at 30 ^{o}C overnight by shaking. Cells were harvested by centrifugation, washed with PBS (Phosphate buffer saline), and resuspended in PBS. GAs were purified from medicinal plant *Gymnema sylvestre* as described earlier [19]. GAs used in our experiments consisted of mixture of GA including GA-III, GA-IV, GA-XIII, GA-XIV, and GA-I. These GA species showed bioactivity as mentioned earlier [19,20]. GAs mixture powder was suspended in sterile PBS as 50 mg/mL stock solution and diluted as required for the experiments.

2.3.3 Inoculation

Female Balb/c mice of age 8-9 weeks old were divided into three groups: *C. albicans* only (disease control), GAs only (GAs control), and *C. albicans* with GAs (test group). Four mice were used per group for handling purpose and experiment was repeated twice. *C. albicans* strain SC5314 grown at 30 ^{o}C in YPD media as yeast form was collected and washed with PBS. 2 x10^5 cells were adjusted in 100 μL PBS and injected intravenously by lateral tail vein injection to both disease control mice and test group mice. GAs (400 μg/100 μL) were injected to GAs control mice group and test mice group via tail vein on the first day then via intraperitoneal route for remaining seven days. Overall schematic is presented in **Figure 2.1**.

2.3.4 Determination of CFU from kidney

One kidney from each mouse was used for CFU and the other kidney was used for histopathology analysis. Kidneys obtained from mice were weighed, homogenized in PBS, and serially diluted. Diluted fractions were plated on YPD agar plates containing 10 μg/mL chloramphenicol (Sigma) and 50 μg/mL kanamycin (Sigma) to inhibit bacterial growth. Plates were incubated at 30 ^{o}C overnight and the number of *C. albicans* colonies on the plates was counted.

2.3.5 Histopathology

Kidneys from control and GAs treated mice were fixed immediately after harvest in 10% formalin. Tissues were embedded in paraffin, sectioned, and stained using hematoxylin and eosin (H&E) stain and Grocott's methenamine silver (GMS) stain. Stained tissue sections were then imaged using a camera on Olympus U-TV0.5XC-3 microscope. Histopathology analyses were performed at the KSDVL (Kansas State Veterinary Diagnostic Laboratory) and scored blindly by a pathologist.

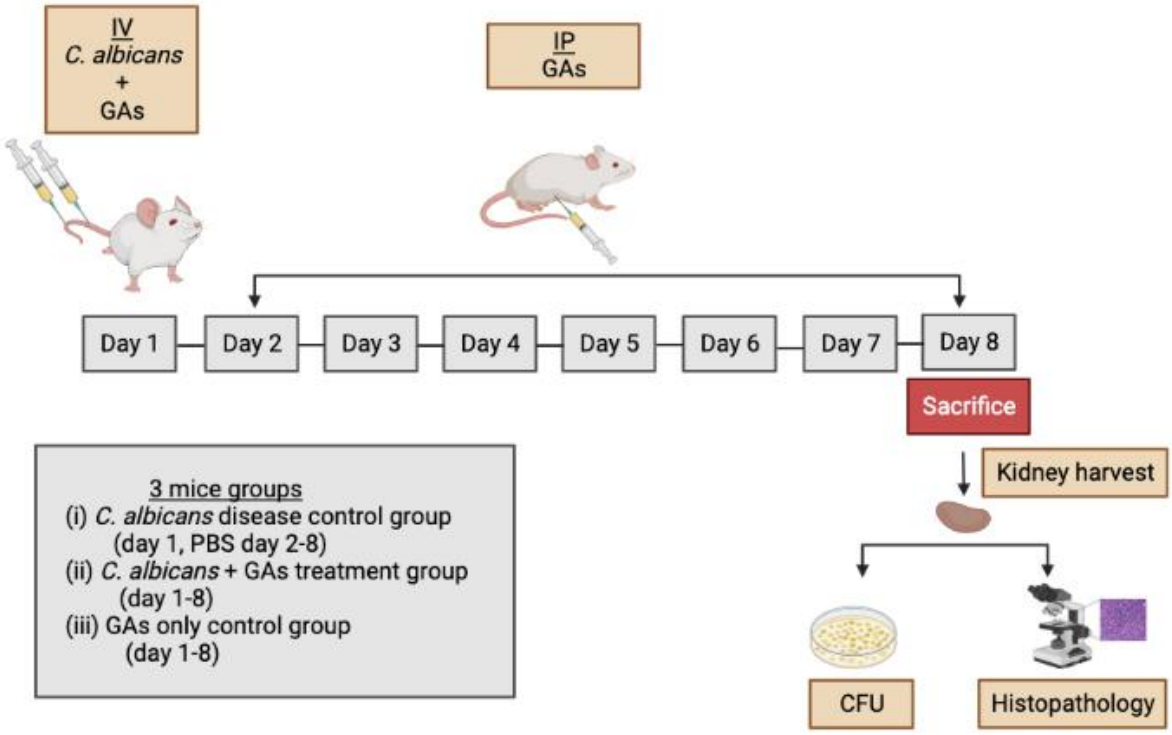

Figure 2.1. Schematic of experimental design to determine the efficacy of GAs in a mouse model of disseminated candidiasis.

Experiment was carried out for eight days to determine the efficacy of GAs followed by survival and pathological analysis. IV-Intravenous; IP-Intraperitoneal. Created in Biorender.com.

2.3.6 Statistical analysis

GraphPad Prism version 7.0 was used to perform statistical analysis to calculate significance between control and GAs treated mice groups. The graphs shown are a representation of two identical separate experiments.

2.4 Results

2.4.1 GAs treatment rescued *C. albicans* infected mice

We tested the efficacy of GAs using mice as a mammalian host model. As the compound is effective in the nematode model of *C. albicans* infection, we hypothesized that GAs would rescue *C. albicans*-infected mice. Consistent with previous studies, by day three, all mice infected with *C. albicans* via tail vein started developing hunched posture with reduced weight and were euthanized. However, the mice treated with GAs at the time of infection and every subsequent day survived until day 8 when mice were sacrificed **(Figure 2.2)**.

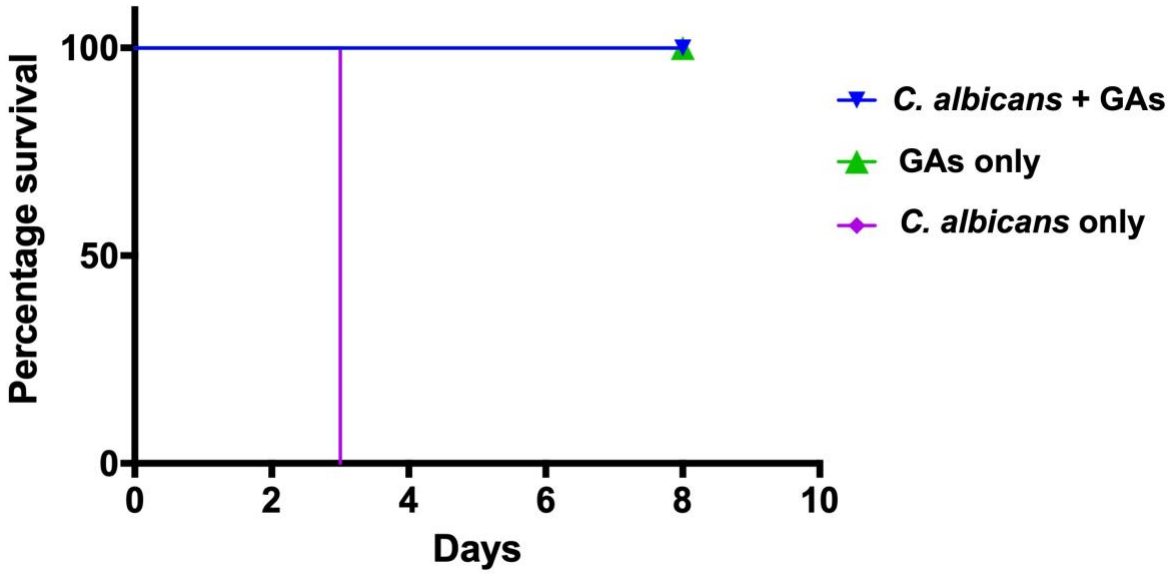

Figure 2.2. GAs rescue *C. albicans* infected mice.

The survival of *C. albicans* infected mice treated with GAs is shown by Kaplan-Meier survival curve. Mice were inoculated with 2 x10^5 *C. albicans* (SC5314) cells directly into the bloodstream via lateral tail vein injection. GAs (400 μg/100 μL) were injected via tail vein on the first day, and then via intraperitoneal route for the remaining seven days. Conditions of mice were assessed daily, and mice that developed disease symptoms such as hunched posture and reduced body weight were sacrificed. Rest of the healthy mice that were treated with GAs were sacrificed at the end of day 8. The mice treated with GAs (blue, inverted triangle), or mice injected with GAs only (compound control, green triangle) survived 100% at the end of the experiment (8 days) as compared to an untreated group (purple, disease control) that died within

day 3 of the experiment. Data were analyzed by Log-rank (Mantel-Cox) test and were statistically significant (P-value = 0.003).

2.4.2 *Candida* infection corresponds to the weight loss in sick animals

The weight of the mice correlates with the progression of the disease. Weights were recorded every day from the start of the experiment until the end, and we found a significant decrease in the weight of infected mice compared to the GAs only control mice group **(Figure 2.3)**.

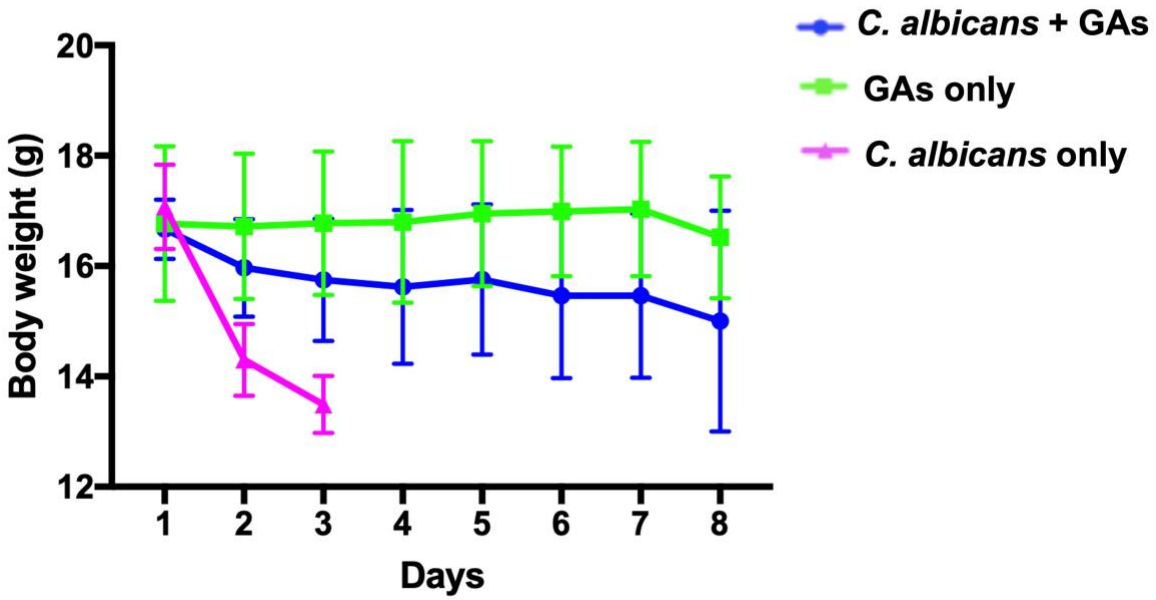

Figure 2.3. GAs lowers the virulence level in *C. albicans* infected mice.

The weights of control and GAs treated mice were measured every day from day 1 to day 8 and plotted in the graph using GraphPad Prism. The level of disease progression correlates to weight loss in mice.

2.4.3 Absence of fungal burden in GAs treated mice correlates with their survival

We performed histopathological analysis using kidney tissues from diseased and GAs treated mice to determine the impact of *C. albicans* on mice. Microscopic analysis of the GMS-

stained tissue section showed spreading of fungal cells in the cortex region of the kidney **(Figure 2.4, top panel)** and H&E stained section showed neutrophil infiltration corresponding to the fungus infected areas of the kidney tissues of diseased mice **(Figure 2.4, lower panel)**. On contrary, the mice that received GAs treatment were cleared of fungal burden and had a reduced or absence of neutrophil infiltration. The GAs alone control group showed kidney histology similar to the treated group.

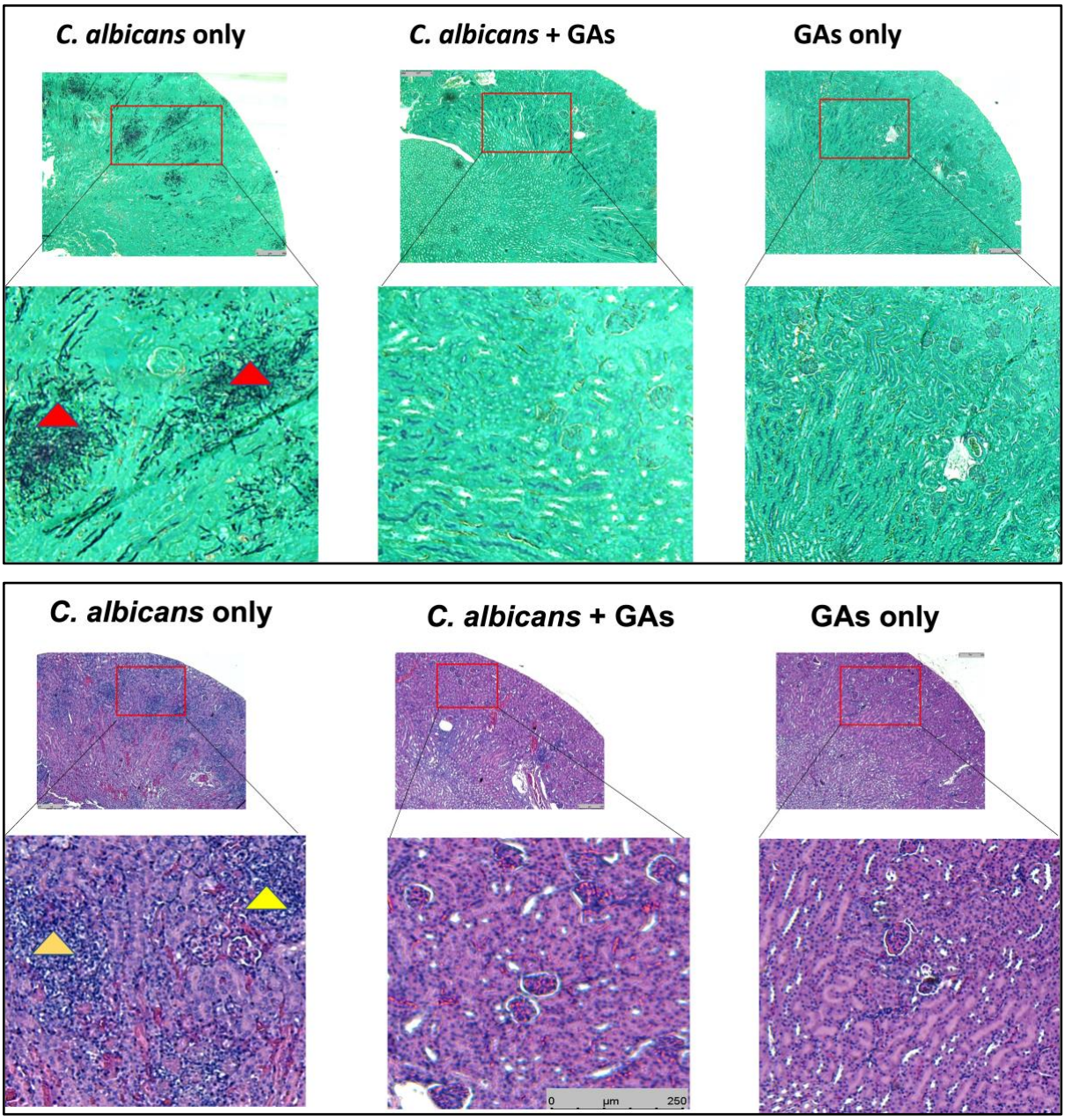

Figure 2.4. Histopathological analyses of kidney sections from diseased, GAs control, and GAs treated test mice groups.

GMS stained (Upper panel) and H&E stained (Lower panel). Neutrophil infiltration in *C. albicans* infected kidney tissue. Red triangle represents fungal cells (fungal yeast & hyphae stained as black, upper panel) and yellow triangle represents neutrophil infiltration around fungus infected areas (stained as blue, lower panel). These symptoms are absent in the treated group or GAs only control group. Regions from square are magnified for better visualization of fungal burden. Scale bar shown applies to both GMS and H&E stained sections.

2.4.4 The CFU analysis correlates with the histopathology results

To verify the histopathology results, we performed CFU analysis of the kidney tissues from diseased and GAs treated mice. As observed in histopathological analysis, we saw a significantly reduced burden of *C. albicans* in GAs treated mice when compared to the diseased control mice group **(Figure 2.5)**.

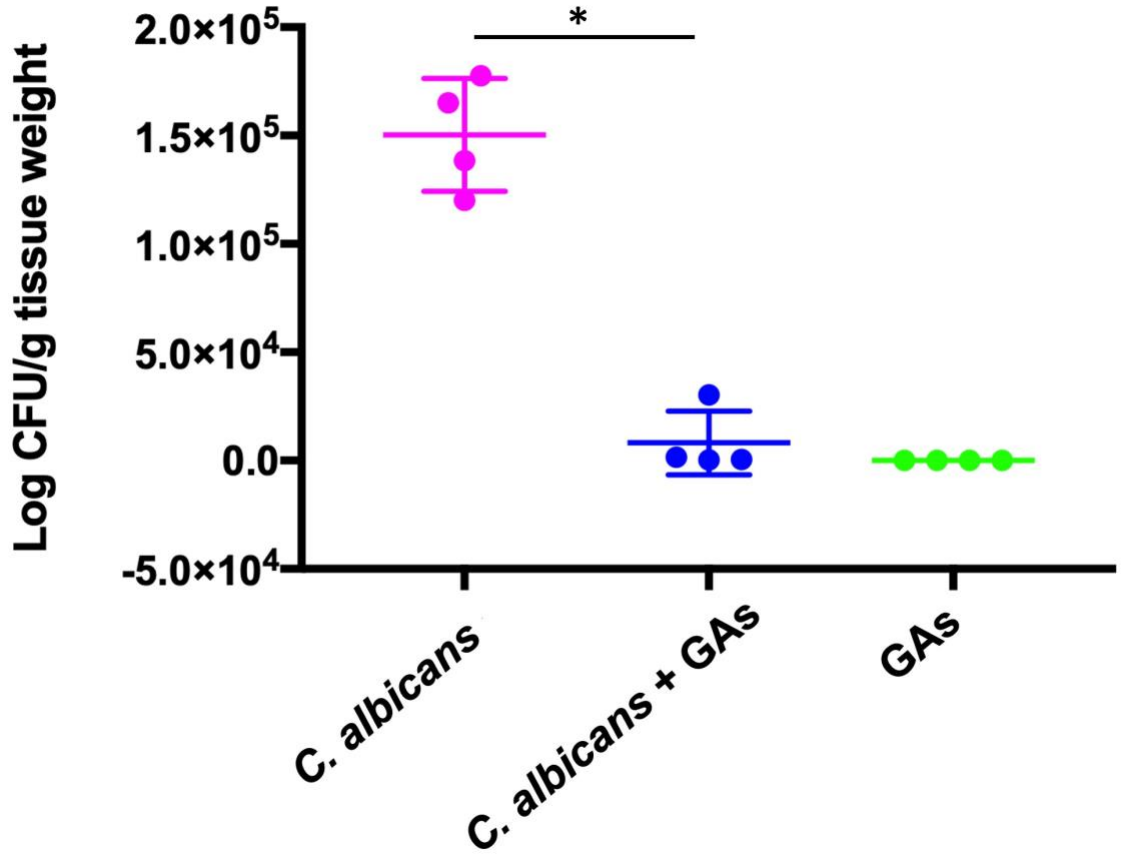

Figure 2.5. CFU analysis of *C. albicans* in control and GAs treated mice.

Graph depicting *C. albicans* colonies from kidney tissue (CFU/g tissue). Kidneys harvested from euthanized mice were grinded in PBS buffer followed by serial dilutions. Diluted kidney extracts were then plated on YPD agar plates. Agar plates were incubated at 30 ºC overnight and the number of colonies grown on the plates were counted. Colony forming units were calculated based on number of colonies, weight of kidney, dilution factor, and volume of extract plated. The Mann-Whitney two-tailed test was applied to determine the significance between disease control and GAs treated mice * ($p<0.001$). Each dot represents one kidney from single mice.

2.5 Discussion

The existing tug of war between rapidly evolving microbes and developing new antimicrobials is a never-ending process. Due to increasing resistance to few available antifungals and the side effects of these drugs in immunocompromised patients, targeting the virulence factors instead of targeting pathogen proliferation, could be an alternative strategy for identifying a new class of drug against pathogenic fungi [21,22]. The transition from yeast to hypha is one of the major virulence factors in *C. albicans* causing pathogenesis in humans. Compounds or drugs that are able to inhibit such morphogenetic switch can be potential antifungal agents capable of lowering pathogenesis [23,24]. Gymenmic acid, a plant derived non-toxic compound is a potential antifungal agent known to target the morphogenetic switch in *C. albicans* by inhibiting yeast to hypha conversion and hyphal growth [19]. In this study, the effectiveness of GAs against *C. albicans* was tested using systemic candidiasis mice model.

Several *in vivo* studies done in the past have highlighted that the hyphal forms are required for causing invasive pathogenesis and inhibiting *C. albicans* hyphal formation during early infection period significantly decreased virulence in the host [17,25–27]. In order to verify if survival data corresponds to the degree of pathogenesis inside the body, histopathological analysis of the kidney tissue was carried out. Fungal cells appear as black after staining kidney tissue sections of infected mice with GMS **(Figure 2.4, upper panel)**, along with neutrophil infiltration observed with H&E staining (lower panel), matched our survival data. The diseased mice group showed symptoms within a couple of days of infection and died. Such fungal cells and neutrophil infiltration were not observed in the kidney tissue sections of GAs treated mice and these mice survived until the end of the experiment **(Figures 2.2 and 2.4)**. The staining results are correlated with CFU analysis done using kidney tissue where kidney of GAs treated

mice had significantly less fungal burden as compared to the untreated diseased mice **(Figure 2.5)**. Also, disease progression in the mice led to the decline of body weight in infected mice. A slight decline in the weight of GAs treated mice can be because there may still *C. albicans* cells in the body yet to be cleared up and the animals may be still recovering. In addition to the inhibition of *C. albicans* yeast to hypha transition and hyphal growth, GAs also prevent its biofilm formation [19] because hyphae are required for biofilm growth. In a recent study with *C. albicans* and *Streptococcus gordonii* dual-species biofilms, GAs inhibited biofilm growth [20]. Since hyphal growth is an important virulence factor in *C. albicans* mediated pathogenesis, GAs' capacity to inhibit hyphal formation *in vivo* might have slowed or stopped disease progression and rescued the GAs treated mice.

The use of disseminated mouse model for systemic candidiasis is an established system to understand pathogenesis of disease and exploring treatment strategies. The tail vein injection is a frequently used method to infect mice with *C. albicans* directly into the bloodstream which mimics bloodstream infection in humans during systemic candidiasis. However, one should note that mice are not the natural host for *C. albicans* and further considerations are needed before extrapolating experimental results from mice study to humans. Also, variation in immune systems among human and mice is important to note as it is challenging to engulf hyphal cells via macrophages, hence evading phagocytic killing [28–31].

In conclusion, our mice survival data correlated with histopathological and CFU analysis validated the effectiveness of GAs in mammalian model system by reducing virulence via inhibition of yeast to hypha switch and hyphal growth.

2.6 References

1. Morrell, M.; Fraser, V.J.; Kollef, M.H. Delaying the Empiric Treatment of *Candida* Bloodstream Infection until Positive Blood Culture Results Are Obtained: A Potential Risk Factor for Hospital Mortality. *Antimicrob Agents Chemother* **2005**, *49*, 3640–3645, doi:10.1128/AAC.49.9.3640-3645.2005.

2. Sanglard, D.; Odds, F.C. Resistance of *Candida* Species to Antifungal Agents: Molecular Mechanisms and Clinical Consequences. *The Lancet Infectious Diseases* **2002**, *2*, 73–85.

3. Ostrosky-Zeichner, L.; Rex, J.H.; Pappas, P.G.; Hamill, R.J.; Larsen, R.A.; Horowitz, H.W.; Powderly, W.G.; Hyslop, N.; Kauffman, C.A.; Cleary, J.; et al. Antifungal Susceptibility Survey of 2,000 Bloodstream *Candida* Isolates in the United States. *Antimicrob Agents Chemother* **2003**, *47*, 3149–3154, doi:10.1128/AAC.47.10.3149-3154.2003.

4. Chamilos, G.; Lionakis, M.S.; Lewis, R.E.; Kontoyiannis, D.P. Role of Mini-Host Models in the Study of Medically Important Fungi. *The Lancet Infectious Diseases* **2007**, *7*, 42–55.

5. Conti, H.R.; Huppler, A.R.; Whibley, N.; Gaffen, S.L. Animal Models for Candidiasis. *Curr Protoc Immunol* **2014**, *105*, 19.6.1-19.6.17, doi:10.1002/0471142735.im1906s105.

6. Clancy, C.J.; Cheng, S.; Nguyen, M.H. Animal Models of Candidiasis. In *Candida albicans: Methods and Protocols*; Cihlar, R.L., Calderone, R.A., Eds.; Methods in Molecular Biology; Humana Press: Totowa, NJ, 2009; pp. 65–76 ISBN 978-1-60327-151-6.

7. Yano, J.; Fidel, Jr., P.L. Protocols for Vaginal Inoculation and Sample Collection in the Experimental Mouse Model of *Candida vaginitis. J Vis Exp* **2011**, 3382, doi:10.3791/3382.

8. Solis, N.V.; Filler, S.G. Mouse Model of Oropharyngeal Candidiasis. *Nat Protoc* **2012**, *7*, 637–642, doi:10.1038/nprot.2012.011.

9. Louria, D.B.; Brayton, R.G.; Finkel, G. Studies on the Pathogenesis of Experimental *Candida albicans* Infections in Mice. *Sabouraudia* **1963**, *2*, 271–283, doi:10.1080/00362176385190431.

10. Papadimitriou, J.M.; Ashman, R.B. The Pathogenesis of Acute Systemic Candidiasis in a Susceptible Inbred Mouse Strain. *The Journal of Pathology* **1986**, *150*, 257–265, doi:10.1002/path.1711500405.

11. MacCallum, D.M.; Odds, F.C. Temporal Events in the Intravenous Challenge Model for Experimental *Candida albicans* Infections in Female Mice. *Mycoses* **2005**, *48*, 151–161, doi:10.1111/j.1439-0507.2005.01121.x.

12. Spellberg, B.; Ibrahim, A.S.; Edwards, J.E., Jr.; Filler, S.G. Mice with Disseminated Candidiasis Die of Progressive Sepsis. *The Journal of Infectious Diseases* **2005**, *192*, 336–343, doi:10.1086/430952.

13. Burgess, D.S.; Hastings, R.W.; Lewis, J.S. A Time-Kill Evaluation of Fluconazole and Amphotericin B against *Candida* Isolates. *Journal of Pharmacy Technology* **2000**, *16*, 102–106, doi:10.1177/875512250001600307.

14. Louie, A.; Liu, W.; Miller, D.A.; Sucke, A.C.; Liu, Q.-F.; Drusano, G.L.; Mayers, M.; Miller, M.H. Efficacies of High-Dose Fluconazole plus Amphotericin B and High-Dose Fluconazole plus 5-Fluorocytosine versus Amphotericin B, Fluconazole, and 5-Fluorocytosine Monotherapies in Treatment of Experimental Endocarditis, Endophthalmitis, and Pyelonephritis Due to *Candida albicans*. *Antimicrob Agents Chemother* **1999**, *43*, 2831–2840.

15. Zhou, Y.; Yang, H.; Zhou, X.; Luo, H.; Tang, F.; Yang, J.; Alterovitz, G.; Cheng, L.; Ren, B. Lovastatin Synergizes with Itraconazole against Planktonic Cells and Biofilms of *Candida albicans* through the Regulation on Ergosterol Biosynthesis Pathway. *Appl Microbiol Biotechnol* **2018**, *102*, 5255–5264, doi:10.1007/s00253-018-8959-8.

16. Garcia-Gomes, A.S.; Curvelo, J.A.R.; Soares, R.M.A.; Ferreira-Pereira, A. Curcumin Acts Synergistically with Fluconazole to Sensitize a Clinical Isolate of *Candida albicans* Showing a MDR Phenotype. *Medical Mycology* **2012**, *50*, 26–32, doi:10.3109/13693786.2011.578156.

17. Lo, H.-J.; Köhler, J.R.; DiDomenico, B.; Loebenberg, D.; Cacciapuoti, A.; Fink, G.R. Nonfilamentous *C. albicans* Mutants Are Avirulent. *Cell* **1997**, *90*, 939–949, doi:10.1016/S0092-8674(00)80358-X.

18. Noble, S.M.; French, S.; Kohn, L.A.; Chen, V.; Johnson, A.D. Systematic Screens of a *Candida albicans* Homozygous Deletion Library Decouple Morphogenetic Switching and Pathogenicity. *Nat Genet* **2010**, *42*, 590–598, doi:10.1038/ng.605.

19. Vediyappan, G.; Dumontet, V.; Pelissier, F.; d'Enfert, C. Gymnemic Acids Inhibit Hyphal Growth and Virulence in *Candida albicans*. *PLoS One* **2013**, *8*, e74189, doi:10.1371/journal.pone.0074189.

20. Veerapandian, R.; Vediyappan, G. Gymnemic Acids Inhibit Adhesive Nanofibrillar Mediated Streptococcus Gordonii–*Candida albicans* Mono-Species and Dual-Species Biofilms. *Front Microbiol* **2019**, *10*, 2328, doi:10.3389/fmicb.2019.02328.

21. Allen, R.C.; Popat, R.; Diggle, S.P.; Brown, S.P. Targeting Virulence: Can We Make Evolution-Proof Drugs? *Nat Rev Microbiol* **2014**, *12*, 300–308, doi:10.1038/nrmicro3232.

22. Clatworthy, A.E.; Pierson, E.; Hung, D.T. Targeting Virulence: A New Paradigm for Antimicrobial Therapy. *Nat Chem Biol* **2007**, *3*, 541–548, doi:10.1038/nchembio.2007.24.

23. Jacobsen, I.D.; Wilson, D.; Wächtler, B.; Brunke, S.; Naglik, J.R.; Hube, B. *Candida albicans* Dimorphism as a Therapeutic Target. *Expert Review of Anti-infective Therapy* **2012**, *10*, 85–93, doi:10.1586/eri.11.152.

24. Vila, T.; Romo, J.A.; Pierce, C.G.; McHardy, S.F.; Saville, S.P.; Lopez-Ribot, J.L. Targeting *Candida albicans* Filamentation for Antifungal Drug Development. *Virulence* **2016**, *8*, 150–158, doi:10.1080/21505594.2016.1197444.

25. Saville, S.P.; Lazzell, A.L.; Monteagudo, C.; Lopez-Ribot, J.L. Engineered Control of Cell Morphology In Vivo Reveals Distinct Roles for Yeast and Filamentous Forms of *Candida albicans* during Infection. *Eukaryot Cell* **2003**, *2*, 1053–1060, doi:10.1128/EC.2.5.1053-1060.2003.

26. Carlisle, P.L.; Banerjee, M.; Lazzell, A.; Monteagudo, C.; López-Ribot, J.L.; Kadosh, D. Expression Levels of a Filament-Specific Transcriptional Regulator Are Sufficient to Determine *Candida albicans* Morphology and Virulence. *Proc Natl Acad Sci U S A* **2009**, *106*, 599–604, doi:10.1073/pnas.0804061106.

27. Saville, S.P.; Lazzell, A.L.; Bryant, A.P.; Fretzen, A.; Monreal, A.; Solberg, E.O.; Monteagudo, C.; Lopez-Ribot, J.L.; Milne, G.T. Inhibition of Filamentation Can Be Used To Treat Disseminated Candidiasis. *Antimicrob Agents Chemother* **2006**, *50*, 3312–3316, doi:10.1128/AAC.00628-06.

28. Dubos, R.J.; Savage, D.C.; Schaedler, R.W. The Indigenous Flora of the Gastrointestinal Tract. *Dis Colon Rectum* **1967**, *10*, 23–34, doi:10.1007/BF02617382.

29. Rehli, M. Of Mice and Men: Species Variations of Toll-like Receptor Expression. *Trends Immunol* **2002**, *23*, 375–378, doi:10.1016/s1471-4906(02)02259-7.

30. Gibbons, D.L.; Spencer, J. Mouse and Human Intestinal Immunity: Same Ballpark, Different Players; Different Rules, Same Score. *Mucosal Immunol* **2011**, *4*, 148–157, doi:10.1038/mi.2010.85.

31. Bain, J.M.; Alonso, M.F.; Childers, D.S.; Walls, C.A.; Mackenzie, K.; Pradhan, A.; Lewis, L.E.; Louw, J.; Avelar, G.M.; Larcombe, D.E.; et al. Immune Cells Fold and Damage Fungal Hyphae. *Proceedings of the National Academy of Sciences* **2021**, *118*, e2020484118, doi:10.1073/pnas.2020484118.

Chapter 3 - Identification of Nrg1p and Ume6p associated proteins during the inhibition of yeast to hyphal transition and hyphal growth in *Candida albicans*

3.1 Abstract

The major fungal pathogen of humans, *Candida albicans* is characterized by its ability to switch from oval yeast cells to tubular hyphae, a process critical for its virulence. Gymnemic acids (GAs), a family of triterpenoid compounds extracted from *Gymnema sylvestre* plant, inhibited the yeast to hypha conversion and hyphal growth *in C. albicans*. Preliminary genetic and gene expression studies showed that GAs act through *NRG1* and *UME6* transcriptional regulators. *UME6* and *NRG1* are positive and negative regulators of *C. albicans* hyphal growth, respectively. *Nrg1-/-* mutants grow into the hyphal form under yeast inducing conditions whereas *ume6 -/-* mutants are defective in hyphal extension. We hypothesized that GAs modulate the interactions of cognate partner proteins with Nrg1p and Ume6p and could disrupt the processes required for yeast to hypha conversion and hyphal growth. In this study, *C. albicans* expressing Tandem Affinity Purification (TAP) tag fused with Nrg1p (P_{PCK1}-*NRG1-TAP*) and Ume6p (P_{PCK1}-*UME6-TAP*) were grown under hypha-inducing conditions in the presence and absence of GAs, and the interacting proteins were affinity purified and identified by LC-MS/MS. We obtained 27 significant proteins co-purified with Nrg1p in absence of GAs and 168 proteins in the presence of GAs. Similarly, we found 19 significant proteins co-purified with Ume6p in the absence of GAs and 142 proteins in the presence of GAs. Classification based on biological functions revealed several DNA binding proteins including Mig1, Mis1, Bre1, and Ade12. Similarly, proteins playing a role in filamentation such as Hmo1 and Ras1 were significantly

different in the presence and absence of GAs. We also found proteins involved in the Hog1 mediated mitogen activated protein kinase (MAPK) pathway and we speculate that GAs inhibit filamentation via MAP kinase pathway. Decreased expression of genes encoding some of these proteins were also verified from gene expression (RNA Seq) studies. In addition, we obtained many ribosomal proteins in GAs treated *C. albicans* compared to control. Reporter fusion assays confirmed the promoter of *NRG1* is upregulated and *UME6* is downregulated in GAs treated sample which may lead to hyphal growth inhibition. Also, GAs inhibited binding of Nrg1p to the promoter of a hypha-specific gene, *ALS3*. Hence, the proteomic approach helped us broaden the knowledge of Nrg1p and Ume6p mediated yeast-hypha morphogenetic changes in the presence and absence of GAs.

3.2 Introduction

C. albicans normally lives as a commensal but it becomes pathogenic when the host becomes immunocompromised. *C. albicans* can cause superficial skin infections, oral thrush or vaginal thrush and affect quality of life. When it reaches to blood, it causes a condition known as candidemia which can lead to death [1–3]. Frequency of fungal infections is increasing as population of immunocompromised patients is rising due to increase in number of HIV-infected patients, organ transplant recipients, cancer patients receiving chemotherapy etc. Reversible morphogenetic switching from yeast to hyphae is an important virulence trait [4]. Both yeast and hyphal forms are important for establishment of infection. Hyphal forms are thought to be important for invasion into host tissues and yeast forms are thought to be important for initial colonization and dispersal through bloodstream after invasion [5–7]. Locking in either yeast or

hyphal form leads to attenuation of virulence in mouse models of systemic candidiasis [5,6,8]. Yeast to hyphae conversion is induced by various environmental conditions including 37 °C temperature, neutral to alkaline pH, serum, nutrient starvation, *N*-acetylglucosamine, microaerophilic conditions, and 5% CO_2 [9]. This morphogenetic switching is governed by a complex network of factors, comprised of parallel pathways including cyclic AMP pathway (cAMP) and MAPK pathway [10–13]. Transcription factors such as Efg1, Cph1, Cph2, Flo8, Tec1, Czf1, Ndt80, and Rim1 are downstream targets of these pathways and promote hyphal morphogenesis. These targets are specific to one particular pathway or targeted by multiple pathways. Hyphal morphogenesis is inhibited by a complex of Tup1 with Nrg1 or Rfg1 [9]. Studies to find the common regulator acting downstream to all hyphal regulatory pathways revealed role of a novel regulator, Ume6p. *UME6* null mutant strain does not form hyphae under any of the environmental conditions. Ume6p expression levels depend on each of the major known hyphal regulators and ectopic expression of Ume6 can induce hyphae in mutant strains lacking *EFG1*, *CPH1* or *RAS1*. Ume6p expression also controls the expression of hyphae-specific genes (HSGs) and has been identified as a common downstream target of several regulatory pathways that are induced by different environmental factors [14,15]. Ume6p controls the level and duration of Nrg1p expression and both Ume6 and Nrg1 function together by a negative feedback mechanism [14]. High level expression of Nrg1p has been shown to block the yeast to hyphae conversion and hyphal growth, leading to attenuated virulence in a mouse model of systemic candidiasis [16,17]. Multiple signaling pathways triggered under different environmental conditions modulate expression of Ume6p and Nrg1p to control filamentation and virulence *in vivo* [18].

In a study, Vediyappan et al. have shown that GAs, a triterpenoid saponin extracted from plants *Gymnema sylvestre* inhibits yeast to hyphae conversion in *C. albicans* in presence of hyphae inducing cues and promotes yeast formation from hyphal cells. Importantly, GAs do not affect the viability of *C. albicans*. GAs inhibited hyphae formation and attenuated virulence in *Caenorhabditis elegans*, an invertebrate animal model of *Candida* infection. GAs inhibited conidial germination and hyphae formation in *Aspergillus fumigatus* [19].

Hyphal formation can be induced directly in conditions such as activation of PKA, expression of Ume6p or deletion of *TUP1*, without the activation of signaling pathways through hypha inducing conditions. GAs have shown to inhibit yeast to hyphae conversion and promote budding from hyphae even under hypha inducing conditions. Dibutiryl-cAMP (db-cAMP) induces hyphal formation by directly activating PKA in the absence of activation of adenylate clyclase-cAMP-PKA-Efg1pathway through inducing cues. Addition of db-cAMP did not relieve the GAs-dependent inhibition of hyphal growth, suggesting that GAs do not act by inhibiting adenylate cyclase [19].

Nrg1p along with corepressor Tup1 is known to repress the expression of hypha-specific genes by binding to the promoters of hyphal genes such as *HWP1*, *ALS3*, *ALS8*, *ECE1*, and more. The promoters of these hypha-specific genes contains one or more *NRG1* response element (NRE) sequences (A/C)(A/C/G)C_3T. Nrg1p was unable to repress hypha-specific gene expression when 2 NREs were deleted from promoter of *ALS8* [17]. *ALS3* contains 2 NREs and Nrg1p was shown to bind to promoter of *ALS3* [17,21]. Small molecule is previously shown to inhibit DNA binding activity of transcription factor [22]. Identifying whether or not GAs inhibit DNA-binding activity of Nrg1p to the promoters of above-mentioned hypha-specific genes would be helpful in understanding mode of action of GAs.

To investigate the molecular basis of inhibition of hyphae formation and induction of budding from hyphae by GAs, we begin with proteomic approach to gain insight into Ume6p and Nrg1p dependent pathways, the two opposing pathways of hyphal morphogenesis in *C. albicans*. Two step affinity purification allows for identifying protein of interest based on protein-protein interaction. Our aim in this study was to identify proteins involved in Nrg1p and Ume6p mediated hyphal growth inhibition by GAs.

3.3 Materials and methods

3.3.1 *C. albicans* strains and growth conditions

All the strains used in this study are listed in **Table 3.1**. Primary cultures of *C. albicans* expressing P_{PCK1}-*NRG1-TAP* and P_{PCK1}-*UME6-TAP* grown overnight in YPD broth medium at 30 ^{o}C were used to inoculate fresh RPMI medium (HyClone, USA) containing 25 mM HEPES and 50 mM glucose. Suspensions of P_{PCK1}-*NRG1-TAP* and P_{PCK1}-*UME6-TAP C. albicans* strains were cultured in petri dishes (100 mm diameter, VWR, USA) separately for 16 h in the presence and absence of GAs (80 µg/mL) at 37 ºC. Although these tagged proteins (Nrg1-Tap & Ume6-Tap) can be induced in *C. albicans* by growing them in a media containing casamino acids [23], we chose to grow them under non-inducing conditions (RPMI without casamino acids) to maintain the native expression of proteins to study protein-protein interaction (and also to avoid non-biological overexpression). For reporter fusion assays, *C. albicans* expressing *NRG1-Pro-lacZ* (DT13) and *UME6-Pro-lacZ* (DT389) strains were also grown in RPMI medium as above with and without GAs at 37 ^{o}C and analyzed for beta-galactosidase activity at different time point intervals.

Table 3.1. List of *C. albicans* strains used in this study

Strain	Genotype	Reference
SC5314	*ura3Δ::λimm434/ura3Δ::λimm434 his1Δ::λimm434/his1Δ::λimm434 arg4Δ::λimm434/arg4Δ::λimm434 iro1Δ::λimm434/ iro1Δ::λimm433*	[23]
P_{PCK1}-*NRG1-TAP*	*ura3Δ::λimm434/ura3Δ::λimm434 arg4Δ::hisG/ARG4 his1Δ::hisG/HIS1 RPS1/RPS1::CIp10-PPCK1-NRG1-TAP tag*	[23]
P_{PCK1}-*UME6-TAP*	*ura3Δ::λimm434/ura3Δ::λimm434 arg4Δ::hisG/ARG4 his1Δ::hisG/HIS1 RPS1/RPS1::CIp10-PPCK1-UME6-TAP tag*	[23]
P_{PCK1}-*GTW-TAP*	*ura3Δ::λimm434/ura3Δ::λimm434 his1Δ::hisG/HIS1 arg4Δ::hisG/ARG4 RPS1/RPS1::CIp10-*P_{PCK1}*-GFP-TAP tag*	[23]
DT13	*ura3Δ::imm434/ura3Δ::imm434 iro1Δ::imm434/IRO1 rps1::NRG1 2.9 kb ur–S.t. lacZ–URA3/RPS1*	[18]
DT389	*ura3Δ::imm434/ura3Δ::imm434 iro1Δ::imm434/IRO1 rps1::UME6 6 kb ur –S.t. lacZ–URA3/RPS1*	[18]

3.3.2 Two-step affinity protein purification

To isolate the interacting partner proteins of Nrg1 and Ume6, P_{PCK1}-*NRG1-TAP* and P_{PCK1}-*UME6-TAP* strains of *C. albicans* were grown in RPMI medium and purified using tandem affinity purification method. The gene encoding target protein is fused with DNA sequences expressing the TAP tag, and the entire construct is integrated into the *RPS1* locus of the *C. albicans* genome. The TAP tag contains calmodulin binding protein peptide and IgG binding domain (Protein A). A TEV site is placed between these binding domains, which allows cleaving of the target protein fused calmodulin tag from the IgG-immobilized beads during the tandem purification step [24] **(Figure. 3.1)**. Vector alone (without target protein) integrated similarly into *C. albicans* chromosome was used as vector control sample during purification.

Two step tandem affinity purification was done as previously described protocol [24]. Briefly, cells were harvested from plates, washed with PBS, and allowed to freeze at -80 ^{o}C. Cells were then resuspended in lysis buffer (50 mM Tris-Cl [pH-8.0], 150 mM NaCl, 0.1%NP-40, protease inhibitor cocktail, PMSF, leupeptin) and lysed using French Press (Sim Aminco) at 19,000 psi. Breaking of cells (>90%) were confirmed under a microscope. Cell lysates were centrifuged at 20,000 x g for 30 mins at 4 ^{o}C in Microfuge 22R Centrifuge. Concentration of proteins was measured using Bradford protein assay and bovine serum albumin as standard. Equal amounts of total proteins from vector control, cells grown without (-GAs), and with GAs (+GAs) were used. The supernatants obtained were incubated overnight with 200 µL of IgG sepharose beads (GE Healthcare) (pre-equilibrated with IPP150 buffer) [24] at 4 ^{o}C. The IgG-sepharose beads were washed with 10 mL of IPP150 buffer. This was followed by treatment with TEV protease of 8 µL in 200 µL TEV protease cleavage buffer (50 mM Tris-Cl [pH-8.0], 0.1 M NaCl, 5 mM DTT) for 1 h at 37 ^{o}C. Flow through were collected and beads were washed with cleavage buffer (-DTT) twice. The second round of purification was done by incubating the flow through from first round i.e TEV cleaved proteins with 200 µL of calmodulin beads (Agilent technologies) equilibrated with binding buffer and 6 mL of calmodulin binding buffer (50 mM Tris-Cl [pH-8.0], 300 mM NaCl, 1 mM Mg^{2+} acetate, 1 mM Imidazole, 2 mM $CaCl_2$, 10 mM DTT). After binding for overnight at 4 ^{o}C, the calmodulin beads were washed with 1 mL of calmodulin binding buffer containing 0.02 % NP-40. The purified protein complexes were eluted from the calmodulin beads with 400 µl calmodulin elution buffer with increased concentration of EGTA 20 mM, 40 mM and 60 mM (10 mM Tris-Cl [pH-8.0], 300 mM NaCl, 0.02% NP-40, 1 mM Mg^{2+} acetate, 1 mM Imidazole, 20 mM EGTA, 10 mM DTT). Pooled samples were processed for mass spectrometry (MS) as required and sent for MS for protein identification.

3.3.3 LC-MS/MS and data analysis

LC-MS/MS was carried out in core facility service (DNA/Protein Resource Facility, Oklahoma State University, Stillwater, OK, USA) using quadrupole-Orbitrap tribrid mass spectrometer (Orbitrap Fusion model, Thermo Fisher, Waltham, MA, USA). Data obtained were processed in Maxquant software and *C. albicans* SC5314 reference genome. Maxquant output obtained were analyzed using Perseus software. We started by comparing vector control (with and without GAs) to their matching bait experiment samples i.e Nrg1p and Ume6p and built a list of proteins that are specific either to Nrg1p or Ume6p. For this, we did Student's t-test against each of the sets and retained only those proteins which were significantly enriched when baits were present. Using these protein sets, we constructed a volcano plot with logarithmic ratios of *P*-value of protein intensities and difference between control treated values. Proteins having *P*-value of less than 0.05 were considered significant and are represented in volcano plots as red and blue colored dots as shown in **Figure 3.1**. Triplicate readings for each and two or more than two matching peptides were only taken into consideration. Two biological replicates of TAP tag purification were carried for both P_{PCK1}-*NRG1-TAP* and P_{PCK1}-*UME6-TAP* grown in the presence and absence of GAs.

3.3.4 GO term analysis

Candida Genome Database (CGD) was used to classify *NRG1* and *UME6* copurified proteins. Proteins were divided based on their biological functions and processes such as DNA-binding, RNA-binding, filamentation, and others.

3.3.5 Reporter fusion assay

Expression of lacZ in the presence and absence of GAs was measured as reported earlier [18]. Briefly, individual colonies of *C. albicans* strains, DT13 and DT389 were inoculated in a 2 mL of YPD broth and were grown overnight at 30 ^{o}C. The overnight cultures were inoculated into fresh RPMI medium containing 50 mM glucose. Cells were grown for 4 hours followed by addition of GAs. Cells were collected, washed with 1 mL of sterile PBS, and resuspended in 500 µL of breaking buffer and homogenized using beads in Precellys 24 (Bertin Technologies, France). 1-100 µL of extracts (for equal protein concentration across the samples) were added to 0.9 mL of Z-buffer and volume was adjusted to 1 mL using breaking buffer. The mixture was incubated in water bath at 28 ^{o}C for 5 minutes. Reaction was initiated by adding 0.2 mL of ortho-nitrophenyl-b-D-galactopyranoside (ONPG) solution and was incubated at 28 ^{o}C until pale yellow color was obtained. Reaction was then terminated by adding 0.5 mL of Na_2CO_3 and β-galactosidase activity was calculated as described earlier [25,26].

3.3.5 Western blot analysis

Cytosolic proteins from *C. albicans* cells for Western blot analysis were prepared by breaking cells using Precellys-24 homogenizer in a sample buffer containing 50 mM Tris, 100 mM NaCl, and protease inhibitors followed by centrifugation at 15,000 x g at 4 ^{o}C for 10 mins. Supernatant or lysates were boiled in reducing buffer for 5 mins at 100 ^{o}C, separated using SDS-PAGE, and transferred into Immobilon-P PVDF membrane (Millipore Sigma, Billerica, MA, USA). Membranes were blotted against specific primary and secondary antibodies. Immuno-detection of protein bands was carried out using the ECL Western blotting substrate (Thermo Scientific, Waltham, MA, USA) and imaged in Azure c600.

3.3.6 Biotin pull-down assay

Biotin DNA pull down assay was performed as described previously [25]. Briefly, the promoter region of a known hyphal regulatory gene, *ALS3* was amplified using biotinylated primers **(Table 3.2)**. The PCR amplified region that is known to contain binding site for Nrg1p (positive control), was coupled to Avidin resin (G Biosciences) for 30 minutes at room temperature in a rotor. The same positive control in the presence of GAs served as our test sample. *ALS3* promoter region without DNA binding sequences and beads alone were used as negative controls. Unbound DNA from bead-DNA complex was removed by washing with TE buffer (10 mM Tris, 2 M NaCl). For lysates containing Nrg1p, P_{PCK1}-*NRG1-TAP* cells were grown overnight in YNB medium with casamino acids and lysed using French press in BS/THES buffer. Lysed cells were centrifuged at 4 ^{o}C for 30 minutes at 20,000 xg and clear lysate was mixed with bead-DNA complex. GAs were added to test sample, mixed for 5 minutes and protein lysates were added to all samples including test sample, positive and negative controls. Protein-DNA-bead complex was incubated in a rotor at 4 ^{o}C overnight, washed with BS/THES buffer and eluted using TE buffer containing 200 mM NaCl. Obtained eluates were run in SDS-PAGE gel followed by Western blot using anti-Nrg1 antibody.

Table 3.2. List of primers used in biotin pull-down assay.

1 and 2 are forward and reverse primers respectively for *ALS3* region containing Nrg1p binding sites. 3 and 4 are forward and reverse primers for control *ALS3* region without Nrg1p binding sites.

S. N	Name of primer	Primer sequence
1	Als3ProF-5biotin	5-CGACGGAAGAAAGAAAGTACAAAG-3
2	Als3ProR-5biotin	5-ACTATCAGACCTCAATTCAAGGG-3
3	Als3ProConF-5biotin	5-TCGTATTCGAAGCAAGGTCTAAT-3
4	Als3ProConR-5biotin	5-GTCTAGCAAATGCATCTCTTTCG-3

3.3.7 Statistical Analysis

Data were analyzed using Perseus and GraphPad Prism version 7 software. Student's t-test was applied to test for the difference between control and GAs treated samples. *P*-value less than 0.05 was considered significant.

3.4 Results

3.4.1 Proteomics profile after TAP-tag purification shows proteins involved in morphogenesis and virulence

A proteomic profile was obtained from the proteins co-purified from *C. albicans* expressing P$_{PCK1}$-*NRG1-TAP* and P$_{PCK1}$-*UME6-TAP* grown in the presence and absence of GAs. *C. albicans* expressing P$_{PCK1}$-*GTW-TAP* served as a vector control and was used in parallel. Two biological samples each with three technical replicates were used for affinity isolation and LC-MS/MS identification. Proteins identified from LC-MS/MS were analyzed using Perseus software. Following analysis, a total of 27 proteins in control (without GAs treatment) and 168

proteins (with GAs treatment) in *C. albicans* expressing Nrg1-TAP tag were co-purified **(Figure 3.1A) (Table S3.1, Appendix A)** whereas 19 proteins in control and 142 proteins in GAs treated for Ume6-TAP were co-purified **(Figure 3.1B) (Table S3.2, Appendix A)**.

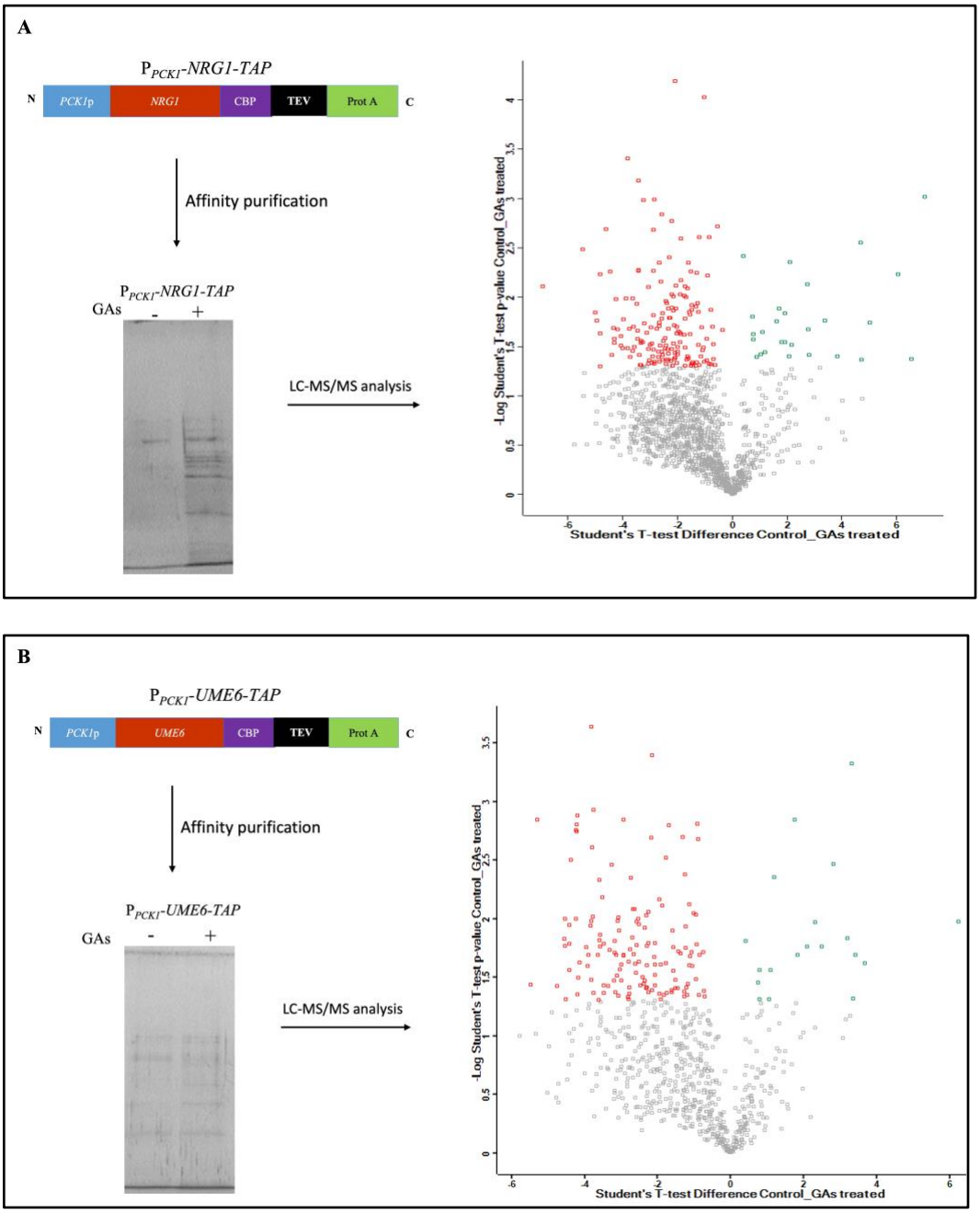

Figure 3.1. Analysis of TAP tag co-purified proteins obtained from LC-MS/MS.

C-terminal TAP tagged strains: P*PCK1*-*NRG1-TAP* **(A)** and P*PCK1*-*UME6-TAP* **(B)** were used as baits for affinity purification of proteins followed by LC-MS/MS analysis. The co-purified

proteins were categorized based on intensity values from LC-MS/MS and volcano plots were constructed using Perseus software (*P*-value <0.05). Red represents proteins having significantly higher intensity in the GAs treated samples whereas green represents significantly higher intensity in control samples without GAs. Grey represents non-significant proteins.

3.4.2 GO term Analysis revealed several DNA binding and filamentation related co-purified proteins in GAs treated *C. albicans*

Significant proteins obtained from LC-MS/MS analysis were categorized based on their biological functions **(Figure 3.2)** for both Nrg1p (upper panel) and Ume6p (lower panel) in the presence and absence of GAs. Majority of proteins had biological functions including hydrolase, transferase, oxidoreductase, protein binding, and DNA binding activities. There were more proteins with oxidoreductase activity and ligase activity in Ume6p co-purified proteins compared to Nrg1p. A total of 12 proteins having DNA binding activity were obtained in GAs treated cells of both Nrg1p-TAP and Ume6p-TAP expressing *C. albicans* **(Table 3.3)**. No DNA binding protein was identified in the Nrg1p-TAP control samples (without GAs exposure) whereas, only 1 protein having DNA binding activity, Skp1, was co-purified with Ume6p-TAP control (-GAs) samples. On the other hand, when proteins were categorized based on biological processes, we found more proteins having role in filamentous growth in GAs treated samples compared to control in both Nrg1p and Ume6 associated co-purified proteins list **(Table 3.4)**. In Nrg1p co-purified list, there were 14 proteins with a role in filamentous growth in GAs treated samples whereas only 5 proteins in the absence of GAs. Similarly, in Ume6p co-purified list, there were 7 proteins in GAs treated samples whereas 4 proteins in the absence of GAs.

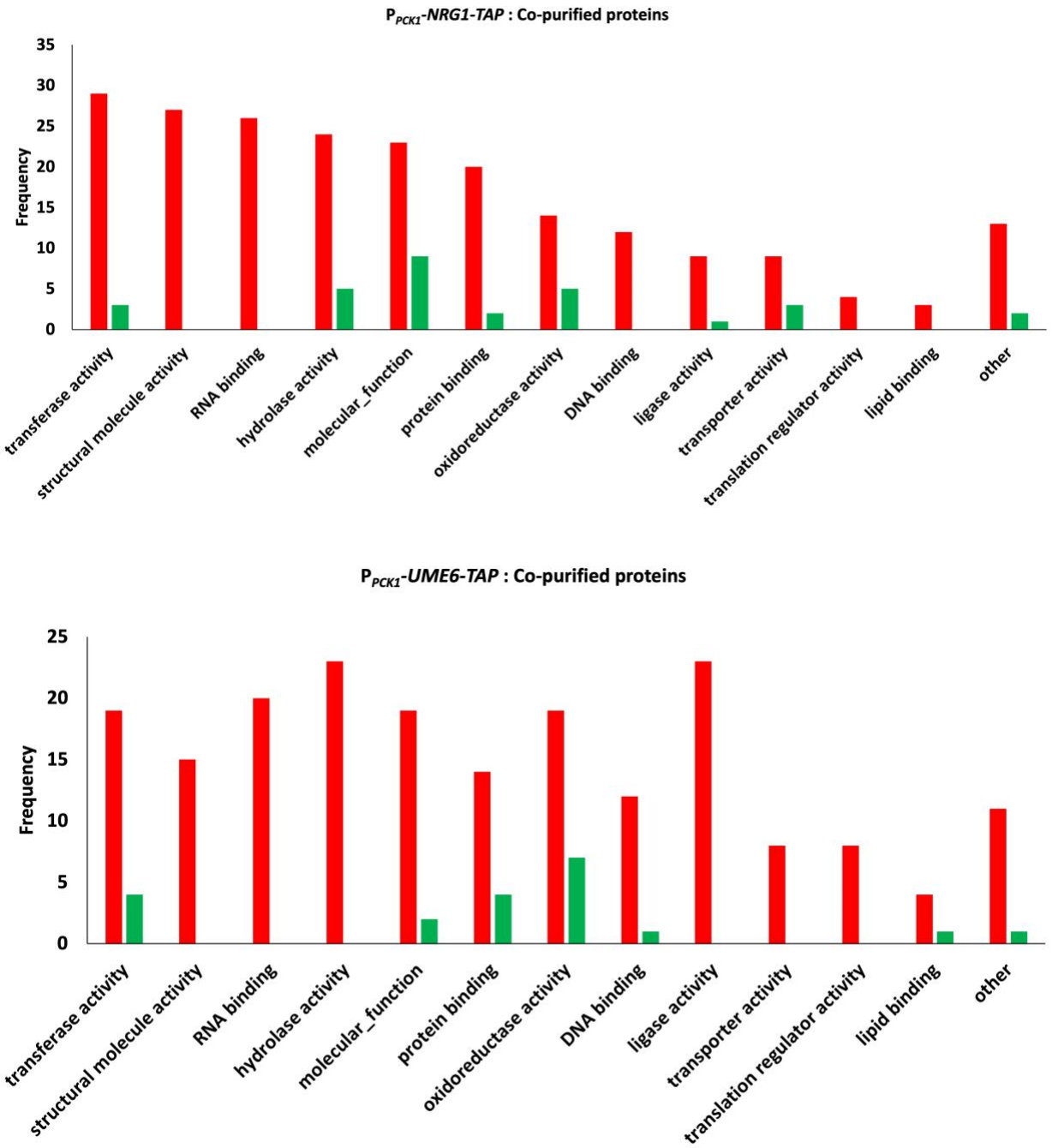

Figure 3.2. GO term analysis of co-purified proteins.

Proteins co-purified with both P*PCK1*-*NRG1-TAP* (upper panel) and P*PCK1*-*UME6-TAP* (lower panel) were categorized based on biological function from Candida Genome Database. Red bars indicate proteins from GAs treated and green bars represent proteins from control (-GAs) samples.

Table 3.3. List of DNA-binding proteins co-purified by TAP.

Proteins co-purified with both Nrg1p and Ume6p were categorized based on biological function using CGD database and only proteins having DNA binding activity are listed. All co-purified proteins listed here are significantly different from control samples (-GAs) based on Student's t-test.

DNA Binding Proteins		
Gene	**Protein**	**Function**
Nrg1p GAs+		
MIG1	A0A1D8PNL1	C2H2 Transcription factor; downregulated during hyphal development
C4_05630W_A	Q5A462	Putative RNA polymerase II subunit B44
RPB7	Q5A8Y7	Essential subunit of RNA Polymerase II
RPB11	A0A8H6C2Q9	Putative RNA polymerase II subunit
BRE1	Q5A4X0	Transcription factor activity, transposon mutation affects filamentous growth, zinc ion binding
C1_09670C_A	Q5APD5	Predicted role in DNA repair, replication
HMO1	Q59PR9	HMG-box transcription factor, repressed in hyphae
ADE12	P0CH96	Adenylosuccinate synthase; upregulated in biofilm; decreased expression in hyphae vs yeast-form cells
CR_05550C_A	Q59M52	Predicted RNA polymerase III activity
C2_04620W_A	A0A1D8PH73	Predicted subunit of the SWI/SNF chromatin remodeling complex; possibly an essential gene
ILV5	A0A1D8PPG7	Ketol-acid reductoisomerase
NAM7	Q5A507	Putative role in nonsense-mediated mRNA decay
Ume6p GA+		
C1_00160C_A	Q5AB84	Putative nucleolar protein with a predicted role in pre-rRNA processing and ribosome biogenesis
MIS11	Q59SM8	Putative protein of glycine catabolism
ADE12	P0CH96	Adenylosuccinate synthase; upregulated in biofilm; decreased expression in hyphae vs yeast-form cells
C1_01590C_A	Q5A8Y5	Putative RNA polymerase II subunit B150
CBF1	Q5A1E3	Transcription factor
C7_02100W_A	G1UAD4	Putative curved DNA-binding protein
RPO21	A0A1D8PUA6	RNA polymerase II, transposon mutation affects filamentous growth
PYC2	A0A1D8PLY4	Putative pyruvate carboxylase
SBP1	Q5ANP6	Similar to RNA binding proteins; downregulated upon adherence to polystyrene
ILV5	A0A1D8PPG7	Ketol-acid reductoisomerase
C1_02850W_A	Q5AI80	Ortholog(s) have RNA binding, DNA binding activity and role in nuclear-transcribed mRNA catabolic process
DOT6	A0A1D8PS02	Protein with a predicted role in telomeric gene silencing and filamentation

Table 3.4. List of filamentation related proteins co-purified by TAP.

Proteins co-purified with both Nrg1p and Ume6p were categorized based on biological process using CGD database and proteins having role in filamentation are listed. All co-purified proteins listed here are significantly different among control and GAs treated samples based on Student's t-test.

Filamentous growth-related proteins		
Gene	**Protein**	**Function**
Nrg1p GA+		
NOP5	Q59S06	Nucleolar protein; mutation affects filamentous growth
VAC8	Q59MN0	Vacuolar protein
RPL6	A0A1D8PCX8	60S ribosomal protein
MIG1	A0A1D8PNL1	C2H2 Transcription factor; downregulated during hyphal development
CSI2	A0A1D8PFE1	Csi2p
RNR1	Q5A0N3	Ribonucleoside-diphosphate reductase
BRE1	Q5A4X0	Transcription factor, transposon mutation affects filamentous growth, zinc ion binding
FGR22	Q5ALJ2	Fgr22p
LAG1	Q5A879	Sphingosine N-acyltransferase
HMO1	Q59PR9	HMG-box transcription factor, repressed in hyphae
IMH3	Q59Q46	Inosine-5-monophosphate dehydrogenase; Filamentation decreases during overexpression
SPT6	Q3MNT0	Transcription elongation factor
SAC1	A0A1D8PEV5	Phosphatidylinositol-3-phosphatase
MKC1	Q5AAG6	Mitogen-activated protein kinase
Nrg1p GA-		
RHO1	O42825	GTP-binding protein
CMD1	A0A1D8PMF8	Calmodulin
RAS1	Q59XU5	Ras-like protein 1
CMP1	A0A1D8PCA8	Serine/threonine-protein phosphatase
C1_11120C_A	Q59WJ7	Uncharacterized protein
Ume6p GA+		
VID27	A0A1D8PP94	Vid27p; Mutation affects filamentous growth
RPL16A	Q5AB87	Ribosomal protein, mutation affects filamentous growth
SSB1	Q5A397	Hsp70 family ATPase; mRNA in yeast and germ tubes
OSH3	Q59TM0	Oxysterol-binding protein ;homozygous null has filamentation defect
IMH3	Q59Q46	Inosine-5-monophosphate dehydrogenase; Filamentation decreases during overwxpression
RPO21	A0A1D8PUA6	RNA polymerase II, transposon mutation affects filamentous growth
AAF1	P46589	Adherence factor
Ume6p GA-		
ALS3	Q59L12	Agglutinin-like protein
TSA1	Q9Y7F0	Peroxiredoxin
PHR1	P43076	pH-responsive protein
RAS1	Q59XU5	Ras-like protein

3.4.3 GAs treated *C. albicans* shows affinity towards ribosomal complex copurified in Nrg1p and Ume6p TAP tagged samples

Classification of significant proteins based on GO term components showed 26 ribosomal proteins copurified when treated with GAs in P*PCK1*-*NRG1-TAP* sample whereas 18 in P*PCK1*-*UME6-TAP* sample. However, no significant ribosomal proteins were copurified in the absence of GAs. **Figure 3.3A** shows ribosomal proteins and their interactions based on STRING database for both Nrg1p and Ume6p co-purified proteins. Rps4a, one of the ribosomal proteins co-purified in both samples in the presence of GAs, was expressed in higher intensity in a GAs treated sample as compared to control in Western blot analysis carried out using anti-Rps4x antibody (human) **(Figure 3.3B)**. Human anti-Rps4x immunogen sequence has approximately 68% similarity with Rps4a.

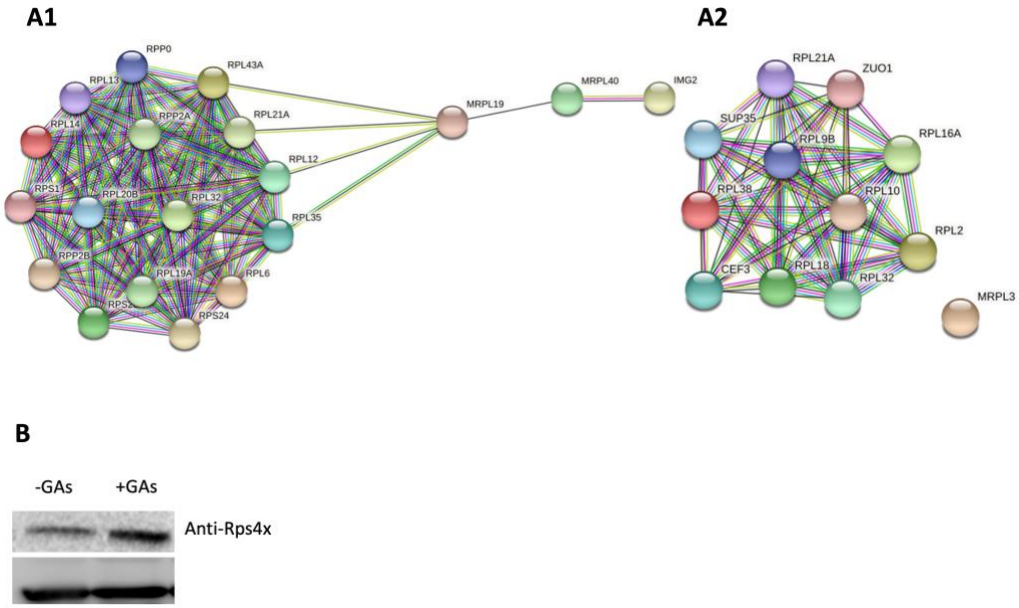

Figure 3.3. Ribosomal proteins co-purified in GAs treated *C. albicans*.

Ribosomal proteins copurified abundantly in GAs treated P*PCK1*-*NRG1-TAP* **(A1)** and P*PCK1*-*UME6-TAP* **(A2)** were analyzed using STRING database based on their interactions. **(B)** Western blot analysis of cytosolic proteins from P*PCK1*-*NRG1-TAP* using anti Rps4x human primary antibody followed by anti-rabbit secondary antibody. Anti-Gapdh antibody was used for loading control (lower panel).

3.4.4 Nrg1p promoter is upregulated and Ume6p promoter is downregulated in GAs treated *C. albicans*

C. albicans Nrg1 is known to regulate hundreds of genes [17]. Our proteomics approach identified several proteins that are associated with Nrg1 in the presence of GAs. To further evaluate the effect of GAs on Nrg1 and Ume6 promoter activities, we used *C. albicans* expressing lacZ under these promoters. Strains having Nrg1p promoter-lacZ reporter (DT13) and Ume6 promoter-lacZ reporter (DT 389) constructs [18] were grown in RPMI medium at 37 ºC in the presence and absence of GAs at different time points and *lacZ* expression (beta-galactosidase) was measured. The *lacZ* expression of DT13 (Nrg1) construct was upregulated in the presence of GAs as compared to the control without GAs. On contrary, *lacZ* expression of DT389 construct (Ume6) was downregulated in the GAs treated sample when compared to the control (-GAs treated), and it was significantly inhibited at 8 hours. Results in **Figure 3.4** show that Nrg1p is upregulated in the presence of GAs which matches with the phenotype observed as we saw all the *C. albicans* were in yeast form when treated with GAs.

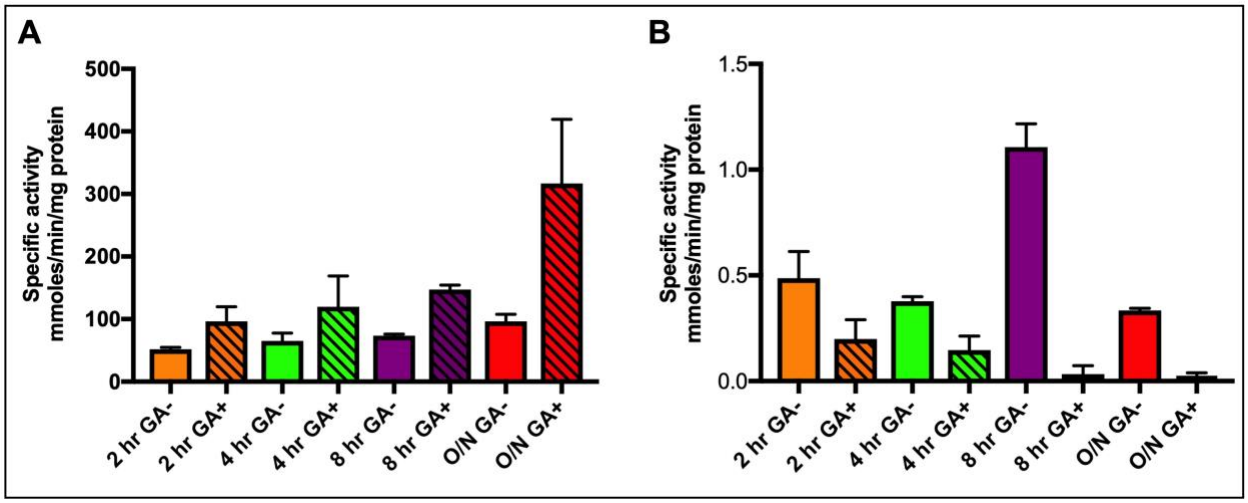

Figure 3.4. Reporter fusion assay of *NRG1* and *UME6* promoter region expression. Strains having *NRG1* promoter-*lacZ* reporter fusion **(A)** and *UME6* promoter-*lacZ* reporter fusion **(B)** [18] were grown at 37 ºC in the presence and absence of GAs. The expression of beta-

galactosidase was measured. The error bars represent standard error of the means of three biological replicates.

3.4.5 GAs increased the expression of Tup1p, a repressor complex of Nrg1p

Tup1p is a transcriptional repressor that represses filamentous growth involving corepressors, Nrg1p and Rfg1p [26,27]. To know the level of Tup1p expression in *C. albicans*, we determined the expression of Tup1p in the presence and absence of GAs under hypha inducing conditions (RPMI & 37 ^{o}C). *C. albicans* (Nrg1p promoter-*lacZ* strain) were grown in the presence and absence of GAs followed by Western blot analysis of cytosolic proteins using anti-Tup1 antibody. As GAs treated cells were in yeast form and we speculated an increased expression of Tup1p in GAs treated cells. As expected, we observed very little or no expression in the absence of GAs when cells were in the hyphal form whereas, strong expression was observed when treated with GAs and cells were in the yeast form **(Figure 3.5)**.

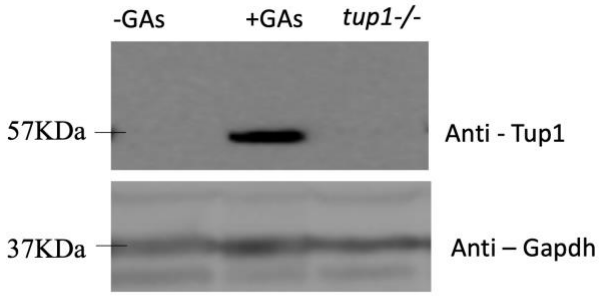

Figure 3.5. Expression of Tup1 in the presence and absence of GAs.

Western blot analysis of cytosolic proteins from *C. albicans* (Nrg1p promoter-*lacZ* strain) cells in the presence and absence of GAs at using Anti-Tup1 monoclonal antibody (clone 10, abcam) (upper panel). *C. albicans tup1-/-* null mutant was used as negative control. Anti-Gapdh (human) antibody was used as loading control (lower panel).

3.4.6 GAs inhibited binding of Nrg1p to the promoter of hypha specific gene *ALS3*

Nrg1p is known to bind to promoter regions of hypha specific genes at binding site (A/C)(A/C/G)C_3T [17]. We used biotinylated primer to amplify promoter region of *ALS3* gene, that is known to have Nrg1p binding site. Then, DNA pull-down experiment was carried out using Avidin beads with the presence and absence of GAs. Interestingly, we observed that addition of GAs prevented Nrg1p binding to *ALS3* promoter region **(Figure 3.6)**.

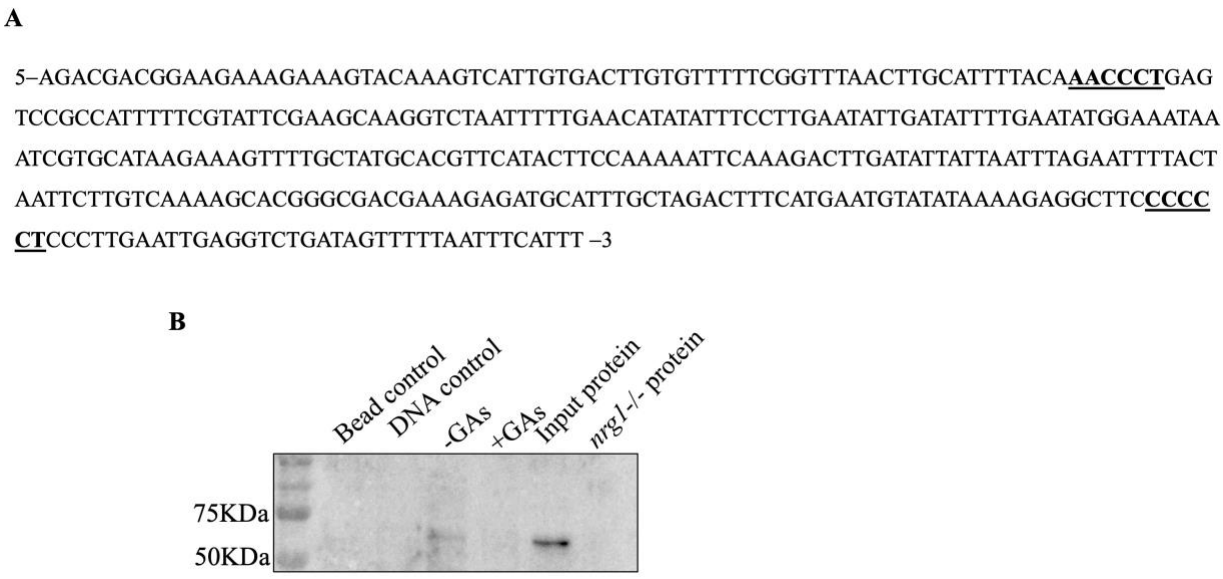

Figure 3.6. GAs inhibit DNA binding activity of Nrg1p.

(A) Promoter region of *ALS3* gene highlighting two Nrg1p binding motif. The promoter DNA (343 bp) was PCR amplified using biotinylated primers and used for pull-down assays. **(B)** Western blot analysis of eluates obtained from biotinylated DNA-Nrg1p pull-down assays using anti-Nrg1p antibody. A 55 kDa Nrg1 protein band is absent in *ALS3* promoter DNA incubated with GAs (lane +GAs). In contrast, *C. albicans* cell lysate containing Nrg1p and the promoter DNA without GAs shows a protein band to that of input protein. Lysates incubated with non-specific DNA or beads alone controls did not show any detectable bands. As expected, lysate from *nrg1-/-* mutant lacks Nrg1p.

3.5 Discussion

C. albicans is an opportunistic fungal pathogen that can cause infection in human and eventually lead to invasive candidiasis especially in immunocompromised individual. Pathogenicity in host is caused by the expression of several virulence factors such as secretion of biomolecules and degrading enzymes, adhesion to host, transition between yeast and hyphal form, and others [28-30]. The transition between yeast and hyphal form involves several transcription factors and is controlled by multiple signaling pathways. Nrg1p and Ume6p are transcription factors acting in opposite direction, where one gets upregulated, the other is downregulated resulting corresponding morphology in *C. albicans* [18]. For example, when Nrg1p overexpress, the Ume6p is repressed resulting yeast growth form and *vice versa*. Our main objective in this study was to identify proteins that co-purify with Nrg1-TAP and Ume6-TAP tags when *C. albicans* were grown in the presence and absence of GAs to know possible interactors. For this, we used tandem affinity purification followed by mass spectrometry which is a commonly used method to find possible interactors of any bait protein. Two-step TAP tag affinity purification technique in combination with mass spectrometry permits the identification of directly and indirectly interacting protein complexes with minimum background [24,31]. Using this method, 168 proteins were co-purified with Nrg1p that had significant higher protein intensity in GAs treated sample whereas 27 proteins had higher intensity in control. Similarly, in case of Ume6p, 142 in GAs treated whereas 19 proteins in control.

DNA binding proteins are a major group of proteins that play role in gene regulation activities such as transcription, DNA replication and repair, cell growth and more. There were 12 DNA binding proteins co-purified with high intensity in GAs treated Nrg1-TAP group whereas none in the absence of GAs **(Table 3.3)**. *HMO1* is one of the transcription factors (TF)

copurified in GAs treated Nrg1-TAP tag cells. Hmo1 is an HMG-box (high mobility group family) TF that binds to the promoters of hexose, ergosterol metabolism, and cell cycle genes (Candida Genome Database, CGD). Further, Hmo1 is considered a generalist TF, and in *S. cerevisiae*, Hmo1 binds to the promoters of ~70% of ribosomal protein genes [33]. As mentioned above, 28 ribosomal proteins were copurified in GAs treated with Nrg1-TAP but not in control (-GAs) cells (**Figure 3.3**). We could hypothesize that GAs exposure could recruit Hmo1 to the transcription machinery and activates the transcription of ribosomal protein-encoding genes as the yeast growth phase may require high protein synthesis due to GAs treatment. Further, some of the ribosomal proteins are involved in hyphal growth-related functions (*e.g*. Rpl6, Rpl16A, etc., **Table 3.4**).

Most of the DNA binding proteins we obtained also had role in filamentation of *C. albicans*. There were 14 proteins that are known to have role in filamentation, copurified in GAs treated Nrg1p sample whereas 5 in control. Similarly, we obtained 7 proteins having role in filamentation in GAs treated Ume6-TAP sample whereas only 4 in the control **(Table 3.4)**. For example, Mig1p, a C2H2 transcription factor was copurified in GAs treated Nrg1-TAP tag sample but not in the control (without GAs) samples. Mig1 is a transcriptional repressor that regulates genes involved in the utilization of carbon sources and functions both Tup1-dependently and independently (CGD). Mig1 expression is known to be downregulated during hyphal development [34] that matches with the yeast morphology of GAs treated sample. In addition, when we analyzed proteins that are near or below cutoff values, we found several proteins involved in the Sln1 branch of the p38/Hog1 MAP kinase pathway (Ypd1, Ssk1/2, Pbs2, and Hog1) that were copurified only in GAs treated but not in control Nrg1-TAP or Ume6-TAP tagged *C. albicans* cells indicating the GAs-mediated cross-talk between Nrg1-Hog1 pathways.

Interestingly, an earlier genetic study in the lab showed the null mutants of the components (*ypd1, ssk1/2, pbs2, and hog1*) of the Hog1 pathway were insensitive to GAs (remain hyphae) and the heterozygous mutants (with one copy of the allele) reversed the hyphae to yeast phenotype when they were exposed to GAs under hypha inducing conditions. A recent study [35] reported the inhibition of SBF G1/S transcription factor complex and controlling of ribosome biogenesis by p38/Hog1MAPK. Overall, GAs exposure to *C. albicans* cells (under hypha-inducing conditions) promotes the recruitment of regulators of metabolic, osmosis, cell wall, and hyphal growth to the transcriptional machinery and modulate the expression of genes resulting in the inhibition of yeast-hyphal transition and hyphal growth. Interactions between proteins involved in these processes are visualized using STRING database (**Figure 3.7**). GO term analysis also showed proteins copurified with Ume6p have a relatively higher number of proteins having ligase activity involving synthesis of tRNA and amino acids when compared to Nrg1p. In *Saccharomyces cerevisiae*, Ume6p, related to *C. albicans* Ume6p, regulates meiosis-specific genes positively. During mitosis, ScUme6 represses the target genes by recruiting the histone deacetylase subunits Sin3p and Rpd3p (yeastgenome.org, SGD). However, little is known about the interaction between CaUme6 and acetylation or deacetylation system in *C. albicans* except a requirement of Ssn6p-Rpd31 complex to activate CaUme6 in hypha-inducing conditions [36]. Als3, a major hypha specific gene, was co-purified in Ume6p sample with significantly high intensity as compared to samples treated with GAs. Based on the evidences from our proteomics, genetics and gene expression studies, we propose the involvement of p38/Hog1 MAP kinase pathways in GAs mediated hyphal inhibition in *C. albicans*. GAs exposure activates the Hog1 MAP kinase pathway and *C. albicans* cells respond to adopt osmotic stress by inhibiting the energy-expensive hyphal growth and initiating the budding.

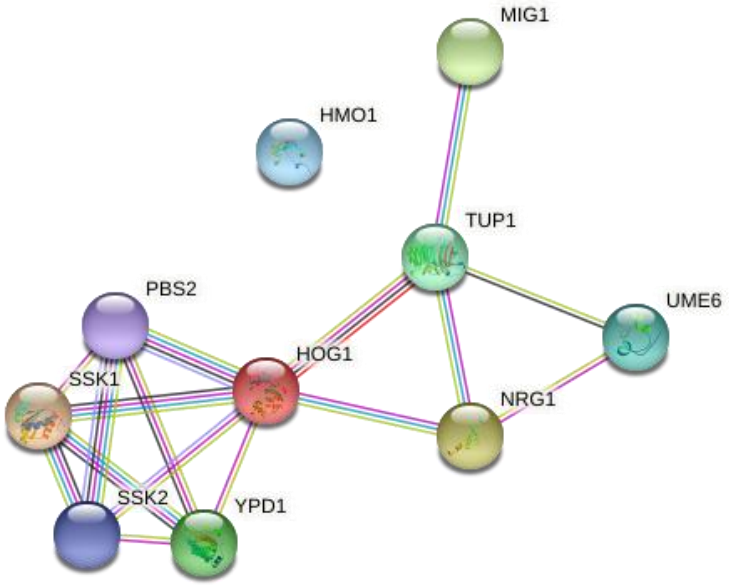

Figure 3.7. Protein interaction network using STRING database.

STRING (Search Tool for the Retrieval of Interacting Genes/Proteins) analysis was performed using proteins co-purified with higher intensity in GAs treated *C. albicans* (e.g. Nrg1-TAP) and with proteins involved in Hog1 pathway.

The inhibition of Ras1 in GAs treated *C. albicans* highlighted the involvement of either cAMP or MAP kinase pathways in GAs mediated hyphal inhibition [37]. Previous study from our group showed that the addition of cAMP could not rescue GAs mediated hyphal growth in *C. albicans* canceling the possibility of GAs acting through cAMP pathway [19] and leaving the Hog1 MAP kinase pathway as a potential target of GAs. With these observations, a tentative model of mode of action of GAs is built as shown in **Figure 3.8**.

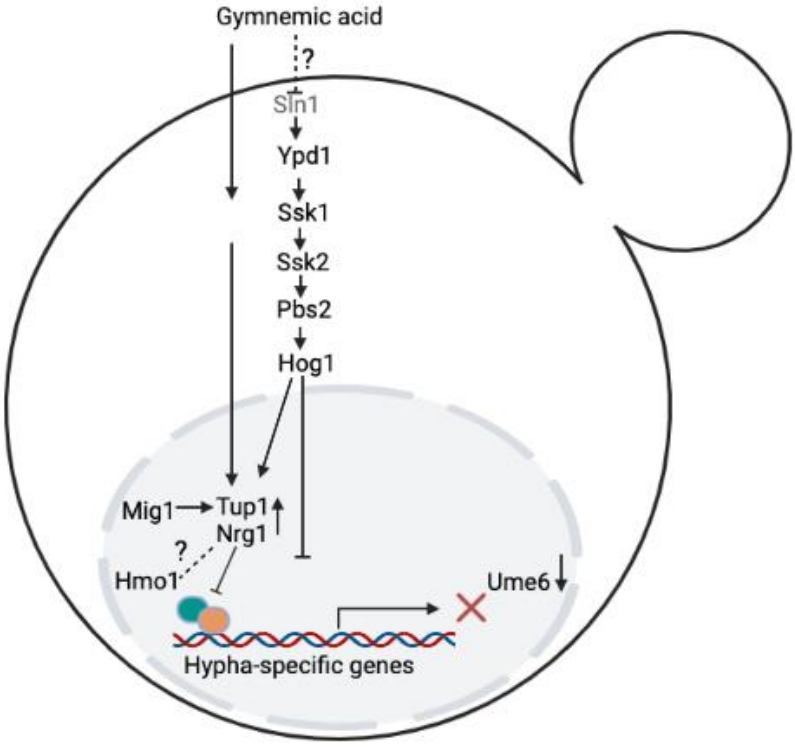

Figure 3.8. Schematic of predicted mode of action of GAs during hyphal growth inhibition. Addition of GAs activates the Hog1 MAP kinase pathway, upregulates Nrg1p/Tup1p, and downregulates Ume6p. Further, exposure of GAs to *C. albicans* recruits several regulatory proteins (Hmo1, Mig1 TFs, and others) to the transcriptional machinery resulting in downregulation of genes involved in various functions (carbon utilization, vesicular transport, cell wall synthesis, etc.) including several hypha-specific genes. Nrg1 protein downregulates hypha-specific genes, including *UME6* by binding to their promoter regions and inhibiting the expression of hypha-specific genes thereby keeping cells in the yeast form. Nrg1p and Ume6p regulate each other via feed-back loop mechanism [14]. Proteins in black color were co-purified during our TAP-tag purification, whereas protein in grey color was not present. Dotted lines with question mark indicate possible link. Upward arrow indicates upregulation of protein and transcripts, whereas downward arrow indicates downregulated protein and transcript. Created in Biorender.com.

Past studies have highlighted the translational changes in gene expression during yeast to hyphal transition. Lorenz and group reported genes involved in ribosome biogenesis and translational control are downregulated when *C. albicans* are converted from yeast to hypha in macrophages [38]. Conversely, Carlisle *et al*., showed reduced levels of genes involved in

protein synthesis during hypha to yeast conversion i.e. reverse morphogenesis [39]. Interestingly, in our current study, we obtained significantly more proteins involved in translational machinery in GAs treated cells compared to control cells without GAs including ribosomal proteins. This finding suggests that the addition of GAs can increase the protein synthesis to maintain the yeast growth form or GAs targeting ribosomal proteins hinders accessibility of ribosomes to hypha specific genes and interfere with the translation of hypha-specific genes resulting in yeast morphology [40–42]. This observation correlates with another recent study that treated Hela cells with GA and showed ribosomal protein complex as its main target [43], but unlike inhibition of protein synthesis in the study, we observed increased protein abundance in the presence of GAs. Also, presence of more RNA binding proteins in GAs treated cells may block ribosome scanning to upstream of hypha specific genes as suggested by Kadosh et al [40].

Nrg1 and Ume6 being key regulator of yeast-hyphal switch, we verified their expression in the presence and absence of GAs, using their specific promoters. A recent study carried out not so long ago, identified serum and temperature mediated response elements in the promoter regions of *NRG1* and *UME6* that are responsible for promoting or inhibiting filamentation in *C. albicans* [18]. In our study, we used these strains having serum and temperature responsive elements and carried out *lacZ*-based reporter fusion assays to check upregulation and downregulation of promoters of *NRG1* and *UME6* in the presence and absence of GAs. As we expected, with the addition of GAs, we observed increased expression of *NRG1* and decreased expression of *UME6*. These results correspond with the previous finding that *NRG1* and *UME6* function together during filamentation in a feedback loop [14].

Besides *UME6, ALS3* is another important hyphal induced gene [44,45]. In our study, we used promoter of *ALS3* gene to check if GAs inhibit, strengthen, or have no effect on the DNA

binding activity of Nrg1p. We chose *ALS3* instead of *UME6* due to the presence of two NREs in *ALS3* promoter compared to one in *UME6*. This allowed for better detection by the avidin-based biotinylated DNA pull-down assay which is comparatively less sensitive compared to other DNA-protein complex detection methods such as radioactive based detection. Since both *ALS3* and *UME6* are hypha-promoting genes, we could expect similar result using *UME6*. Surprisingly, we found that GAs inhibited binding of Nrg1p to promoter of *ALS3 in vitro*. We expected GAs would strengthen the binding of Nrg1p to *ALS3* promoter region as this binding inhibits the expression of *ALS3* which is hypha promoting gene. Also, our LC-MS/MS data show inhibition of Als3 in *C. albicans* treated with GAs. The rationale for this observation could be either this *in vitro* scenario might be different from actual *in vivo* condition or GAs recruit other hypha repressing proteins and continue repressing hypha-specific genes. We do not know if GAs can directly bind to Nrg1p that resulted in the observed inhibition. Further studies are needed to be done to clarify this complete mechanism.

In conclusion, by using tandem affinity purification followed by LC/MS-MS analysis, we have identified several Nrg1p and Ume6p associated co-purified proteins that are significantly different during the inhibition of *C. albicans* yeast-to-hyphal transition and hyphal growth by GAs. These include several transcriptional regulators (*MIG1*, *HMO1*, and other TFs) that are known to affect yeast-to-hyphal transition and hyphal growth. Proteomics and gene expression data hinted the involvement of MAP kinase pathway in GAs mediated hyphal inhibition. We highlighted that addition of GAs copurified several ribosomal proteins. We have also shown the upregulation of Nrg1p promoter and downregulation of Ume6p promoter in the presence of GAs that suggest us that GAs act partly through these two transcription factors. Besides, we observed

that GAs inhibit binding of Nrg1p to promoter region of *ALS3*, a hypha-specific gene. These findings add new insight into GAs mediated hyphal inhibition in *C. albicans*.

3.6 References

1. Odds, F.C. Activity of Cilofungin (LY121019) against *Candida* Species *in Vitro*. *Journal of Antimicrobial Chemotherapy* **1988**, *22*, 891–897, doi:10.1093/jac/22.6.891.

2. Dupont, P.F. *Candida albicans*, the Opportunist. A Cellular and Molecular Perspective. *J Am Podiatr Med Assoc* **1995**, *85*, 104–115, doi:10.7547/87507315-85-2-104.

3. Weig, M.; Groß, U.; Mühlschlegel, F. Clinical Aspects and Pathogenesis of *Candida* Infection. *Trends in Microbiology* **1998**, *6*, 468–470, doi:10.1016/S0966-842X(98)01407-3.

4. Mitchell, A.P. Dimorphism and Virulence in *Candida albicans*. *Current Opinion in Microbiology* **1998**, *1*, 687–692, doi:10.1016/S1369-5274(98)80116-1.

5. Saville, S.P.; Lazzell, A.L.; Monteagudo, C.; Lopez-Ribot, J.L. Engineered Control of Cell Morphology In Vivo Reveals Distinct Roles for Yeast and Filamentous Forms of *Candida albicans* during Infection. *Eukaryot Cell* **2003**, *2*, 1053–1060, doi:10.1128/EC.2.5.1053-1060.2003.

6. Noble, S.M.; French, S.; Kohn, L.A.; Chen, V.; Johnson, A.D. Systematic Screens of a *Candida albicans* Homozygous Deletion Library Decouple Morphogenetic Switching and Pathogenicity. *Nat Genet* **2010**, *42*, 590–598, doi:10.1038/ng.605.

7. Gow, N.A.R.; van de Veerdonk, F.L.; Brown, A.J.P.; Netea, M.G. *Candida albicans* Morphogenesis and Host Defence: Discriminating Invasion from Colonization. *Nat Rev Microbiol* **2012**, *10*, 112–122, doi:10.1038/nrmicro2711.

8. Lo, H.-J.; Köhler, J.R.; DiDomenico, B.; Loebenberg, D.; Cacciapuoti, A.; Fink, G.R. Nonfilamentous *C. albicans* Mutants Are Avirulent. *Cell* **1997**, *90*, 939–949, doi:10.1016/S0092-8674(00)80358-X.

9. Sudbery, P.E. Growth of *Candida albicans* Hyphae. *Nat Rev Microbiol* **2011**, *9*, 737–748, doi:10.1038/nrmicro2636.

10. Biswas, S.; Van Dijck, P.; Datta, A. Environmental Sensing and Signal Transduction Pathways Regulating Morphopathogenic Determinants of *Candida albicans*. *Microbiol Mol Biol Rev* **2007**, *71*, 348–376, doi:10.1128/MMBR.00009-06.

11. Whiteway, M.; Bachewich, C. Morphogenesis in *Candida albicans*. *Annu Rev Microbiol* **2007**, *61*, 529–553, doi:10.1146/annurev.micro.61.080706.093341.

12. Shapiro, R.S.; Robbins, N.; Cowen, L.E. Regulatory Circuitry Governing Fungal Development, Drug Resistance, and Disease. *Microbiol Mol Biol Rev* **2011**, *75*, 213–267, doi:10.1128/MMBR.00045-10.

13. Odds, F.C.; Kerridge, D. Morphogenesis in *Candida albicans*. *CRC Critical Reviews in Microbiology* **1985**, *12*, 45–93, doi:10.3109/10408418509104425.

14. Banerjee, M.; Thompson, D.S.; Lazzell, A.; Carlisle, P.L.; Pierce, C.; Monteagudo, C.; López-Ribot, J.L.; Kadosh, D. UME6, a Novel Filament-Specific Regulator of *Candida albicans* Hyphal Extension and Virulence. *Mol Biol Cell* **2008**, *19*, 1354–1365, doi:10.1091/mbc.E07-11-1110.

15. Zeidler, U.; Lettner, T.; Lassnig, C.; Müller, M.; Lajko, R.; Hintner, H.; Breitenbach, M.; Bito, A. UME6 Is a Crucial Downstream Target of Other Transcriptional Regulators of True Hyphal Development in *Candida albicans*. *FEMS Yeast Research* **2009**, *9*, 126–142, doi:10.1111/j.1567-1364.2008.00459.x.

16. Braun, B.R.; Kadosh, D.; Johnson, A.D. NRG1, a Repressor of Filamentous Growth in *C. albicans*, Is down-Regulated during Filament Induction. *EMBO J* **2001**, *20*, 4753–4761, doi:10.1093/emboj/20.17.4753.

17. Murad, A.M.A.; Leng, P.; Straffon, M.; Wishart, J.; Macaskill, S.; MacCallum, D.; Schnell, N.; Talibi, D.; Marechal, D.; Tekaia, F.; et al. NRG1 Represses Yeast–Hypha Morphogenesis and Hypha-Specific Gene Expression in *Candida albicans*. *EMBO J* **2001**, *20*, 4742–4752, doi:10.1093/emboj/20.17.4742.

18. Childers, D.S.; Kadosh, D. Filament Condition-Specific Response Elements Control the Expression of NRG1 and UME6, Key Transcriptional Regulators of Morphology and Virulence in *Candida albicans*. *PLoS One* **2015**, *10*, e0122775, doi:10.1371/journal.pone.0122775.

19. Vediyappan, G.; Dumontet, V.; Pelissier, F.; d'Enfert, C. Gymnemic Acids Inhibit Hyphal Growth and Virulence in *Candida albicans*. *PLoS One* **2013**, *8*, e74189, doi:10.1371/journal.pone.0074189.

20. Lu, Y.; Su, C.; Wang, A.; Liu, H. Hyphal Development in *Candida albicans* Requires Two Temporally Linked Changes in Promoter Chromatin for Initiation and Maintenance. *PLOS Biology* **2011**, *9*, e1001105, doi:10.1371/journal.pbio.1001105.

21. Huang, W.; Dong, Z.; Chen, Y.; Wang, F.; Wang, C.J.; Peng, H.; He, Y.; Hangoc, G.; Pollok, K.; Sandusky, G.; et al. Small-Molecule Inhibitors Targeting the DNA-Binding Domain of STAT3 Suppress Tumor Growth, Metastasis and STAT3 Target Gene Expression in Vivo. *Oncogene* **2016**, *35*, 783–792, doi:10.1038/onc.2015.215.

22. Chauvel, M.; Nesseir, A.; Cabral, V.; Znaidi, S.; Goyard, S.; Bachellier-Bassi, S.; Firon, A.; Legrand, M.; Diogo, D.; Naulleau, C.; et al. A Versatile Overexpression Strategy in the Pathogenic Yeast *Candida albicans*: Identification of Regulators of Morphogenesis and Fitness. *PLOS ONE* **2012**, *7*, e45912, doi:10.1371/journal.pone.0045912.

23. Puig, O.; Caspary, F.; Rigaut, G.; Rutz, B.; Bouveret, E.; Bragado-Nilsson, E.; Wilm, M.; Séraphin, B. The Tandem Affinity Purification (TAP) Method: A General Procedure of Protein Complex Purification. *Methods* **2001**, *24*, 218–229, doi:10.1006/meth.2001.1183.

24. Rigaut, G.; Shevchenko, A.; Rutz, B.; Wilm, M.; Mann, M.; Séraphin, B. A Generic Protein Purification Method for Protein Complex Characterization and Proteome Exploration. *Nat Biotechnol* **1999**, *17*, 1030–1032, doi:10.1038/13732.

25. Rupp, S. LacZ Assays in Yeast. *Methods Enzymol* **2002**, *350*, 112–131, doi:10.1016/s0076-6879(02)50959-9.

26. Osipov, S.; Tutyaeva, V.; Preobrazhenskaya, O.; Karpov, V. A Rapid Method for Liquid β-Galactosidase Reporter Assay in *Saccharomyces Cerevisiae*. *World J Microbiol Biotechnol* **2011**, *27*, 1255–1259, doi:10.1007/s11274-010-0546-9.

27. Jutras, B.L.; Verma, A.; Stevenson, B. Identification of Novel DNA Binding Proteins Using DNA Affinity Chromatography-Pulldown. *Curr Protoc Microbiol* **2012**, *CHAPTER*, Unit1F.1, doi:10.1002/9780471729259.mc01f01s24.

28. Braun, B.R.; Johnson, A.D. Control of Filament Formation in *Candida albicans* by the Transcriptional Repressor TUP1. *Science* **1997**, *277*, 105–109, doi:10.1126/science.277.5322.105.

29. Kadosh, D.; Johnson, A.D. Induction of the *Candida albicans* Filamentous Growth Program by Relief of Transcriptional Repression: A Genome-Wide Analysis. *Mol Biol Cell* **2005**, *16*, 2903–2912, doi:10.1091/mbc.E05-01-0073.

30. Calderone, R.A.; Fonzi, W.A. Virulence Factors of *Candida albicans*. *Trends in Microbiology* **2001**, *9*, 327–335, doi:10.1016/S0966-842X(01)02094-7.

31. Hube, B. From Commensal to Pathogen: Stage- and Tissue-Specific Gene Expression of *Candida albicans*. *Current Opinion in Microbiology* **2004**, *7*, 336–341, doi:10.1016/j.mib.2004.06.003.

32. Li, C.X.; Gleason, J.E.; Zhang, S.X.; Bruno, V.M.; Cormack, B.P.; Culotta, V.C. *Candida albicans* Adapts to Host Copper during Infection by Swapping Metal Cofactors for Superoxide Dismutase. *Proceedings of the National Academy of Sciences* **2015**, *112*, E5336–E5342, doi:10.1073/pnas.1513447112.

33. Kasahara, K.; Ohyama, Y.; Kokubo, T. Hmo1 Directs Pre-Initiation Complex Assembly to an Appropriate Site on Its Target Gene Promoters by Masking a Nucleosome-Free Region. *Nucleic Acids Res* **2011**, *39*, 4136–4150, doi:10.1093/nar/gkq1334.

34. Harcus, D.; Nantel, A.; Marcil, A.; Rigby, T.; Whiteway, M. Transcription Profiling of Cyclic AMP Signaling in *Candida albicans*. *Mol Biol Cell* **2004**, *15*, 4490–4499, doi:10.1091/mbc.E04-02-0144.

35. Sellam, A.; Chaillot, J.; Mallick, J.; Tebbji, F.; Richard Albert, J.; Cook, M.A.; Tyers, M. The P38/HOG Stress-Activated Protein Kinase Network Couples Growth to Division in *Candida albicans*. *PLoS Genet* **2019**, *15*, e1008052, doi:10.1371/journal.pgen.1008052.

36. Lee, J.E.; Oh, J.H.; Ku, M.; Kim, J.; Lee, J.S.; Kang, S.O. Ssn6 has dual roles in *Candida albicans* filament development through the interaction with Rpd31. *FEBS Lett* **2015**, 589(4):513-20. doi:10.1016/j.febslet.2015.01.011.

37. Leberer, E.; Harcus, D.; Dignard, D.; Johnson, L.; Ushinsky, S.; Thomas, D.Y.; Schröppel, K. Ras Links Cellular Morphogenesis to Virulence by Regulation of the MAP Kinase and CAMP Signalling Pathways in the Pathogenic Fungus *Candida albicans*. *Molecular Microbiology* **2001**, *42*, 673–687, doi:10.1046/j.1365-2958.2001.02672.x.

38. Lorenz, M.C.; Bender, J.A.; Fink, G.R. Transcriptional Response of *Candida albicans* upon Internalization by Macrophages. *Eukaryot Cell* **2004**, *3*, 1076–1087, doi:10.1128/EC.3.5.1076-1087.2004.

39. Carlisle, P.L.; Kadosh, D. A Genome-Wide Transcriptional Analysis of Morphology Determination in *Candida albicans*. *Mol Biol Cell* **2013**, *24*, 246–260, doi:10.1091/mbc.E12-01-0065.

40. Kadosh, D. Regulatory Mechanisms Controlling Morphology and Pathogenesis in *Candida albicans*. *Curr Opin Microbiol* **2019**, *52*, 27–34, doi:10.1016/j.mib.2019.04.005.

41. Mignone, F.; Gissi, C.; Liuni, S.; Pesole, G. Untranslated Regions of MRNAs. *Genome Biology* **2002**, *3*, reviews0004.1, doi:10.1186/gb-2002-3-3-reviews0004.

42. Pickering, B.M.; Willis, A.E. The Implications of Structured 5' Untranslated Regions on Translation and Disease. *Semin Cell Dev Biol* **2005**, *16*, 39–47, doi:10.1016/j.semcdb.2004.11.006.

43. Capolupo, A.; Esposito, R.; Zampella, A.; Festa, C.; Riccio, R.; Casapullo, A.; Tosco, A.; Monti, M.C. Determination of Gymnemic Acid I as a Protein Biosynthesis Inhibitor Using Chemical Proteomics. *J. Nat. Prod.* **2017**, *80*, 909–915, doi:10.1021/acs.jnatprod.6b00793.

44. Sorgo, A.G.; Heilmann, C.J.; Dekker, H.L.; Brul, S.; de Koster, C.G.; Klis, F.M. Mass Spectrometric Analysis of the Secretome of *Candida albicans*. *Yeast* **2010**, *27*, 661–672, doi:10.1002/yea.1775.

45. Hoyer, L.L.; Payne, T.L.; Bell, M.; Myers, A.M.; Scherer, S. *Candida albicans* ALS3 and Insights into the Nature of the ALS Gene Family. *Curr Genet* **1998**, *33*, 451–459, doi:10.1007/s002940050359.

Chapter 4 - Cell Surface Expression of Nrg1 Protein in *Candida auris*

Reprinted with permission from "Cell Surface Expression of Nrg1 Protein in *Candida auris*" by Anuja Paudyal and Govindsamy Vediyappan 2017. Journal of Fungi; 7(4): 262
doi: 10.3390/jof7040262

4.1 Abstract

Candida auris is an emerging antifungal resistant human fungal pathogen increasingly reported in healthcare facilities. It persists in hospital environments, and on skin surfaces, and can form biofilms readily. Here, we investigated the cell surface proteins from *C. auris* biofilms grown in a synthetic sweat medium mimicking human skin condition. Cell surface proteins from both biofilm and planktonic control cells were extracted with a buffer containing β-mercaptoethanol and resolved by 2-Dimensional (2-DE) gel electrophoresis. Some of the differentially expressed proteins were excised and identified by mass spectrometry. *C. albicans* orthologs Spe3p, Tdh3p, Sod2p, Ywp1p, and Mdh1p were overexpressed in biofilm cells when compared to the planktonic cells of *C. auris*. Interestingly, several proteins with zinc ion binding activity were detected. Nrg1p is a zinc- binding transcription factor that negatively regulates hyphal growth in *C. albicans*. *C. auris* does not produce true hypha under standard in vitro growth conditions, and the role of Nrg1p in *C. auris* is currently unknown. Western blot analyses of cell surface and cytosolic proteins of *C. auris* against anti-*Cal*Nrg1 antibody revealed the Nrg1p in both locations. Cell surface localization of Nrg1p in *C. auris*, an unexpected finding, was further confirmed by immunofluorescence microscopy. Nrg1p expression is uniform across all four clades of *C. auris* and is dependent on growth conditions. Taken together, the data

indicate that *C. auris* produces several unique proteins during its biofilm growth, which may assist in the skin-colonizing lifestyle of the fungus during its pathogenesis.

4.2 Introduction

Skin, a major interface between host and environment, is a habitat for several microbial populations. Many skin residing microbes have the ability to form skin biofilms that can lead to skin infection, and in certain conditions, can enter the body to cause life threatening bloodstream infections [1].

Candida auris is an emerging multi-drug resistant human fungal pathogen detected in many countries simultaneously [2]. It colonizes skin surfaces and can be invasive in immunocompromised patients [3]. *C. auris* has been isolated from blood, wounds, body fluids, and skin [4], where bloodstream infection is the most common infection leading to a mortality rate as high as 30–60% [5]. Additionally, the ability of *C. auris* to adhere to and to form drug-resistant biofilms has been a serious issue [6,7]. Until recently, *C. albicans* has been considered the major pathogen but recently, there has been increasing evidence showing *C. auris* involved in biofilm formation resulting in fatal bloodstream infections [8]. Unlike *C. albicans*, *C. auris* does not produce hyphae under *in vitro* conditions but it can form hyphae *in vivo* [9] or elongated pseudo hyphae in the presence of genotoxic compounds [10].

Nrg1p is a zinc-finger domain containing DNA-binding protein and is a key transcription factor that negatively regulates hyphal growth in *C. albicans* [11,12]. The *NRG1* transcript is down-regulated during hypha-inducing growth conditions, and its deletion has caused constitutive filamentous growth, similar to the *tup1* null mutant under yeast-promoting growth conditions because the expression of hypha-specific genes (e.g., *UME6*, *ECE1*, *HWP1*, etc.,) was

derepressed [12]. In a transcriptomic study, hundreds of genes were found to be differentially regulated in a *NRG1*-dependent and *NRG1-TUP1*-dependent manner. Studies have also shown that *C. albicans* Nrg1p plays important roles in biofilm formation and dispersion, and deletion or overexpression of *NRG1* blocks the yeast-to-hypha transition resulting in attenuated virulence [12–14]. However, the expression of *C. auris NRG1* and its role in virulence is unknown. Sweat media that mimics axillary skin condition promotes *C. auris* biofilm formation *in vitro* and biofilm produced by *C. auris* in this media was ten times more robust than that of biofilms formed by *C. albicans*. According to a recent study, high salinity and fatty acids mimicking sweat favors growth of *C. auris* allowing it to survive for 14 days whereas *C. albicans* survived for less than a week [15]. Since cell surface proteins play a major role in host cell adherence and biofilm formation, understanding their expression and their cellular roles in the pathogenicity of *C. auris* will help develop effective intervention strategies. We used sweat medium to study *C. auris* biofilm proteins.

In this study, we extracted non-glucan attached cell surface proteins from *C. auris* biofilm and planktonic cells, separated by 2-D gel electrophoresis, and identified some of the differentially expressed proteins by liquid chromatography coupled with mass spectrometry. We have also demonstrated an unexpected finding of cell surface localization of *C. auris* Nrg1p, which is a zinc-finger transcription factor and is predicted to be nuclear.

4.3 Materials and Methods

4.3.1 *C. auris* Strains and Growth Conditions

Candida species were routinely maintained on YPD (1% yeast extract, 2% peptone, and 2% dextrose) agar (1.5%). *Candida auris* isolated from Saudi Arabia by Abdalhamid et al. [16]

(South Asian, clade-I) was used for most of the experiments in this study. A single colony of this *C. auris* was inoculated into YPD broth medium and grown overnight at 37 °C with shaking at 200 rpm. For planktonic cells, overnight grown cells were used to inoculate 100 mL of fresh sweat medium to make a suspension of approximately 2×10^5 cells at an optical density of 0.05 (OD_{600}) and grown at 37 °C for 48 h with shaking (200 rpm). Sweat medium was prepared as mentioned by Horton et al. [15]. Biofilms were formed in cell culture treated dishes using the same cell density as for planktonic growth. They were allowed to grow at 37 °C for 48 h without disturbance. For pseudohyphal induction by hydroxyurea (HU) in *C. auris* [10], the sweat medium was used with and without 100 mM HU and grown statically for 48 h at 37 °C. *C. auris* strains **(Table 4.1)** (Clades II-IV), representing those from different countries, were obtained from the Centers for Disease Control and Prevention (CDC) and the Food and Drug Administration (FDA) Antibiotic Resistance (AR) isolate bank (Atlanta, GA, USA). List of all other strains used in this study are listed in **Table 4.1**.

Table 4.1. List of *Candida* fungal strains used in this study

Strains	Source
Candida auris (Lab strain #1126, Clade I)	Abdalhamid et. al. (2018) [16]
C. auris (AR#0381, Clade II)	Antibiotic Resistance (AR) Isolate Bank, the Centers for Disease Control and Prevention (CDC) and the Food and Drug Administration (FDA)
C. auris (AR#0383, Clade III)	AR Isolate Bank, CDC/FDA
C. auris (AR#0386, Clade IV)	AR Isolate Bank, CDC/FDA
C. albicans (Lab strain #1)	Wildtype (SC5314) [17]
C. albicans nrg1$^{-/-}$	Noble's deletion mutants [18]

4.3.2 Cell Surface Proteins Preparation

Planktonic cells were collected by centrifugation while biofilm cells were scraped from cell culture dishes using a cell scraper. Fungal cells were washed twice with sterile phosphate

buffered saline (PBS), pH 7.5, to remove residual media components. Cell surface proteins (non-glucan bound) were extracted from both planktonic and biofilm cells by resuspending them in ammonium carbonate (1.89 g/L) buffer containing 1% β-mercaptoethanol (BME) and incubated at 37 °C for 30 min as described [19,20]. Pooled BME extracts were dialyzed thoroughly against water and lyophilized before analyses.

4.3.3 2-Dimensional Gel Electrophoresis (2-DE)

Lyophilized cell surface proteins were resuspended in a small volume of sterile water and their concentration determined using the Bradford dye-binding method [21]. 2-DE was performed using the immobilized pH gradient (IPG) gels (Immobiline Drystrip, pH 3–10, NL, 7 cm, Cytiva, MA, USA). Aliquots of protein suspensions were diluted in IPG buffer as described by the manufacturer and applied to IPG gels. The gel strips were rehydrated overnight at room temperature. First dimension electrofocusing was performed using Multiphore-II unit (Pharmacia Biotech, Uppsala, Sweden) at 20 °C, 3500 volts for 6 h. Gels were equilibrated first in an equilibration buffer containing dithiothreitol for 15 min, then in a buffer containing iodoacetamide for another 15 min as recommended by the manufacturer. Electrofocused gel strips were run in the second dimension using 12.5% SDS-PAGE for 90 min at 100 V. Resolved proteins were stained by silver stain (Sigma-Aldrich, St. Louis, MO, USA) and images were recorded against a white light background. Cell surface proteins from at least two different biological samples were analyzed by 2-DE. Proteins that were differentially expressed were identified and some were excised for LC-MS/MS analysis. When necessary, 2-DE separated proteins were transferred to an Immobilon-P polyvinylidene fluoride (PVDF) membrane (Millipore Sigma, Billerica, MA, USA) electrophoretically for Western analysis.

4.3.4 Mass Spectrometry Analysis

Proteins from 2-DE were analyzed by a core facility service (DNA/Protein Resource Facility, Oklahoma State University, Stillwater, OK, USA). Proteins from the excised gel spots were digested with trypsin and collected. Peptides were dissolved in 0.1% formic acid, and injected onto a 75-micron × 55 cm nano HPLC column packed with 2-micron C18 media (Thermo Fisher PN 164942). Peptides were separated using 0.1% aqueous formic acid as mobile phase A and acetonitrile/water/formic acid (80:20:0.1) as mobile phase B to develop a gradient of 0–35% over 60 min. The column was terminated with stainless-steel emitter within a Nanospray Flex Ion source (Thermo Fisher, Waltham, MA, USA). The ion stream was analyzed in a quadrupole-Orbitrap tribrid mass spectrometer (Orbitrap Fusion model, Thermo Fisher, Waltham, MA, USA), using a data-dependent 5-second Top Speed method, wherein peptide precursors were measured in the Orbitrap sector, isolated in the quadrupole sector and fragmented in the ion routing multipole. After dissociation, peptide fragment ions were analyzed in the ion trap sector. The results were analyzed using MaxQuant software and the *C. auris* B8441 reference genome. Criteria such as peptide ion signal peak intensity, peptide spectral match (PSM)-based quantity, *Q* values, peptide mass, pI, and sequence coverage were included during analysis.

4.3.5 Bioinformatic Analyses

The amino acid sequence of Nrg1p from *C. albicans* (C7_04230W_A, Candida Genome Database, CGD) was blasted (NCBI blast) against that of *C. auris* (B9J08_005429, B8441, CGD) to determine the percent homology between them. Iterative Threading ASSEmbly Refinement (I-TASSER) [22] was used to generate a 3D model of *C. auris* and *C. albicans* Nrg1 protein based on previously available 3D structures of one or more closely related proteins.

Using 3D models from I-TASSER, structural alignment of *C. auris* and *C. albicans* Nrg1 was carried out using RaptorX structural alignment tool [23].

4.3.6 *NRG1* Cloning, Nrg1p Purification and Antibody Production

The gene (*NRG1*) encoding Nrg1p of *C. albicans* was synthesized and cloned in-frame in an *Escherichia coli* overexpression vector (pET24a, Kan^R, *Nde*I and *Xho*I, Epoch Life Sciences Inc., TX) that contains a 6-Histidine tag at its C-terminus. The plasmid was transformed into *E. coli* (BL21-DE3 or Rosetta) cells. Nrg1p was overexpressed by induction with 1 mM of isopropyl-β-d-1-thiogalactopyranoside (IPTG) in antibiotic containing medium. Expressed cells were pelleted and resuspended in phosphate buffer containing a protease inhibitors cocktail followed by cell lysis using a French press (19,000 psi) with centrifugation at 10,000 g for 10 min at 4 °C. Nrg1p from the supernatant was purified using Ni-NTA agarose beads (Qiagen, Valencia, USA) as recommended by the manufacturer. Thus, the purified Nrg1p was dialyzed against water, verified for homogeneity on SDS-PAGE and used for antibody production (*Cal*Nrg1 antibody) in a rabbit (LAMPIRE Biological Laboratories Pipersville, PA, USA).

4.3.7 Immunoblotting

*Cal*Nrg1 polyclonal antibody was used to detect *C. auris* Nrg1p. Cell surface and cytosolic proteins from both planktonic and biofilm cells were separated by SDS-PAGE after boiling and reducing conditions and transferred to an Immobilon-P PVDF membrane (Millipore Sigma, Billerica, MA, USA). The membrane was blocked using 5% non-fat dry milk in a buffer containing Tris-HCl, NaCl, and Tween-20 and blotted against an anti-rabbit *Cal*Nrg1 antibody followed by an anti-rabbit IgG-HRP conjugate (R & D System, Minneapolis, MN, USA). The

ECL Western Blotting Substrate (Thermo Scientific, Waltham, MA, USA) was used to detect the protein bands followed by imaging in Azure c600.

4.3.8 Immunofluorescence

C. auris cells grown in sweat medium for 48 h at 37 °C were collected and washed twice using PBS to remove media constituents. Immunofluorescence of *C. auris* after immunostaining was performed as described [24] with slight modifications. Briefly, cells were fixed in 4% formaldehyde for 15 min followed by a PBS wash. Fixed cells were then blocked with 3% BSA in PBS containing 0.1% Tween-20, washed with PBS and incubated with 1:100 anti-*Cal*Nrg1 antibody raised in a rabbit overnight at 4 °C. Cells were washed twice with PBS and further incubated in an anti-rabbit Alexa Fluor-secondary antibody (Thermo Fisher Scientific, Waltham, MA, USA) 1:100 for 2 h. Cells were washed three times and mounted on a slide to examine under a fluorescence microscope (Leica DM 6 B with a camera attached).

4.4 Results

4.4.1 Cell surface proteins are differentially expressed in planktonic and biofilm cells

Cell surface proteins play a major role in adhesion and biofilm formation. To identify the differentially expressed non-glucan attached cell surface proteins from biofilm and planktonic *C. auris* cells (strain #1126, Clade I, **Table 4.1**), we used proteomics approaches. Using 2-D gel electrophoresis followed by silver staining, several differentially expressed proteins can be found and representative images are shown **(Figure 4.1)**. Selected protein spots from the biofilm sample were excised from the gel and analyzed by mass spectrometry. These cell surface proteins are listed in **Table 4.2**. *C. albicans* ortholog proteins including Spe3p, Tdh3p, Sod2p,

Ywp1p and Mdh1p were present in high intensities in *C. auris* biofilm cells when compared to planktonic cells.

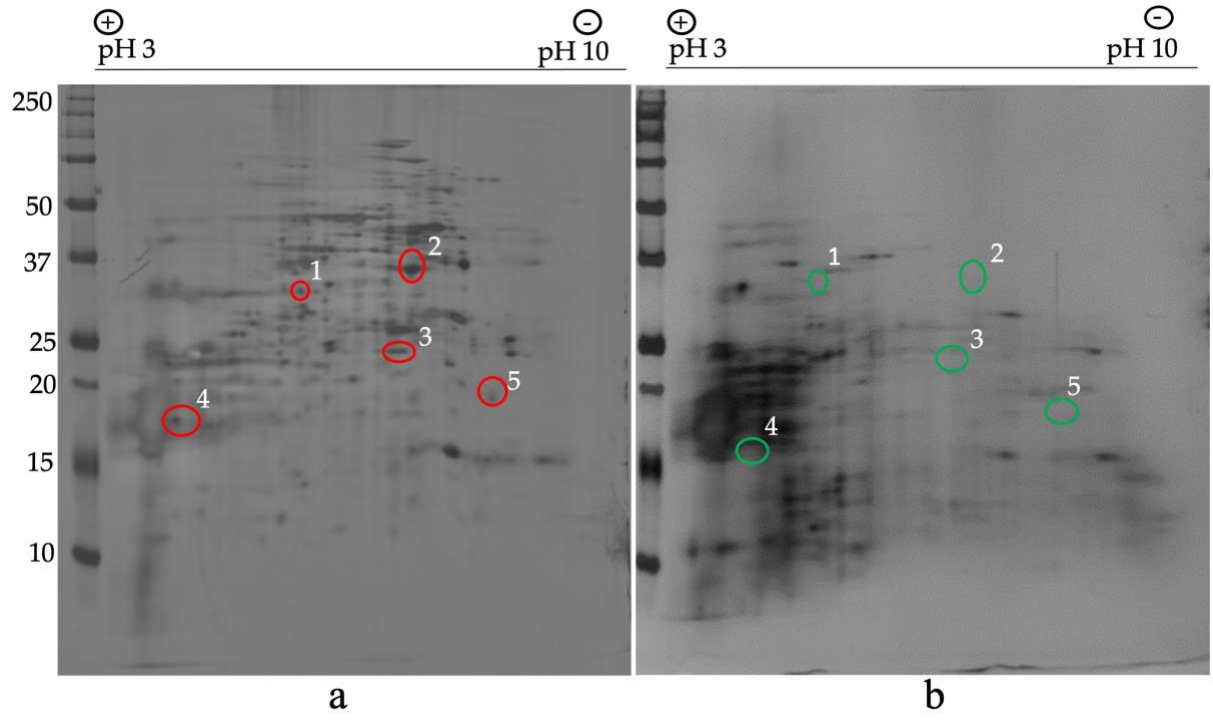

Figure 4.1. Cell surface proteins extracted from *Candida auris* biofilm and planktonic cells and resolved by 2-Dimensional Gel Electrophoresis (2-DE).

Silver stained gel images of proteins from biofilm **(a)** and planktonic cells **(b)**. Protein spots marked with red circles are excised out and identified by mass spectrometry. These proteins were expressed less or were absent in planktonic cells (marked in green circles).

Table 4.2. List of proteins identified by MS.

Proteins are selected on the basis of their peptide ion signal intensity, matching peptide and sequence coverage. Q-value of zero applies to all identified proteins.

Spot no.	Protein *C. auris*	Intensity	Number of Peptide	Seq. coverage (%)	Molecular Weight (kDa)		PH		Localization	Function	*C. albicans* ortholog
					Predicted	Experimental	Predicted	Experimental			
1	A0A2H0ZC50	85544000	8	18.3	33.618	25-37	5.12	5.9	Extracellular region	Spermidine synthase	Spe3p
2	A0A2H1A5V9	131870000	20	66.2	34.541	37	6.81	6.5	Extracellular region, mitochondria	Malate dehydrogenase precursor	Mdh1p
3	A0A2H1A3N7	8158000	10	42.2	25.404	25	7.16	6.5	Cytoplasm, mitochondria	Superoxide dismutase	Sod2p
4	A0A2H0ZMT8	305020	3	7	46.13	15-20	4.65	5	Cell surface, cell wall	Yeast form wall protein	Ywp1p
5	A0A2H0ZM53	46601000	9	29.3	35.336	20	7.13	7.3	Cytoplasm, cell wall, cell surface	Glyceraldehyde 3-phosphate dehydrogenase activity	Tdh3

Protein spot #1 is spermidine synthase (Spe3p). It localizes in the extracellular region and plays role in spermidine and pantothenate biosynthesis. Similarly, Tdh3p was also expressed more in the biofilm cells which are known to be located in the cytoplasm, cell wall and cell surface regions. An increased *TDH3* transcript has been reported in *C. albicans* biofilm [25]. The next protein that showed increased expression in biofilm cells was Sod2p (spot #3) which has superoxide dismutase activity and is known to be found in the mitochondrial matrix [26,27]. Ywp1p is a yeast wall protein-1 found on the cell surface and cell wall of yeasts known to be involved in adhesion and biofilm formation [28]. Mdh1 is a predicted malate dehydrogenase precursor and is found in the extracellular regions and mitochondria. It was upregulated in *C. albicans* when grown as a biofilm [29]. Future studies are required to identify additional proteins that are differentially expressed and validate them.

4.4.2 Nrg1 protein expresses in *C. auris* biofilm and planktonic Cells

C. albicans is known to cause biofilm-related infections and strains that are defective in hyphal growth fail to produce robust biofilm and matrix polysaccharides [30,31]. Nrg1p is a negative regulator of hyphal growth in *C. albicans*, but its role and expression of Nrg1 in *C.*

auris is unknown. Since *C. auris* produces yeast cells during *in vitro* biofilm growth and a gene encoding Nrg1p is present in *C. auris* (B8441 genome, B9J08_005429, *C. albicans* ortholog), we were interested in investigating it in *C. auris*. Further, Nrg1p is a zinc-binding transcription factor and we identified other zinc-binding proteins including Fba1p, Adh1p, Xyl2p and Pmi1p in our MS analysis, prompting us to investigate Nrg1p further.

To determine Nrg1p expression and localization in *C. auris*, we used an anti-*Cal*Nrg1 antibody (polyclonal) that we raised in our laboratory. Briefly, *C. albicans NRG1* with 6His tag at the C-terminus was cloned, overexpressed and purified in an *E. coli* expression system. The purified Nrg1 protein with a molecular weight of approximately 36 kDa reacted to both the anti-His and anti-*Cal*Nrg1 antibody **(Figure 4.2a)**. To examine Nrg1 protein expression in *C. auris*, it was grown in sweat medium as planktonic and biofilm cells. Using the *Cal*Nrg1 antibody, we detected an Nrg1 protein band of ~52 kDa in both the *C. auris* cell surface and cytosolic protein extracts of biofilm and planktonic cells **(Figure 4.2b)**. The predicted molecular weight of *C. auris* Nrg1p is 26.1 kDa (B9J08_005429) and the 52 kDa reactive band is likely to be a dimer of Nrg1p. Nrg1p is expressed slightly more in the cell surface proteins of biofilm than that of planktonic cells even though an equal amount of protein was used (Ponceau staining, data not shown). The antibody reacted to *C. albicans* cytosolic Nrg1 protein but none in the cell surface proteins (data not shown). The *Cal*Nrg1 antibody did not react to the cytosolic proteins of *C. albicans nrg1* -/- (null) mutant [18], consistent with its specificity for Nrg1p **(Figure 4.2b)**. Anti-GAPDH antibody (human, HRP-conjugated, Santa Cruz Biotechnology, TX, USA) reacted with a cytosol protein component but not with a cell surface protein component.

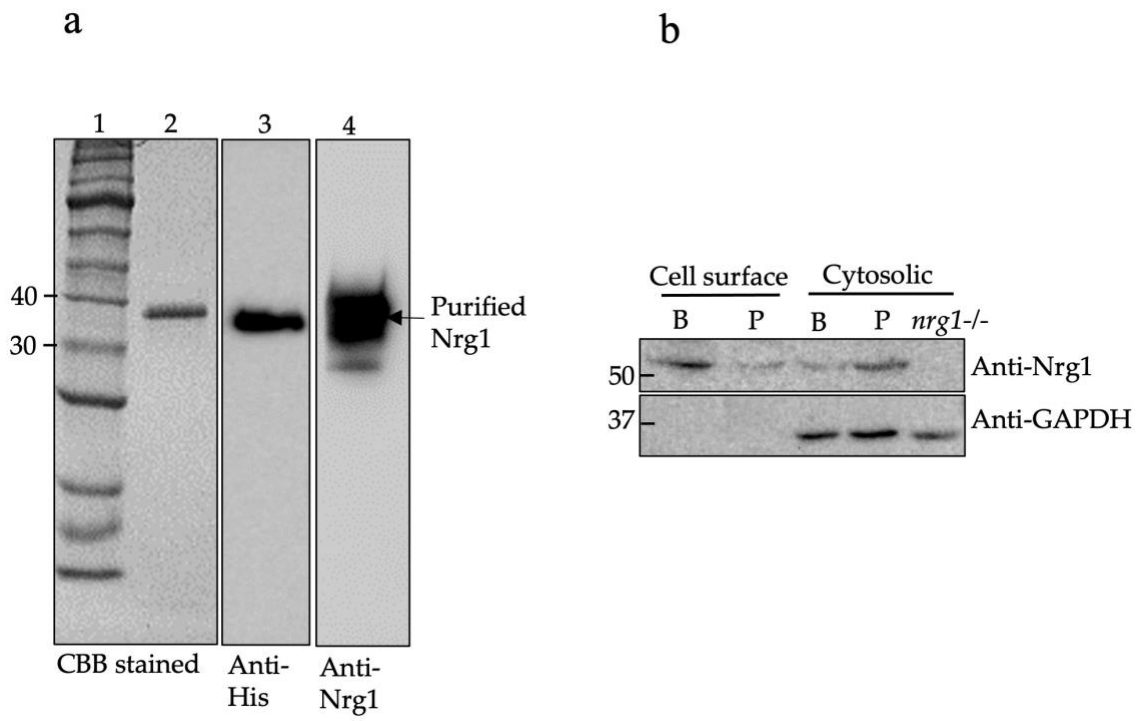

Figure 4.2. Purification of *C. albicans* Nrg1 protein overexpressed in *Escherichia coli* and the expression of Nrg1p in *C. auris* biofilm and planktonic cells.

(a) Purified r*Cal*Nrg1-6His protein separated on SDS-PAGE. Lane 1. Protein ladder (New England Biolab, Boston, MA, USA), Lane 2. Ni^{++} affinity purified *Cal*Nrg1p (Coomassie blue stained), Lane 3. Western blot of purified *Cal*Nrg1p against anti-His antibody, and Lane 4. Western blot of purified *Cal*Nrg1p against anti-*Cal*Nrg1 antibody. **(b)** Western blot of cell surface and cytosolic proteins of *C. auris* biofilm (B) and planktonic (P) cells probed with anti-*Cal*Nrg1 antibody. *C. albicans* $nrg^{-/-}$ was included as negative control. Anti-GAPDH HRP-conjugate provides loading and subcellular location controls.

4.4.3 Nrg1 proteins of *C. albicans* and *C. auris* are structurally similar

As a transcription factor, Nrg1p is predicted to be in the nucleus in *C. albicans* and the cell surface expression of this protein is unexpected. To understand the similarities of Nrg1 proteins between *C. auris* and *C. albicans*, we compared their amino acid sequences and aligned their predicted 3D structures using software. *C. albicans* and *C. auris* Nrg1 proteins contain 310 and 236 amino acids with predicted molecular weights of 34.3 kDa and 26.1 kDa, respectively. Sequence

alignment using Clustal Omega shows a total of 38% identity **(Figure 4.3a)**, and BLAST result shows 67% identity in the region between 185 to 220 of *C. auris* and 219 to 254 region of *C. albicans* Nrg1p. Based on structure prediction software, five structures were predicted for both *C. auris* and *C. albicans* Nrg1. Structures with the least C-score were picked for both proteins **(Figure 3b,c)**. Using these predicted structures, structural alignment was performed using RaptorX software **(Figure 4.3d)** and a TM (Template modeling) score of 0.667 was obtained which suggests that these two proteins share a similar fold. Interestingly, the C-terminal C_2H_2 zinc-finger domains between these two proteins are highly conserved **(Figure 4.3a–d)**. The zinc-finger domain is involved in DNA binding activity and this type of Class 1 zinc-finger protein is common in most of the eukaryotes [32]

a

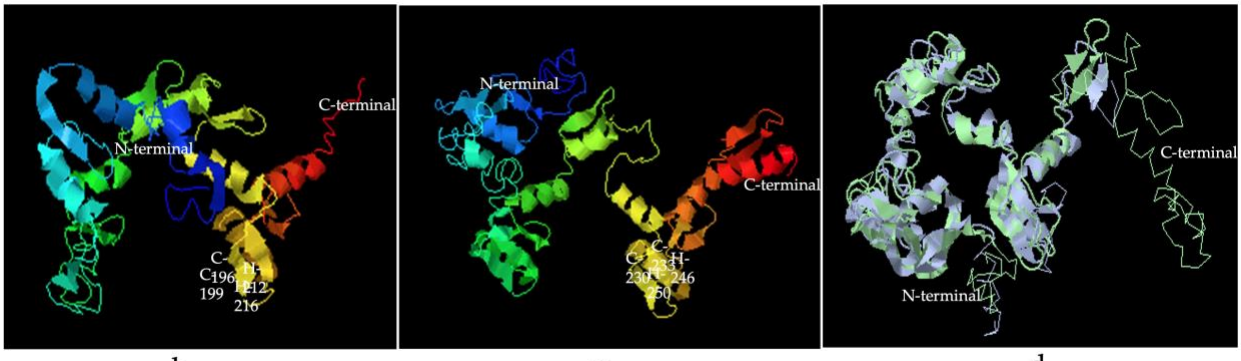

b c d

Figure 4.3. Comparison between Nrg1p of *C. auris* and *C. albicans*.

Alignment of amino acid sequences of Nrg1p of *C. auris* and *C. albicans* **(a)**. The Cys and His residues (C_2H_2 zinc-finger) and the identities between the amino acid residues are marked by gray boxes and asterisks, respectively. Predicted 3D structures of Nrg1p of *C. auris* **(b)** and *C. albicans* **(c)** using Iterative Threading ASSEmbly Refinement (I-TASSER). N-terminus, C-terminus and predicted zinc-binding domains are marked. **(d)** Structure alignment of *C. auris* Nrg1p (purple) and *C. albicans* Nrg1p (green) using predicted structures from I-TASSER. Note *C. auris* lacks 44 residues after the C_2H_2 zinc-finger domain (Class 1) at its C-terminus. The aligned image was tilted forward for better viewing, and hence the N-terminal regions appear different from images (b,c).

4.4.4 Nrg1 protein localizes on *C. auris* cell surface

Having verified bioinformatically the similarities of Nrg1 proteins between *C. auris* and *C. albicans* and detected the Nrg1p in the cell surface extract of *C. auris* during the 1st-dimensional SDS-PAGE/Western analysis **(Figures 4.2 and 4.3)**, we next wanted to determine if Nrg1p can be detected from the cell surface fraction of *C. auris* after 2-DE. This is also because we did not identify Nrg1p in our initial proteomic analyses of *C. auris* biofilm cell surface proteins (2-DE and MS, **Figure 4.1** and **Table 4.2**).

We used cell surface proteins (BME extract) collected from *C. auris* biofilm cells grown in the sweat medium and resolved by 2-DE **(Figure 4a)** as above and analyzed by Western blot against the *Cal*Nrg1 antibody. The result shows a single protein spot that reacted to the *Cal*Nrg1 antibody that matches the predicted size of 26 kDa of *C. auris* Nrg1 protein **(Figure 4b)**. To further validate the specificity of the *Cal*Nrg1 antibody to Nrg1 proteins of *Candida* species, the *Cal*Nrg1 antibody was depleted against the purified *C. albicans* rNrg1-6His protein and used for Western analysis. The depleted antibody failed to detect Nrg1 proteins of *C. auris* cytosolic proteins, suggesting its specificity to Nrg1p **(Figure S4.1).**

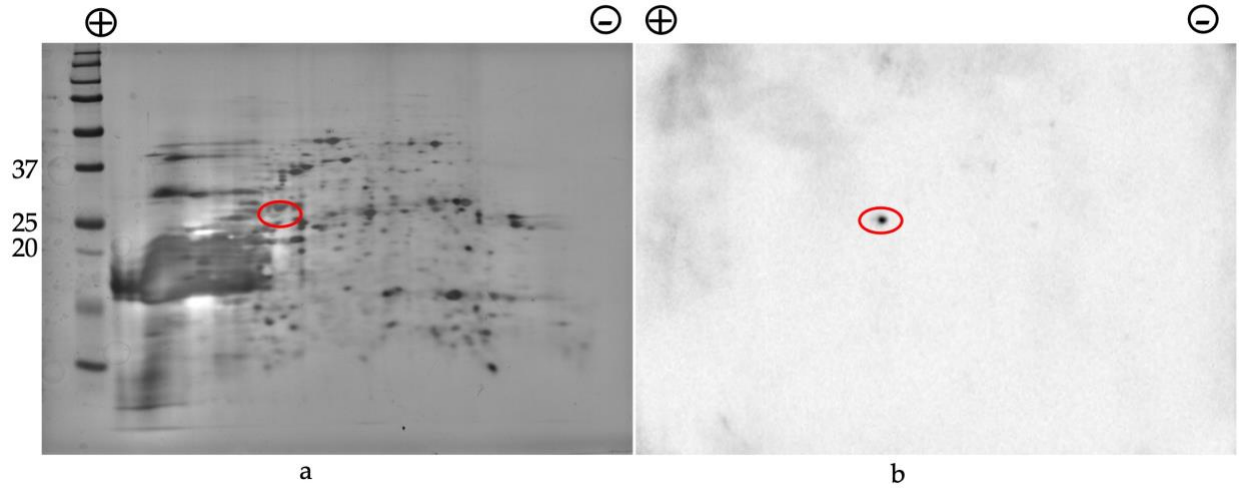

Figure 4.4. Nrg1p is localized in the cell surface extract of *C. auris*.

(a) The silver-stained SDS-PAGE gel image of cell surface proteins after 2-DE. **(b)**, Western analysis of the same proteins against rabbit anti-*Cal*Nrg1 antibody. The antibody reactive Nrg1p spot (marked in a red circle) with a molecular weight of around 26 kDa is shown in panel (b). All blue prestained protein standard (Bio-Rad, Hercules, CA, USA) was included in the 2nd dimension gel (a). Potential Nrg1p is marked in red circle (a).

To determine the surface localization of the Nrg1p on *C. auris* cells *in vivo*, we performed an immunofluorescence assay. *C. auris* cells were grown in synthetic sweat medium for 48 h and used *Cal*Nrg1 antibody (primary antibody) followed by a fluorescent secondary antibody as described in the Materials and Methods Section.

Interestingly, we observed Nrg1p expression on the surface of *C. auris* cells where several punctate fluorescence signals can be seen **(Figure 4.5)**. These fluorescence signals were discrete and found throughout the cell surface. Cells stained with a second antibody coupled with Alexa Fluor only (minus the primary antibody) did not show any fluorescent signal **(Figure 4.5, lower panel)**.

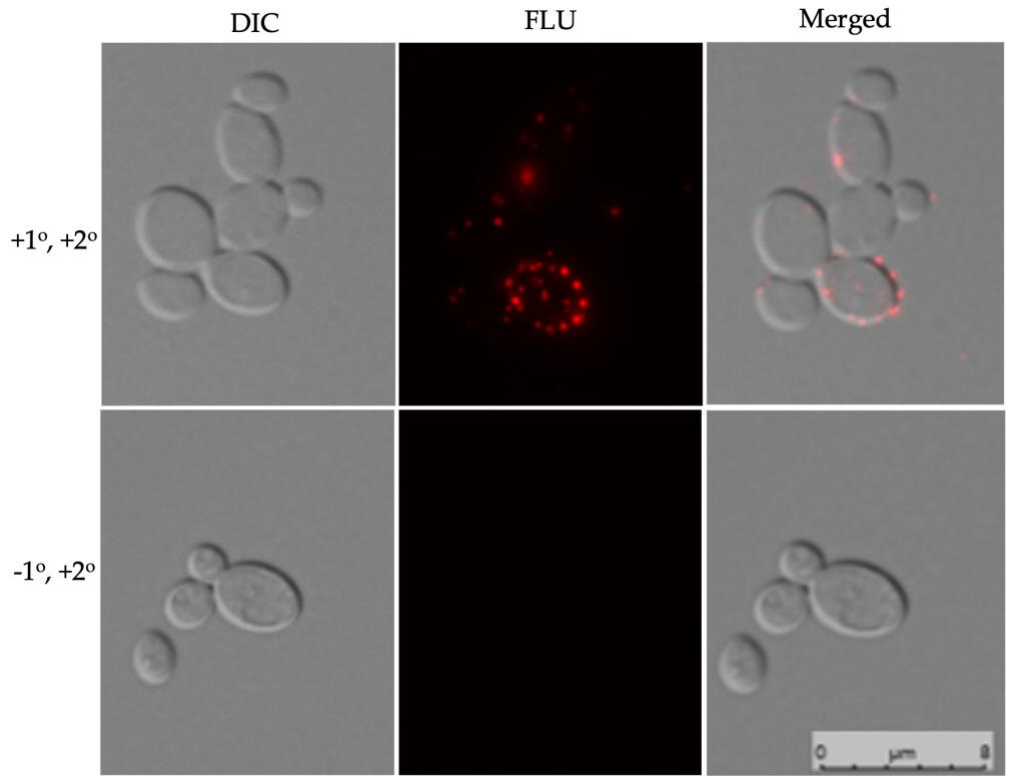

Figure 4.5. Immunofluorescence of cell surface expressed Nrg1p in *C. auris*.

Synthetic sweat media grown *C. auris* cells were stained with anti-*Cal*Nrg1 antibody followed by anti-rabbit Alexa Fluor-secondary antibody and observed under a fluorescence microscope **(upper panel)**. Cells without primary antibody (anti-*Cal*Nrg1 antibody) and with anti-rabbit Alexa Fluor-secondary antibody are showed in **lower panel** (control). Scale bar = 8 μm.

4.4.5 Nrg1 protein expresses in different clades of *C. auris* and is dependent on growth conditions

To know if Nrg1p expresses in different clades of *C. auris*, we obtained a panel of *C. auris* strains (Clades II-IV) from the CDC and used one strain from each clade along with *C. auris* strain #1126 (Clade I) to analyze Nrg1p expression. Cells grown in the sweat medium were homogenized and the cytosolic proteins were used for Western analysis. Results shown in **Figure 4.6a** indicate Nrg1p expresses in all the four strains representing different clades. We

also determined the expression of Nrg1p in a rich medium, YPD broth, and found it was poorly expressed in this medium when compared to the sweat medium **(Figure 4.6b)**.

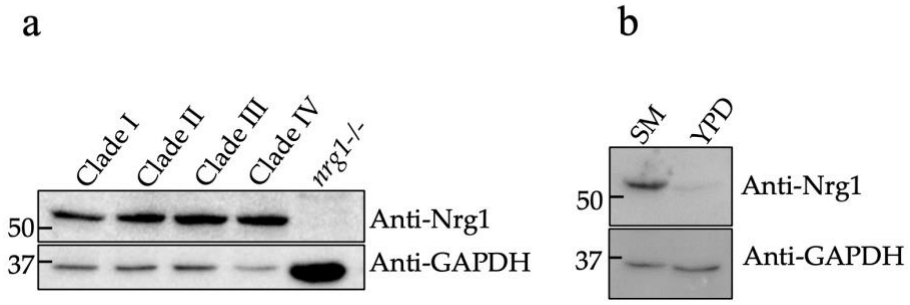

Figure 4.6. Nrg1p expression among different clades of *C. auris* and in different growth conditions.

(a) Western blot of cytosolic proteins of 4 different clades of *C. auris*. Clade 1 (South Asia, Saudi Arabia, lab strain #1126), Clade II (AR bank #0381, East Asia), Clade III (AR bank #0383, Africa), Clade IV (AR bank #0386, South America). *C. albicans nrg1*$^{-/-}$ null mutant was included as a negative control. Anti-GAPDH (human, HRP-conjugate) was used as a loading control. **(b)** Cytosolic proteins from *C. auris* grown in synthetic sweat medium (SM) and YPD broth medium were probed against anti-*Cal*Nrg1 antibody (upper panel). Equal amounts of protein loading were confirmed by use of anti-GAPDH-HRP conjugate (human) antibody.

4.4.6 Yeast-hypha regulation in *C. auris* could be different from *C. albicans*

C. albicans produces hyphae under hypha-inducing conditions (growth temperature at 37 °C, RPMI-1640 medium and media containing serum, etc.) whereas *C. auris* remains in the yeast form under these conditions, hinting that its hyphal regulatory pathway(s) may be non-functional or different. However, *C. auris* forms elongated pseudohyphal phenotype when treated with a genotoxic compound, hydroxyurea (HU) [10], while the control cells (without HU) were mostly yeast cells which allowed us to determine whether *C. auris* Nrg1 plays any role in the pseudohyphal growth. Western analysis of cytosolic proteins from these two growth forms showed no differences in the expression levels of Nrg1p **(Figure 4.7)**.

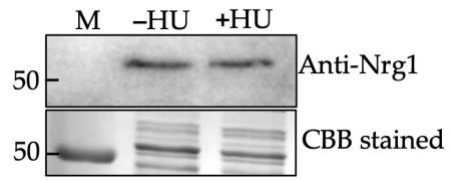

Figure 4.7. Nrg1p expression in *C. auris* treated with hydroxyurea (HU).

Western analysis of cytosolic proteins from *C. auris* against *Cal*Nrg1 antibody **(upper panel)**. Lane 1. Marker, Lane 2. Without HU, and Lane 3. With HU. SDS-PAGE gel of proteins from *C. auris* cells grown in sweat medium with and without HU followed by Coomassie brilliant blue (CBB) staining **(lower panel)**.

4.5 Discussion

Candida auris, a newly emerged drug-resistant human fungal pathogen, was first reported in 2009 in Japan [33] and since then it has been isolated in over 40 countries across 6 continents [34]. *C. auris* is resistant to almost all clinical antifungal drugs and the CDC has listed this pathogen at an urgent threat level (fact sheet, CDC).

Although *C. auris* can be isolated from multiple sites in the body, it predominantly colonizes the skin and also persists in the environment, particularly in healthcare settings. Skin infections caused by *C. auris* in humans could be in a biofilm status. Despite the fact that *C. auris* produces fewer dense biofilms than *C. albicans* [35,36], *C. auris* can survive at high salt and other stress conditions [37] normally found in the skin niche and able to produce biofilms. Researchers have shown that *C. auris* is able to form 10-fold more biofilm than that of *C. albicans* in a skin-mimicking synthetic sweat medium that contains high salts and various lipids [15]. *C. auris* also has a high ability to colonize the skin, as demonstrated using porcine skin as an ex vivo model [15]. The high tolerance of this fungus to salty sweat medium mimicking skin conditions may play a role in its pathogenicity and persistence. We, therefore, as a first step, aimed to analyze the cell surface proteins from *C. auris* biofilms grown in the sweat medium.

Fungal cell surface proteins play a major role in pathogenesis. These proteins are one of the major groups of molecules that mediate the initial contact with its surrounding environment. Some cell surface proteins are covalently attached to mannan and other polysaccharides. Earlier studies have shown that the cell surface proteins can be extracted using an alkaline buffer containing β-mercaptoethanol (BME) [19,20,38]. By employing this method, we extracted a covalently attached cell surface and other soluble proteins from *C. auris* biofilms developed in sweat medium. As a control, we used planktonic cells grown in the same medium. Using 2-DE and silver staining, several differentially expressed proteins were detected from the BME extract of biofilm cells **(Figure 4.1)**. This result shows that the *C. auris* biofilm produces some cell surface proteins at a higher level compared to planktonic cells. Although a limited number of protein spots were excised and analyzed by mass spectrometry, several of those detected are known to be found in the cell wall and/ or on the cell surface.

Upregulated proteins that we identified by proteomics of biofilm cells include Spe3, Mdh1, Sod2, Ywp1 and Tdh3 **(Table 4.2)**. Spe3p is involved in the biosynthesis of spermidine in *C. albicans* and also in many other fungi [39,40]. Spermidine is one of the three types of polyamines (putrescine and spermine are the others) that play a major role in various cellular processes including growth, oxidative and osmotic stress responses [39]. It is worth noting that *C. auris hog1* mutant was acutely sensitive to organic oxidative- and osmotic-stress-inducing agents [37]. Similarly, increased expression of Sod2p, the mitochondrial Mn-containing superoxide dismutase in *C. auris* biofilms, may provide antioxidant properties to the fungus against environmental or host oxidative stress. These proteins were shown to be overexpressed in *C. albicans* biofilms [41]. Certain proteins are involved in more than one cellular functions as in the case of *C. glabrata* Tdh3p that expressed more in biofilm than planktonic cells [42].

Proteomic analyses of cell surface proteins (BME) and extracellular vesicles of *C. albicans* yeast and hyphal morphologies were shown to contain Tdh3p [43,44]. Since Tdh3p is a moonlighting protein (involved in glycolysis, oxidoreductase activity and host–pathogen interaction), it may have some of these roles in *C. auris* biofilm growth. Future genetic studies (gene deletion or controlled expression) will determine the functional roles of these proteins in *C. auris* biofilm growth and virulence. *C. albicans* is known to cause biofilm-related infections and strains that are defective in hyphal growths fail to produce robust biofilms [30,31]. In contrast to the *C. albicans* biofilm production phenotype, *C. auris* produces ten-fold more biofilm without producing hyphae but with yeast cells [15]. This distinctive *C. auris* phenotype prompted us to search for a major negative regulator(s) of hyphal growth in *C. auris*. In conjunction with this notion, we have also identified some zinc-binding proteins in our 2-DE mass spectometry analyses. Nrg1p is a zinc-binding transcription factor that regulates hyphal growth negatively in co-operation with Tup1p in *C. albicans* [11], and the role and expression levels of Nrg1p in *C. auris* is unknown, although an ortholog is present. Further, Tup1, a zinc transcription factor similar to Nrg1p, has no hyphal regulatory function in *C. auris* [10]. Using an anti-Nrg1 antibody, we showed that Nrg1p is present in the cell surface extracts from both types of cells **(Figure 4.2a).** To confirm that the cell surface proteins are not contaminated with the cytosolic proteins during BME extraction, we probed these proteins with an anti-GAPDH (human) antibody that reacts only to the cytosolic proteins but not to the cell surface proteins. The presence of Nrg1p in the BME extract of *C. auris* biofilm cells was further demonstrated by a 2-DE resolved Western blot **(Figure 4.4b)**. Interestingly, the immunofluorescence assay clearly showed the presence of Nrg1p on the cell surfaces of *C. auris in vivo* **(Figure 4.5)**. Taken together, a zinc transcription factor Nrg1p, normally found in the

nucleus, can also be present on the cell surface of *C. auris* cells. However, the mechanism of Nrg1p transport to the cell surface and its function(s) on the cell surface remain to be determined.

Structural data for fungal Nrg1p are not available. However, the three-dimensional prediction of Nrg1 proteins from *C. auris* and *C. albicans* by the I-TASSER program and their structural alignment by RaptorX programs rendered a superimposed model showing Nrg1 proteins from both species have a similar fold **(Figure 3,b–d)**. Importantly, the zinc-binding and the DNA-binding C-terminal regions are highly conserved and similar in structure, including the alpha-helices and ß-sheet folds of the DNA binding regions of the Class-I zinc-finger transcription factors [32]. It is unclear if the lack of 44 residues at the C-terminus of Nrg1 in *C. auris* may have functional implications.

It is reasonable to speculate that the hyphal regulatory role of Nrg1p in *C. auris* may be different or absent from *C. albicans* Nrg1p. For example, *C. albicans* hyphae and pseudohyphae were shown to convert into yeast cells when they were treated with hyphal growth inhibitors called gymnemic acids (GAs) [45]. However, when pseudohyphae of *C. auris* were treated with GAs, they did not revert to yeasts and they remain pseudohyphae (data not shown). Further, the expression level of Nrg1p in yeast and pseudohyphal growth forms of *C. auris* without and with HU, respectively, did not show any differences between the two growth forms **(Figure 4.7)** which may suggest that Nrg1p may have a limited role in the yeast-hyphal morphogenesis in *C. auris*. Alternatively, the growth condition or host niche-dependent cues may regulate hyphal morphogenesis in this fungus. When *C. auris* was grown in YPD with 10% NaCl, elongated pseudohyphal-like cells were formed [46]. Similarly, *C. auris* can filament when it is passaged in the mammalian body [9]. It is also worth mentioning that the representative strains from all four

clades (Clade I-IV) that we analyzed contain Nrg1p **(Figure 4.6a)**. Thus, *C. auris* is more tolerant to various stress conditions when compared to other *Candida* species which might help in the unique lifestyle of *C. auris*.

In conclusion, *C. auris* produces several differentially expressed cell surface proteins during its biofilm growth. Despite its predominant yeast form of growth, *C. auris* produces robust biofilm, and the Nrg1 ortholog is expressed on the cell surface of *C. auris*. While the function of Nrg1p is currently unknown, representative strains from all four known clades of *C. auris* express Nrg1p.

4.6 References

1. Krüger, W.; Vielreicher, S.; Kapitan, M.; Jacobsen, I.D.; Niemiec, M.J. Fungal-Bacterial Interactions in Health and Disease. *Pathogens* **2019**, *8*, 70.

2. Lockhart, S.R.; Etienne, K.A.; Vallabhaneni, S.; Farooqi, J.; Chowdhary, A.; Govender, N.P.; Colombo, A.L.; Calvo, B.; Cuomo, C.A.; Desjardins, C.A.; et al. Simultaneous Emergence of Multidrug-Resistant *Candida auris* on 3 Continents Confirmed by Whole-Genome Sequencing and Epidemiological Analyses. *Clin. Infect Dis.* **2017**, *64*, 134–140.

3. Iguchi, S.; Itakura, Y.; Yoshida, A.; Kamada, K.; Mizushima, R.; Arai, Y.; Uzawa, Y.; Kikuchi, K. *Candida auris*: A pathogen difficult to identify, treat, and eradicate and its characteristics in Japanese strains. *J. Infect. Chemother.* **2019**, *25*, 743–749.

4. Adams, E.; Quinn, M.; Tsay, S.; Poirot, E.; Chaturvedi, S.; Southwick, K.; Greenko, J.; Fernandez, R.; Kallen, A.; Vallabhaneni, S.; et al. *Candida auris* in Healthcare Facilities, New York, USA, 2013–2017. *Emerg. Infect. Dis.* **2018**, *24*, 1816–1824.

5. Chowdhary, A.; Sharma, C.; Duggal, S.; Agarwal, K.; Prakash, A.; Singh, P.K. New clonal strain of *Candida auris*, Delhi, India. *Emerg. Infect. Dis.* **2013**, *19*, 1670–1673.

6. Calvo, B.; Melo, A.S.; Perozo-Mena, A.; Hernandez, M.; Francisco, E.C.; Hagen, F.; Meis, J.F.; Colombo, A.L. First report of *Candida auris* in America: Clinical and microbiological aspects of 18 episodes of candidemia. *J. Infect.* **2016**, *73*, 369–374.

7. Chakrabarti, A.; Sood, P.; Rudramurthy, S.M.; Chen, S.; Kaur, H.; Capoor, M.; Chhina, D.; Rao, R.; Eshwara, V.K.; Xess, I.; et al. Incidence, characteristics and outcome of ICU-acquired candidemia in India. *Intensiv. Care Med.* **2014**, *41*, 285–295.

8. Borman, A.M.; Szekely, A.; Johnson, E.M. Comparative Pathogenicity of United Kingdom Isolates of the Emerging Pathogen *Candida auris* and Other Key Pathogenic Candida Species. *mSphere* **2016**, *1*, e00189-16.

9. Yue, H.; Bing, J.; Zheng, Q.; Zhang, Y.; Hu, T.; Du, H.; Wang, H.; Huang, G. Filamentation in *Candida auris*, an emerging fungal pathogen of humans: Passage through the mammalian body induces a heritable phenotypic switch. *Emerg. Microbes Infect.* **2018**, *7*, 188.

10. Bravo Ruiz, G.; Ross, Z.K.; Gow, N.A.R.; Lorenz, A. Pseudohyphal Growth of the Emerging Pathogen *Candida auris* Is Triggered by Genotoxic Stress through the S Phase Checkpoint. *mSphere* **2020**, *5*, doi:10.1128/mSphere.00151-20.
11. Braun, B.R.; Kadosh, D.; Johnson, A.D. NRG1, a repressor of filamentous growth in *Candida albicans*, is down-regulated during filament induction. *EMBO J.* **2001**, *20*, 4753–4761.

12. Murad, A.A.; Leng, P.; Straffon, M.; Wishart, J.; Macaskill, S.; Maccallum, D.M.; Schnell, N.; Talibi, D.; Marechal, D.; Tekaia, F.; et al. NRG1 represses yeast-hypha morphogenesis and hypha-specific gene expression in *Candida albicans*. *EMBO J.* **2001**, *20*, 4742–4752.

13. Uppuluri, P.; Pierce, C.G.; Thomas, D.P.; Bubeck, S.S.; Saville, S.P.; Lopez-Ribot, J.L. The Transcriptional Regulator Nrg1p Controls *Candida albicans* Biofilm Formation and Dispersion. *Eukaryot. Cell* **2010**, *9*, 1531–1537.

14. Saville, S.P.; Lazzell, A.L.; Monteagudo, C.; Lopez-Ribot, J.L. Engineered Control of Cell Morphology in vivo Reveals Distinct Roles for Yeast and Filamentous Forms of *Candida albicans* during Infection. *Eukaryot. Cell* **2003**, *2*, 1053–1060.

15. Horton, M.V.; Johnson, C.J.; Kernien, J.F.; Patel, T.D.; Lam, B.C.; Cheong, J.Z.A.; Meudt, J.J.; Shanmuganayagam, D.; Kalan, L.R.; Nett, J.E. *Candida auris* Forms High-Burden Biofilms in Skin Niche Conditions and on Porcine Skin. *mSphere* **2020**, *5*, doi:10.1128/msphere.00910-19.

16. Abdalhamid, B.; Almaghrabi, R.; Althawadi, S.; Omrani, A. First report of *Candida auris* infections from Saudi Arabia. *J. Infect. Public Health* **2018**, *11*, 598–599.

17. Gillum, A.M.; Tsay, E.Y.H.; Kirsch, D.R. Isolation of the *Candida albicans* gene for orotidine-5′-phosphate decarboxylase by complementation of S. cerevisiae ura3 and E. coli pyrF mutations. *Mol. Genet. Genom.* **1984**, *198*, 179–182.

18. Noble, S.M.; French, S.; Kohn, L.A.; Chen, V.; Johnson, A.D. Systematic screens of a *Candida albicans* homozygous deletion library decouple morphogenetic switching and pathogenicity. *Nat. Genet.* **2010**, *42*, 590–598.

19. Casanova, M.; Chaffin, W.L. Cell wall glycoproteins of *Candida albicans* as released by different methods. *J. Gen. Microbiol.* **1991**, *137*, 1045–1051.

20. Vediyappan, G.; Bikandi, J.; Braley, R.; Chaffin, W.L. Cell surface proteins of *Candida albicans*: Preparation of extracts and improved detection of proteins. *Electrophoresis* **2000**, *21*, 956–961.

21. Bradford, M.M. A rapid and sensitive method for the quantitation of microgram quantities of protein utilizing the principle of protein-dye binding. *Anal. Biochem.* **1976**, *72*, 248–254.

22. Roy, A.; Kucukural, A.; Zhang, Y. I-TASSER: A unified platform for automated protein structure and function prediction. *Nat. Protoc.* **2010**, *5*, 725–738.

23. Peng, J.; Xu, J. Raptorx: Exploiting structure information for protein alignment by statistical inference. *Proteins Struct. Funct. Bioinform.* **2011**, *79*, 161–171.
24. Pemberton, L.F. Preparation of Yeast Cells for Live-Cell Imaging and Indirect Immunofluorescence. *Adv. Struct. Saf. Stud.* **2014**, *1205*, 79–90.

25. Bonhomme, J.; Chauvel, M.; Goyard, S.; Roux, P.; Rossignol, T.; D'Enfert, C. Contribution of the glycolytic flux and hypoxia adaptation to efficient biofilm formation by *Candida albicans*. *Mol. Microbiol.* **2011**, *80*, 995–1013.

26. Hwang, C.S.; Rhie, G.; Kim, S.T.; Kim, Y.R.; Huh, W.K.; Baek, Y.U.; Kang, S.O. Copper- and zinc-containing superoxide dismutase and its gene from *Candida albicans*. *Biochim. Biophys. Acta* **1999**, *1427*, 245–255.

27. Rhie, G.E.; Hwang, C.S.; Brady, M.; Kim, S.T.; Kim, Y.R.; Huh, W.K.; Baek, Y.U.; Lee, B.H.; Lee, J.S.; Kang, S.O. Manganese-containing superoxide dismutase and its gene from *Candida albicans*. *Biochim. Biophys. Acta* **1999**, *1426*, 409–419.

28. Granger, B.L.; Flenniken, M.L.; Davis, D.A.; Mitchell, A.P.; Cutler, J.E. Yeast wall protein 1 of *Candida albicans*. *Microbiology* **2005**, *151*, 1631–1644.

29. Seneviratne, C.J.; Wang, Y.; Jin, L.; Abiko, Y.; Samaranayake, L.P. *Candida albicans* biofilm formation is associated with increased anti-oxidative capacities. *Proteomics* **2008**, *8*, 2936–2947.

30. Mitchell, K.F.; Zarnowski, R.; Andes, D.R. Fungal Super Glue: The Biofilm Matrix and Its Composition, Assembly, and Functions. *PLoS Pathog.* **2016**, *12*, e1005828.

31. Richard, M.L.; Nobile, C.J.; Bruno, V.M.; Mitchell, A.P. *Candida albicans* Biofilm-Defective Mutants. *Eukaryot. Cell* **2005**, *4*, 1493–1502.

32. MacPherson, S.; LaRochelle, M.; Turcotte, B. A Fungal Family of Transcriptional Regulators: The Zinc Cluster Proteins. *Microbiol. Mol. Biol. Rev.* **2006**, *70*, 583–604.

33. Satoh, K.; Makimura, K.; Hasumi, Y.; Nishiyama, Y.; Uchida, K.; Yamaguchi, H. *Candida auris* sp. nov., a novel ascomycetous yeast isolated from the external ear canal of an inpatient in a Japanese hospital. *Microbiol. Immunol.* **2009**, *53*, 41–44.

34. Du, H.; Bing, J.; Hu, T.; Ennis, C.L.; Nobile, C.J.; Huang, G. *Candida auris*: Epidemiology, biology, antifungal resistance, and virulence. *PLoS Pathog.* **2020**, *16*, e1008921.

35. Sherry, L.; Ramage, G.; Kean, R.; Borman, A.; Johnson, E.M.; Richardson, M.D.; Rautemaa-Richardson, R. Biofilm-Forming Capability of Highly Virulent, Multidrug-Resistant *Candida auris*. *Emerg. Infect. Dis.* **2017**, *23*, 328–331.

36. Larkin, E.; Hager, C.; Chandra, J.; Mukherjee, P.K.; Retuerto, M.; Salem, I.; Long, L.; Isham, N.; Kovanda, L.; Borroto-Esoda, K.; et al. The Emerging Pathogen *Candida auris*: Growth Phenotype, Virulence Factors, Activity of Antifungals, and Effect of SCY-078, a Novel Glucan Synthesis Inhibitor, on Growth Morphology and Biofilm Formation. *Antimicrob. Agents Chemother.* **2017**, *61*, doi:10.1128/aac.02396-16.

37. Day, A.M.; McNiff, M.M.; Dantas, A.D.S.; Gow, N.A.R.; Quinn, J. Hog1 Regulates Stress Tolerance and Virulence in the Emerging Fungal Pathogen *Candida auris*. *mSphere* **2018**, *3*, e00506-18.

38. Chaffin, W.L. *Candida albicans* cell wall proteins. *Microbiol. Mol. Biol. Rev.* **2008**, *72*, 495–544.

39. Valdés-Santiago, L.; Ruiz-Herrera, J. Stress and polyamine metabolism in fungi. *Front. Chem.* **2014**, *1*, 42.

40. Rocha, R.O.; Wilson, R.A. Essential, deadly, enigmatic: Polyamine metabolism and roles in fungal cells. *Fungal Biol. Rev.* **2019**, *33*, 47–57.

41. Martínez-Gomariz, M.; Perumal, P.; Mekala, S.; Nombela, C.; Chaffin, W.L.; Gil, C. Proteomic analysis of cytoplasmic and surface proteins from yeast cells, hyphae, and biofilms of *Candida albicans*. *Proteomics* **2009**, *9*, 2230–2252.

42. Seneviratne, C.J.; Wang, Y.; Jin, L.; Abiko, Y.; Samaranayake, L.P. Proteomics of drug resistance in *Candida glabrata* biofilms. *Proteomics* **2010**, *10*, 1444–1454.

43. Gil-Bona, A.; Parra-Giraldo, C.M.; Hernáez, M.L.; Reales-Calderon, J.A.; Solis, N.V.; Filler, S.G.; Monteoliva, L.; Gil, C. *Candida albicans* cell shaving uncovers new proteins involved in cell wall integrity, yeast to hypha transition, stress response and host–pathogen interaction. *J. Proteom.* **2015**, *127*, 340–351.

44. Gil-Bona, A.; Amador-García, A.; Gil, C.; Monteoliva, L. The external face of *Candida albicans*: A proteomic view of the cell surface and the extracellular environment. *J. Proteom.* **2018**, *180*, 70–79.

45. Vediyappan, G.; Dumontet, V.; Pelissier, F.; D'Enfert, C. Gymnemic Acids Inhibit Hyphal Growth and Virulence in *Candida albicans*. *PLoS ONE* **2013**, *8*, e74189.

46. Wang, X.; Bing, J.; Zheng, Q.; Zhang, F.; Liu, J.; Yue, H.; Tao, L.; Du, H.; Wang, Y.; Wang, H.; et al. The first isolate of *Candida auris* in China: Clinical and biological aspects. *Emerg. Microbes Infect.* **2018**, *7*, 93.

Chapter 5 - Interaction of *Candida auris* with a skin colonizing bacterium *Staphylococcus aureus*

5.1 Abstract

Candida auris is a recently emerged antifungal-resistant human fungal pathogen that is stable in the environment for weeks and causes severe illness in hospitalized patients. It colonizes on skin surface and can cause systemic infections especially in immunocompromised individuals. Several other fungal and bacterial species reside on skin such as other *Candida* spp., *Malassezia*, *Staphylococcus* spp., and others. Polymicrobial infections are tough to treat especially when they form adherent biofilms and are resistant to antimicrobials such as *C. auris* and *Staphylococcus aureus*. *S. aureus* is an antibiotic-resistant bacterial pathogen and is known to cause community- and hospital-associated infections. Both pathogens colonize on skin surfaces and can spread systemically if the mucosal barrier is compromised. We hypothesized that these two pathogens can interact synergistically and could form a mixed-species biofilm that could be more virulent than either species alone. To test our hypothesis, we grew these two microbes as a mixture and individually on an environment that mimics human skin conditions. Biofilms were quantified along with determination of enzymatic activities. Interestingly, *C. auris*-*S. aureus* mixed biofilms showed significantly increased biomass when compared to single-species biofilms. Similarly, enhanced hemolytic activity was also observed in the mixed-species biofilms whereas, *C. auris* alone did not show any hemolytic activity. We have also analyzed the culture medium for quorum sensing (QS) molecule from *C. auris* and demonstrated that *C. auris* secretes a quorum sensing molecule that inhibits filamentation in *C. albicans*. Taken together, being drug-resistant, environmentally stable, and skin-colonizing pathogens, *C.*

auris and *S. aureus* can co-exist as biofilms and can cause augmented lethal infections if not diagnosed and treated promptly.

5.2 Introduction

Microbes interact with each other directly or indirectly in several niches of human body. Human skin microflora consists of a diverse range of microbes. Particularly, the microbes that are able to form biofilms are of major concern [1]. Biofilm related polymicrobial infections are difficult to treat, especially when mixed biofilms consist of bacteria and fungi. This is mostly due to the development of several virulence factors and resistance against antimicrobials when they colonize together adhering to one another or any available substrates. Due to these characteristics, it becomes difficult to get rid of the adherent biofilm with antimicrobials and may require surgical interventions [2]. Hence, studies to identify microbial interactions is important in developing effective therapeutic strategies.

C. auris colonizes on the skin and has also been found to form persistent biofilms on the surface areas of wounds, catheters, medical equipment, and devices which can lead to bloodstream infection especially in immunocompromised individuals. It has been found to be resistant against almost all antifungals available. Also, its ability to adhere, and remain viable for more than two weeks has been a major concern [3–6]. On the other hand, *S. aureus* is a ubiquitous Gram-positive bacterium mostly residing in nasal mucosa and skin. When it colonizes skin, it can grow to form biofilm leading to damage to epidermal and dermal layers of the skin and causing deeper infection. And when it enters the body, it can spread to different body parts including circulatory system that can lead to fatal bloodstream infection [2]. *S. aureus* and *C. auris* (mono-species) have developed resistance against existing antibiotics and antifungals,

respectively. The mono-species biofilms serve as the source of systemic infection (*e. g.* blood-stream infections and endocarditis) and are highly resistant to conventional antimicrobials resulting in therapeutic failure [7] .

Synthetic sweat medium mimics the human skin environment and favors the growth of *C. auris*. In fact, *C. auris* was able to form a denser biofilm than *C. albicans* in sweat medium. This medium typically consists of salt, glucose, amino acids, and fatty acids [6]. As *S. aureus* grow well on skin and high salt environment, we used sweat medium for establishing both mono- and dual-species biofilms.

During polymicrobial interaction and especially when cell density is high, microbes secrete quorum sensing (QS) molecules that act as signaling molecules to cope with the changing environment. Both *C. albicans* and *S. aureus* secrete QS molecules. Farnesol is one of the major quorum sensing molecules known to be produced by *C. albicans* along with several other *Candida* species [8,9]. However, whether or not *C. auris* produces farnesol is unknown. Farnesol inhibits biofilm formation in *S. aureus* at a concentration of 200 μM or more along with sensitization of resistant *S. aureus* to antimicrobials [10]. Although a different study showed that the nanomolar concentration of farnesol increases *S. aureus* growth and biofilm [11]. So, we were interested in knowing if *C. auris* produces farnesol or farnesol-like molecules and if such molecules have any effect on *S. aureus* biofilm.

Both *C. auris* and *S. aureus* reside on skin and wound surfaces, and both are capable of forming biofilms on skin surface [6,12], but to our knowledge, their interactions and combined virulence effects have not been studied at all. In this study, we identified ability of dual biofilm formation by *C. auris* and *S. aureus* in skin mimicking environment. We also determined their biochemical properties such as hemolytic, phospholipase and proteolytic activities. We also

demonstrated farnesol-like molecule produced by *C. auris* in the growth medium that blocked filamentation in *C. albicans* and this molecule slightly increased biofilm in *S. aureus*.

5.3 Materials and Methods

5.3.1 Strains and Growth Conditions

Candida auris (South Asian, clade-I) strain was used in this study [13] and was routinely maintained in YPD (yeast extract, peptone, dextrose, and agar) agar plate. *Staphylococcus aureus* (USA 300, JE-2 strain, NARSA/BEI) was routinely maintained on TSA (Tryptic Soy Agar: tryptone, soytone, dextrose, sodium chloride, dipotassium phosphate, and agar) plate. Both *C. auris* and *S. aureus* were grown in synthetic sweat medium at 37^{o}C for 48 h in 96-well microtiter plates (TPP, Cell culture treated) for biofilm assays. Synthetic sweat medium mimicking our sweat and skin environment was prepared as mentioned previously [6]. The main ingredients of the medium are amino acids, salt, and fatty acids (lauric acid, myristic acid, and palmitic acid instead of human fat) [6]. For testing QS molecule secretion, *C. auris* and *C. albicans* (SC5314, as a control) were grown in RPMI (buffered with MOPS, 50 mM, glucose) medium by shaking for 24 h at 37 ^{o}C. *S. aureus agrA* (BEI) mutant was grown in TSB medium.

5.3.2 Mono-Species and Dual-Species Biofilm Assay

To identify if *C. auris* and *S. aureus* can grow together as a biofilm, we grew them alone and in combination in synthetic sweat medium. Biofilms were formed as described previously for *C. albicans* and *S. aureus* mono- and dual-species biofilms [14]. For mono-species biofilm formation, single colony of *C. auris* was grown overnight at 30 ^{o}C in YPD broth medium. 1×10^{6} cells/mL cells were adjusted in synthetic medium and 100 μL of this suspension was grown in a

flat 96-well microtiter plate. Similarly, for *S. aureus* biofilm, overnight tryptic soy broth (TSB) grown *S. aureus* cells was used to adjust 1×10^8 cells/mL in synthetic sweat medium and 100 µL of this was added in 96-well plate. For dual-species biofilm, 100 µL of both *C. auris* and *S. aureus* were added together in 96-well plate. The plate was then incubated at 37 ^{o}C for 48 h under static condition.

5.3.3 Crystal violet (CV) staining

Biofilm intensity was measured using crystal violet staining method as described previously [15]. Media was removed from the wells after 48 h of incubation and the wells were washed with phosphate buffered saline (PBS) buffer to remove unattached cells. 0.1% of crystal violet solution was added to the wells for 10 min followed by removal of excess crystal violet using sterile distilled water for 3 times. Plates were air-dried and dissolved in 30% acetic acid. Optical density was then measured at 600 nm using a microplate reader.

5.3.4 Scanning Electron Microscopy (SEM)

Biofilms were grown on the surface of Thermanox plastic strips (Miles Scientific, USA) placed in 24-well plate for 48 h at 37 ^{o}C. Unattached cells were removed by washing with PBS whereas attached biofilms were fixed using 2% paraformaldehyde and 2% glutaraldehyde in 0.15 M cacodylate buffer as described previously in a standard protocol [16]. The cacodylate buffer having pH 7.4 contained 0.15% Alcian blue that was used for improved detection of cell surface structures [17]. Biofilms were washed and dehydrated in a series of increasing ethanol

concentrations followed by coating with 1 nm platinum using ion beam coater and observed under microscope (Field Emission Scanning Electron Microscope, Versa 3D Dual Beam, Nikon).

5.3.5 Biochemical assays

Cells were collected from mono- and dual-species biofilms grown in 96 well plate aseptically by centrifugation (2000 x g) and resuspended in a fresh medium. Two μL of cells were spotted on separate agar plates each containing different substrates such as sheep blood (5%), egg yolk (5%), and casein (6%) to identify their hemolytic, phospholipase, and proteolytic activities, respectively. Plates were incubated at 37 ^{o}C for 24 h and zones of lysis/hydrolyses were measured. To confirm hemolytic activity in culture filtrates, media from both mono- and dual-species biofilms were collected, filter sterilized, and 20 μL was spotted on the wells on sheep blood agar plate made by using a sterile pipette tip as described earlier [18]. After 24 h of incubation at 37 ^{o}C, plates were imaged. Three independent experiments were performed.

5.3.6 QS molecules extraction from *C. auris*

QS molecules extraction was performed following a protocol previously described [8]. Briefly, *C. auris* approximately 10^7 cells/mL was grown in 50 ml of RPMI medium for 24 h at 30 ^{o}C under shaking condition. Cultures were centrifuged at 8000 x g for 10 min. Supernatant obtained was filter sterilized and extracted with 1/5th volume of ethyl acetate. Ethyl acetate was removed, and residue was solubilized in 100% methanol for QS molecule bioassay and in 100% ethyl acetate for thin layer chromatography.

5.3.7 Thin Layer Chromatography (TLC)

The residue after the removal of ethyl acetate was solubilized in ethyl acetate and spotted on silica gel plate with 4:1 ethyl acetate: n-hexane as mobile phase as previously described [8]. Iodine was used as indicator for spot detection.

5.3.8 QS molecule bioassay

As farnesol inhibits germ tube formation in *C. albicans* that results in yeast morphology, we used QS molecules extracted from *C. auris* to evaluate if it can inhibit germ tube formation in *C. albicans*. Two microliters of methanol-solubilized QS molecules extract from *C. auris* was added to the wells containing *C. albicans* in RPMI media and incubated at 37 ^{o}C for 3 h (hypha inducing conditions). Percentage of budding yeasts and germ tubes were documented. As positive controls, *C. albicans* extract and commercially available farnesol were used whereas as negative controls, media alone and methanol alone were used.

5.3.9 Effect of *C. auris* QS molecules on *S. aureus* biofilm

S. aureus biofilms were established in 96-well plates as mentioned above with and without *C. auris* extract. Ethyl acetate was used as solvent control and two different concentrations (5 nM and 150 nM) of commercial farnesol (Sigma) were used as controls. Plates were incubated at 37 ^{o}C for 24 h. Biofilm growths were determined by CV assay as mentioned above.

5.3.10 Statistical analyses

Experiments were repeated, and data obtained were expressed as Mean ± SD. Student's t-test was used to calculate significance and *P*-value of less than 0.01 was considered significant. Data were analyzed using both Excel and GraphPad Prism 7.0 version.

5.4 Results

5.4.1 *C. auris* forms mixed biofilm with *S. aureus* under *in vitro* growth condition in synthetic sweat medium

C. auris and *S. aureus* both being skin colonizers, their interaction with each other is not known. To understand if these two microbes can interact with each other in skin environment, we used sweat medium that contained various salts and lipids mimicking human skin conditions [6]. After 48 h biofilm growth on plastic wells, they were processed and quantified by a standard crystal violet (CV) staining method. As shown in **Figure 5.1**, *C. auris* and *S. aureus* dual culture showed higher biofilms than their mono-species biofilms.

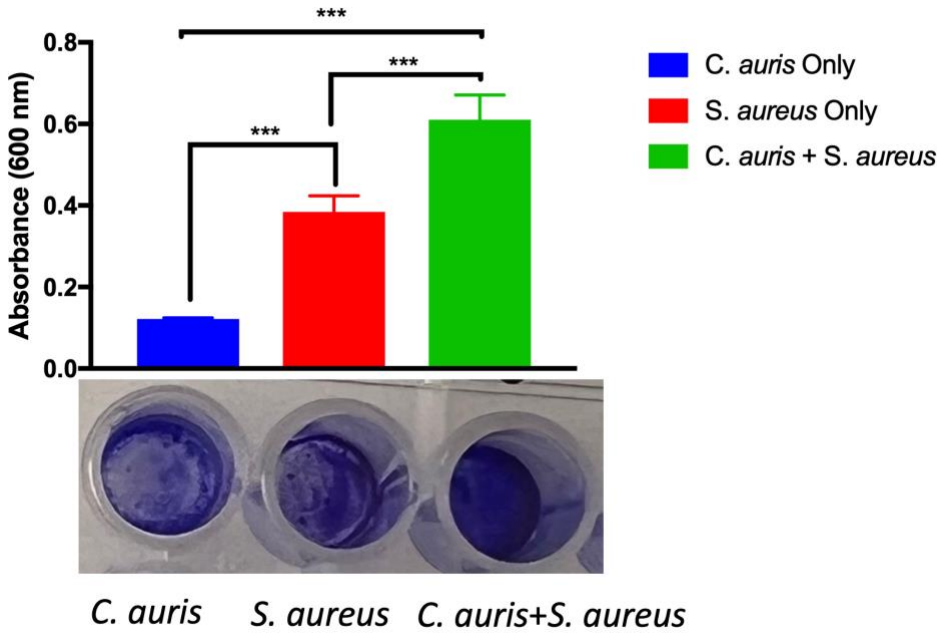

Figure 5.1. *C. auris* and *S. aureus* mixed-species biofilm formation in skin mimicking environment.

(Top panel) Overnight grown *C. auris* and *S. aureus* cells were inoculated into fresh sweat medium having starting cell density of *C. auris* ($1x10^6$ cells/ml) and *S. aureus* ($1x10^8$ cells/mL) into 96 well plate and grown at 37 ^oC for 48 h as stationary mono- and dual biofilm cultures. Biofilm formation was measured using Crystal Violet (CV) assay. Data were analyzed by students t-test; *** $p<0.001$. **(lower panel)** Biofilm containing wells imaged after removing crystal violet solution.

5.4.2 *S. aureus* cells are physically attached to *C. auris* cells

To confirm that these biofilms indeed contained both species, we used scanning electron microscopy which shows that *C. auris* and *S. aureus* growing well together in dual-species biofilm, and *S. aureus* can physically attach to *C. auris* yeast cell surface (**Figure 5.2, arrows)**.

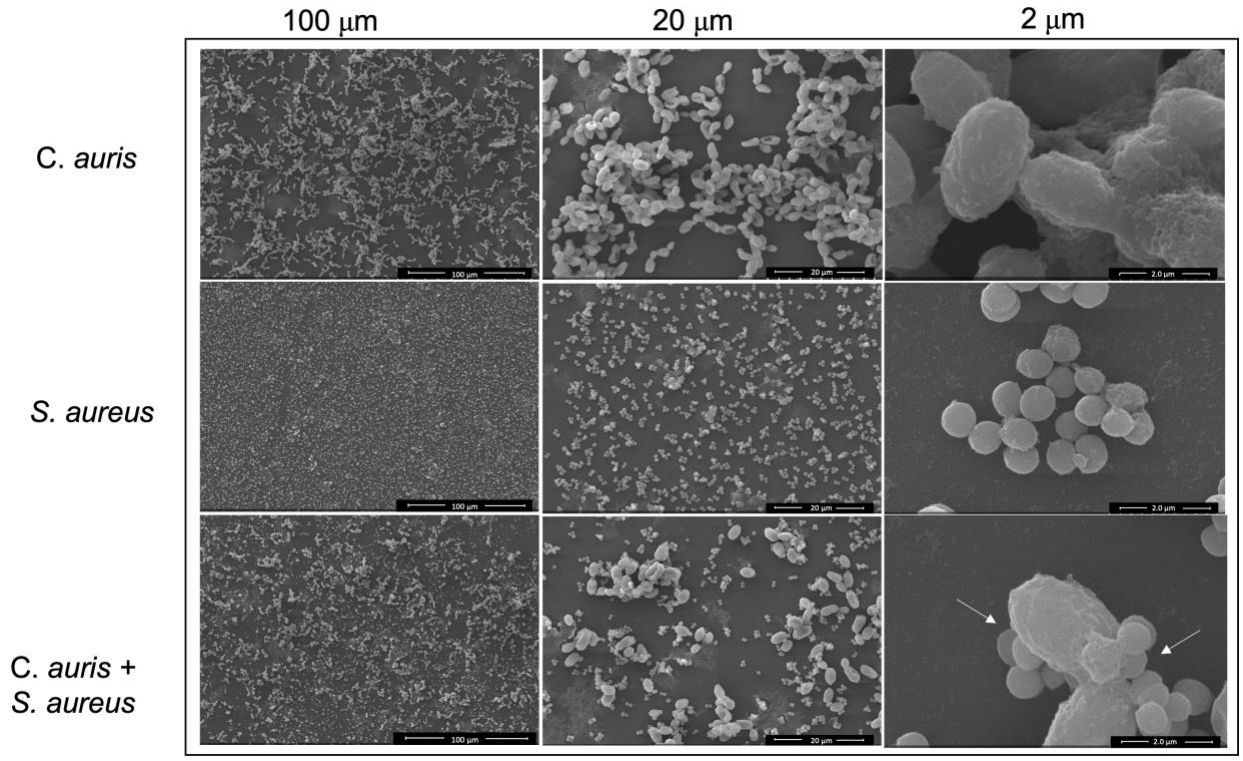

Figure 5.2. *S. aureus* cells are physically attached to *C. auris* cells.

Scanning electron microscopy (SEM) images of *C. auris* **(Top panel)**, *S. aureus* **(Middle panel)** and mixed biofilms **(Lower panel)** grown on the surface of Thermanox plastic strips (Miles Scientific, USA) placed in 24-wells microtiter plate using synthetic sweat medium for 48 h at 37 ^{o}C. Arrows show *S. aureus* cells attachment to *C. auris* cells.

5.4.3 *C. auris* enhances the hemolytic activity of *S. aureus* when grown together

To colonize and to invade host skin cells, the colonizing pathogens need to produce and secrete various types of hydrolytic enzymes. Some of them include proteolytic, lipolytic, and hemolytic enzymes. These enzymatic activities were determined by spotting small aliquots of cell suspensions from freshly collected biofilm cells on agar media containing different substrates. We used blood as substrate to identify hemolytic activity, egg yolk to identify phospholipase activity, and casein to identify proteolytic activity. Plates were incubated for 24 h at 37 ^{o}C and images were recorded. *C. auris* by itself did not produce hemolytic activity. On the

other hand, *S. aureus* which is known to produce beta-hemolytic activity displayed hemolysis with *S. aureus* on our blood agar plates. Interestingly, the dual biofilm cells showed increased hemolysis which either suggests that *C. auris* might have augmented *S. aureus*' beta-hemolytic activity or increased amounts of *S. aureus* could have grown in presence of *C. auris*. Although proteolytic and phospholipases activities were seen in these biofilms, no distinguishable differences were observed (**Figure 5.3A**). Since the accessory gene regulator (Agr) QS system of *S. aureus* is controlled by *AgrBDCA* operon and the *agrA* is one of the major global regulators of biofilm growth and virulence [19,20], we analyzed *agrA* mutant with and without *C. auris* co-culture. *S. aureus agrA* mutant alone as well as with *C. auris* did not show pronounced hemolytic activity (**Figure S5.1**). To further confirm increased hemolysis by dual biofilms on sheep blood agar (SBA), culture filtrates of both *S. aureus* and dual-species grown culture were placed the wells of SBA plate and incubated for 24 h at 37 ^{o}C. As observed above, an increased hemolysis with culture filtrate from dual-species as compared to *S. aureus* alone was observed (**Figure 5.3B, upper panel**). We also verified if live *C. auris* cells are required for this enhanced hemolytic activity and interestingly, we found that heat-killed *C. auris* was unable to enhance hemolytic activity of *S. aureus*. (**Figure 5.3B, lower panel**).

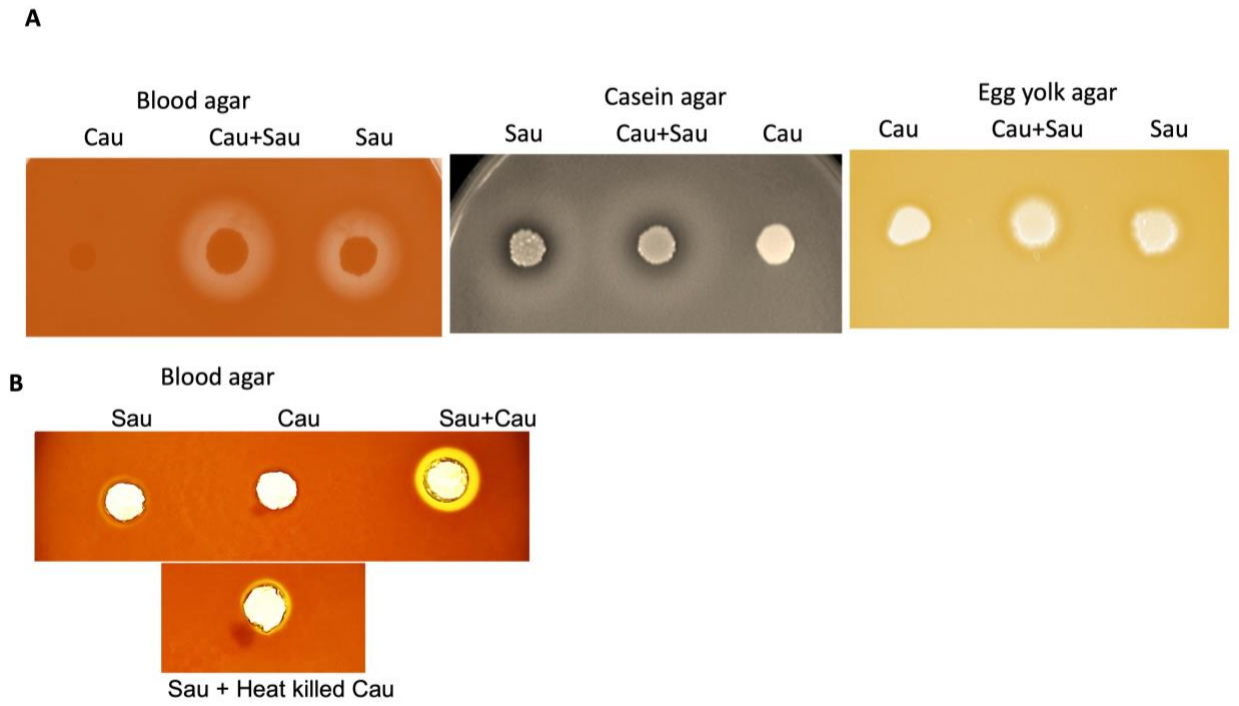

Figure 5.3. Biochemical assays of mono- and dual-species biofilm cultures.

(A) Mono- and dual-species biofilm cells spotted on blood, casein, and egg yolk agar plates to identify their hemolytic, proteolytic, and phospholipase activities respectively. Cells were scraped from wells and 2uL cells were spotted on sheep blood agar plate and grown at 37 ^{o}C for 24 h. Lysis zones were noted. **(B)** Sterile culture filtrates from mono- and dual cultures were added into the wells of sheep blood agar and incubated at 37 ^{o}C for 24 h **(B, upper panel)**. Also, hemolytic activity of *S. aureus* in the presence of heat killed *C. auris* was analyzed and found it did not increase hemolytic activity suggesting live *C. auris* is required **(B, lower panel)**.

5.4.4 *C. auris* secretes QS molecule that inhibits filamentation in *C. albicans*

QS molecules play important roles during polymicrobial cultures and since QS molecules secreted by *S. aureus* have been thoroughly studied in the past, we were curious to know if *C. auris* secretes any QS molecules which is unknown. For this, we used solvent extraction method as done previously [8]. QS molecules were extracted from sterile culture filtrates of *C. auris* using one fifth volume of ethyl acetate solvent. Dried extract redissolved in methanol and was used to evaluate if it blocks *C. albicans* filamentation under hypha inducing conditions. *C. auris*

doesn't form filamentations under *in vitro* hypha-inducing conditions and to determine the *C. auris* extracts for QS activity, we used *C. albicans*, which readily forms filaments under similar conditions. The bioassay shows that addition of *C. auris* extract resulted in more than fifty percent of *C. albicans* cells in the yeast form **(Figure 5.4A)**. Both *C. albicans* extract and commercial farnesol showed majority of cells in yeast form and both negative controls media alone extract, and methanol (solvent control) showed majority of cells with germ tubes. The results obtained were quantified by counting number of budding yeast and germ tube **(Figure 5.4B)** and represent results from three independent experimental replicates.

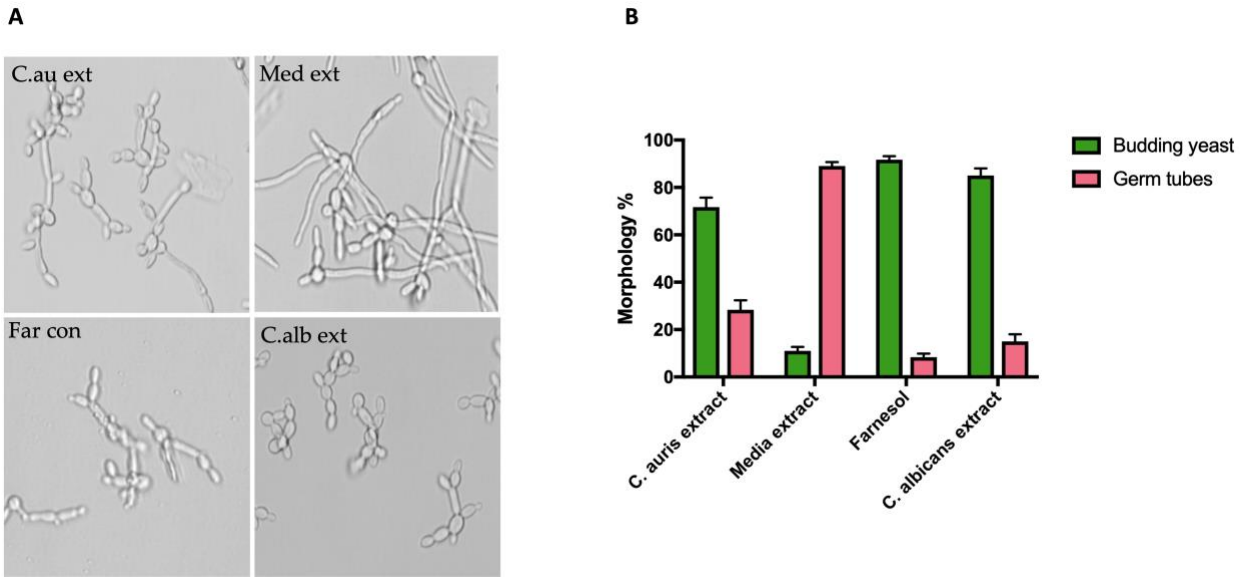

Figure 5.4. Bioactivity of QS molecules secreted by *C. auris*.

(A) *C. auris* grown culture filtrate was filter sterilized and QS molecules were extracted using solvent extraction method. To check the ability of extract to inhibit filamentation, the extract was added to *C. albicans* cells and grown in RPMI medium with 50 mM glucose at 37 ^{o}C for 3 hours. Culture filtrate extract from *C. albicans* and commercial farnesol served as positive controls whereas media extract was used as negative control. **(B)** After 3 hours, number of budding yeast and filaments were counted and quantified.

5.4.5 *C. auris* secretes QS molecule different from farnesol

Since we observed that the extract from *C. auris* was able to inhibit filamentation in *C. albicans*, we analyzed if the molecule is farnesol. Farnesol is known to block filamentation in *C. albicans*. For this, we separated ethyl acetate extracts from *C. auris* on a thin layer chromatography plate (TLC) **(Figure 5.5A)** and noticed two major spots in both *C. auris* and *C. albicans* extracts. Top spot was close to the spot shown by commercial pure farnesol. No such spots were seen in medium control ethyl acetate extract. Molecules from both top and bottom spots of *C. auris* were extracted and tested for their ability to block *C. albicans* filamentation. Top spot showed good bioactivity than the bottom spot **(Figure 5.5B)**. Extracts from both spots of TLC plate were analyzed by GC-MS **(Figure 5.6A)** and peaks that are different in top spot as compared to bottom spot were found to be 9-Cedranone **(Figure 5.6B)** and 9-Octadecenoic acid(Z)-phenylmethyl ester **(Figure 5.6C)** by database search.

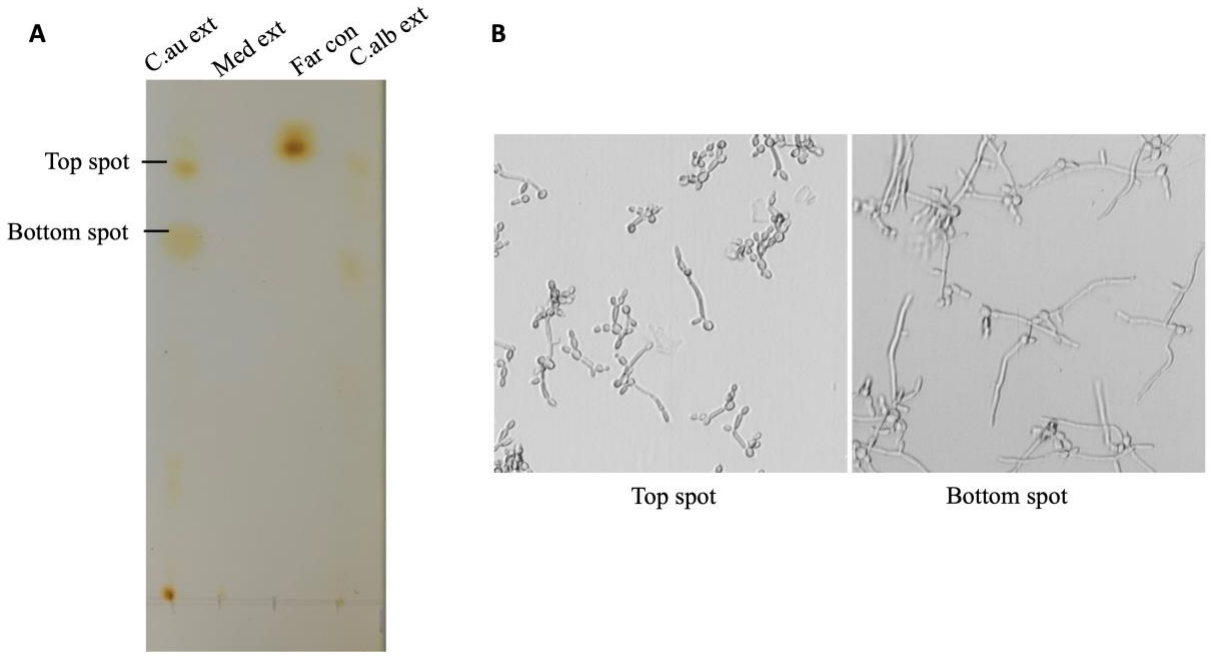

Figure 5.5. Thin Layer Chromatography analysis of QS molecules from *C. auris*.

(A) Ethyl acetate extracts of *C. auris* grown culture filtrates along with *C. albicans* extract, medium extract, and farnesol were run on TLC silica glass plate with ethyl acetate: hexane (4:1)

as mobile solvent. Two major spots were observed after iodine staining of the plates. **(B)** Both top and bottom spots were scraped, eluted, and tested on *C. albicans* cells to check their filament inhibition activity. Top spot showed good bioactivity as compared to the bottom spot.

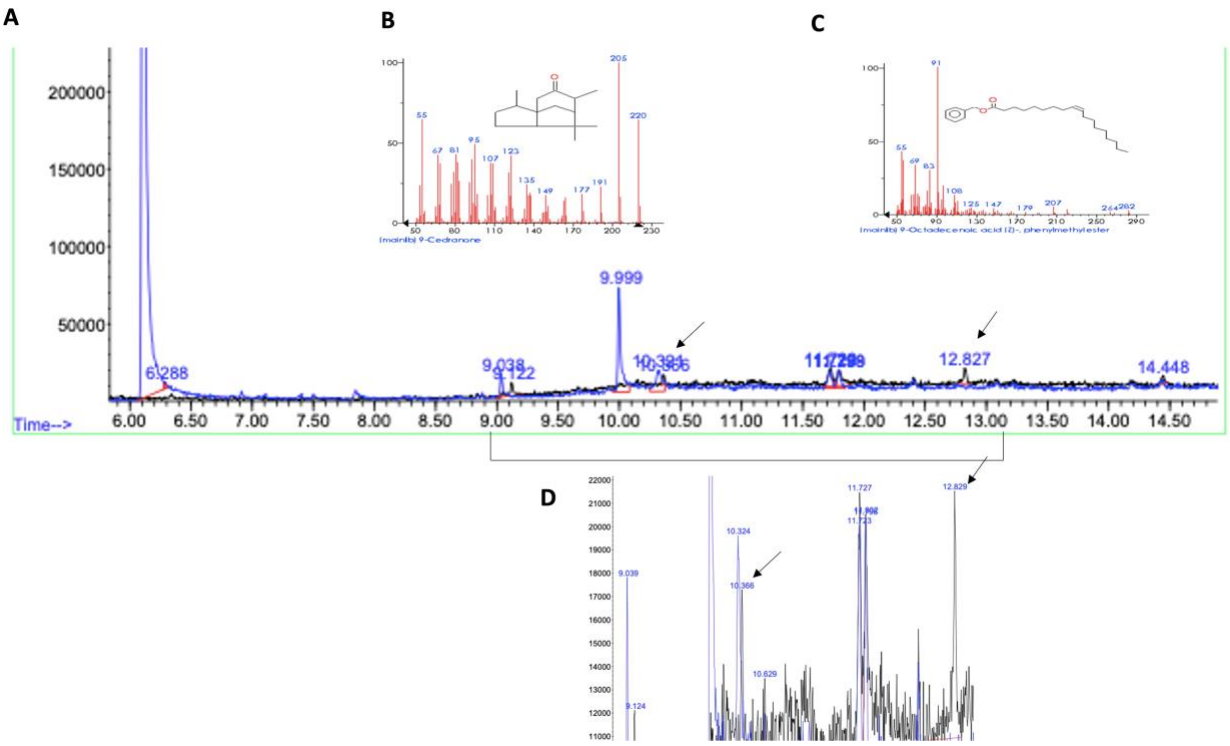

Figure 5.6. GC-MS analysis of TLC detected QS molecules from *C. auris*.

(A) TLC separated spots (top and bottom) were run through GC-MS. Peaks shown in black color represent top spot from TLC (good bioactivity) and peaks in blue color represent bottom spot from TLC (less activity). Peaks that were unique to top spot (black) were identified by database search (marked by arrows) as **(B)** 9-Cedranone and **(C)** 9-Octadecenoic acid (Z)-phenylmethyl ester**. (D)** Small section of chromatogram is enlarged for better visualization. (Kansas Lipidomics Research Center, Division of Biology, KSU).

5.4.6 *C. auris* extract augments biofilm forming ability of *S. aureus*

QS molecule extracted from *C. auris* was tested (1 µl/100 µl of *S. aureus* culture) to verify if the extract influences biofilm forming ability of *S. aureus*. Ethyl acetate was used as solvent control. We observed significant increase in *S. aureus* biofilm intensity in the presence of *C. auris*

extract (*P*-value: 0.0055). Similarly, 5 nM of farnesol increased *S. aureus* growth in biofilms and high concentration of farnesol lowered biofilm intensity as reported earlier [11].

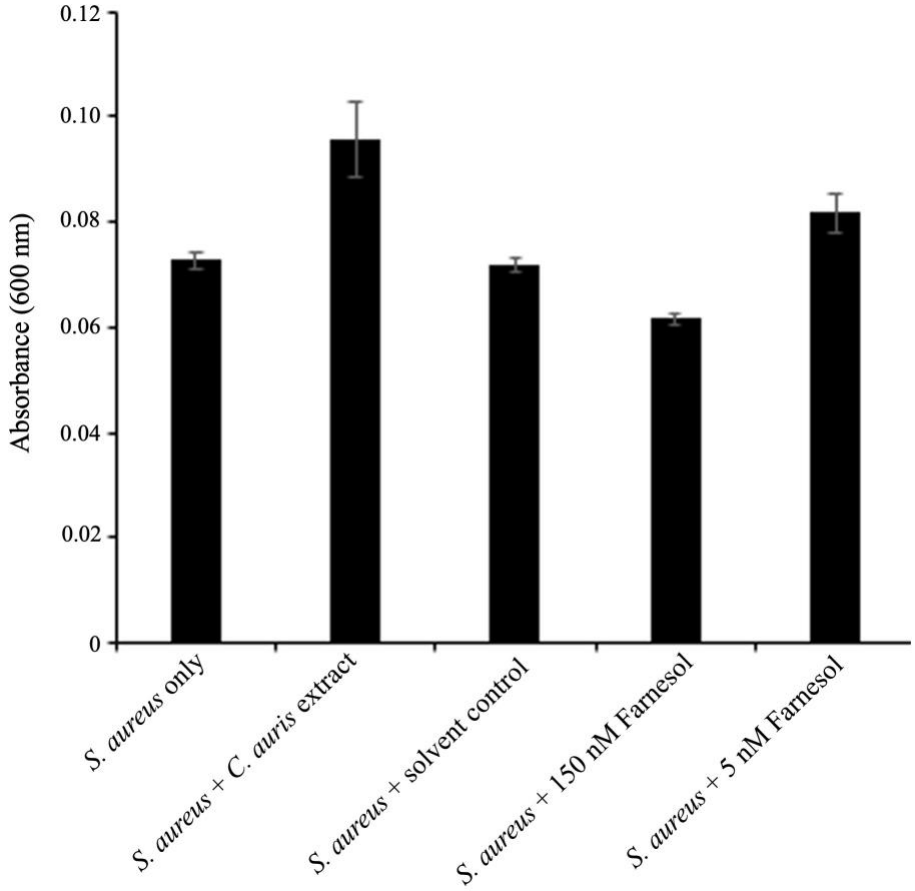

Figure 5.7. Biofilm quantification of *S. aureus* treated with *C. auris* extract.

S. aureus cells were inoculated in 96-well plate in triplicate in synthetic sweat medium. *C. auris* extract, solvent, and two concentrations of farnesol (150 nM and 5 nM) were added to *S. aureus* culture. Plate was incubated at 37 ^{o}C for 24 h and biofilms were quantified using crystal violet method. *S. aureus* showed increased biofilm formation when grown along with *C. auris* extract (*P*-value<0.05, two-tailed Student t-test between biofilm formed by *S. aureus* only and biofilm formed by *S. aureus* grown in the presence of *C. auris* extract).

5.5 Discussion

Candida related biofilms lead to increased morbidity and mortality and so far, *C. albicans* has been considered as the major pathogen. But recently, there has been increasing

evidence showing non-*C. albicans* species such as *C. auris* involved in biofilm formation resulting in fatal bloodstream infections. *C. auris* has been isolated from skin wounds and catheters, which are also the active colonizing sites for *S. aureus* [21–23]. Previous studies have shown that *S. aureus* interacts physically with *C. albicans* and increases virulence factor by making the biofilm more adherent and resistant. On the contrary, *S. aureus* is shown to have antagonistic relation with another *Candida* species, *Candida glabrata* [24]. However, interaction between *S. aureus* and *C. auris* is currently unknown. Since both *C. auris* and *S. aureus* are clinically relevant pathogens found in shared niche space and both form biofilms with drug resistance, we first demonstrated that if these two microbes can grow together and establish biofilm on skin mimicking environment.

Synthetic sweat medium favored the growth of both *C. auris* and *S. aureus* and interestingly, we found increased biofilm intensity when both were grown together. *C. auris* outbreak in United Kingdom was associated with the common use of reusable skin-surface temperature probes and this was speculated to be so due to biofilm forming ability of *C. auris* in the skin [6,25]. Similarly, the ability of *S. aureus* to form biofilm on medical devices has been known for decades [26,27]. Based on our observation that these two microbes formed increased biofilm when grown together in skin mimicking environment, we proposed that *C. auris* and *S. aureus* can form robust biofilms on skin with increased virulence in the skin environment.

Images from scanning electron microscopy showed that these two microbes are closely associated. Physical interaction plays major role in polymicrobial infection leading to adhesion and drug ineffectiveness. *C. albicans* Als proteins and hyphal wall proteins are key players that allow *C. albicans* to adhere to several bacteria and host surfaces [28,29]. More specifically, in *C. albicans* and *S. aureus* dual-species biofilm, Als3 of *C. albicans* was identified as a receptor that

binds to *S. aureus* [30]. In fact, homologue of Als3 is found in *C. auris* as well and is found to be upregulated when *C. auris* is grown as biofilms [31]. However, many studies on *C. albicans* and *S. aureus* interactions are linked to hypha mediated interaction. Although *C. auris* does not produce hyphae under *in vitro* conditions, studies showing hyphal or pseudohyphal forms exist [32,33].

The first straight forward thing to do after identifying that two pathogenic microbes coexist, is to determine whether major virulence factors alter in presence of one another. For this study, we chose to identify three relevant virulence traits of *C. auris* such as hemolysis, phospholipase, and proteolytic activities. We did not observe any hemolysin activity by *C. auris* in our study. However, a case study reported isolation of *C. auris* with hemolytic activity from a patient having vulvovaginal candidiasis [34]. Glucose and CO_2 rich environment are known to favor hemolytic activity in *Candida* species. On the other hand, hemolysis in *S. aureus* is the result of hemolysin toxins produced that result in the lysis of red blood cells (RBC). Our results demonstrated increased lysis of RBC when *S. aureus* cells were spotted on sheep blood agar plate in the presence of *C. auris* as compared to *S. aureus* alone. On top of that, culture filtrate from *S. aureus* and *C. auris* mixed culture also showed increased hemolysis in blood agar plate as compared to culture filtrate from *S. aureus* alone. Similar results were reported during polymicrobial interaction of *C. albicans* and *S. aureus* where authors suggested alpha-toxin dependent activities resulted in such phenotypes [18]. Given similar phenotypes in our experiment, agr and toxin can be the key players in increased biofilm and hemolysis. Also, this assumption is strengthened by the observation from our experiment where *agrA* mutant failed to hemolyze RBC with or without *C. auris*. We did not see significant difference in phospholipase and proteolytic activities in dual-species biofilm as compared to mono-species biofilm.

Small-secreted molecules and secreted effectors such as QS molecules play major roles during polymicrobial infections [35,36]. *Candida* species are also known to secrete QS molecules and most of the studies are done in *C. albicans*. *C. albicans* secretes QS molecules such as farnesol and tyrosol along with phenylethyl alcohol, tryptophol, and morphogenic autoregulatory substance [8,37–40]. Weber et al., [9] looked at farnesol secretion in eight different *Candida* species and found the highest farnesol secretion by *C. albicans* as compared to other *Candida* species. However, if *C. auris* secretes any QS molecule has not been reported yet. This leaves a gap in understanding the complete mechanism of interaction between *C. auris* and other coexisting microbes. To fill this gap and to identify if QS molecule from *C. auris* exists and has role in its interaction with *S. aureus*, we explored secreted molecules by *C. auris* and tested. Ethyl acetate-based extraction of secreted molecule initially hinted us that *C. auris* secreted QS molecule could be farnesol as the extract was able to block filamentation in *C. albicans* similar to that of farnesol. Though the effect of *C. auris* extract was comparatively less than that of *C. albicans* extract and commercial pure farnesol, there was a significant difference in the percentage of yeast and germ tubes. This might suggest that *C. auris* produces farnesol like QSM but lesser than that of *C. albicans*. To confirm if it is farnesol, we separated the extract on TLC plate where we saw two major spot, top spot and bottom spot having Rf values of 0.476 and 0.312 respectively. Similar spots were obtained for *C. albicans*. Rf value of commercial farnesol was 0.50. Interestingly, based on GC-MS analysis of active TLC spots, farnesol was not detected. In fact, two other molecules were detected namely 9-Cedranone and 9-Octadecenoic acid(Z)-phenylmethyl ester in top spot based on the database search. As per a recent study, 9-Cedranone has been identified as a fungal metabolite [41], however this may be the first study where 9-Cedranone is detected in *C. auris* with possible QS role (blocking filamentation). On the

other hand, octadecanoic acid obtained in our GC-MS data are major components of extracellular vesicles (EVs) in *C. albicans*. These octadecanoic compounds are long chain fatty acids that did not inhibit filamentation in *C. albicans* [42]. However, latest studies show octadecanoic acid inhibited filamentation and identified as major components of *C. albicans* EVs that inhibited filamentation, biofilm formation, and were avirulent in *Galleria mellonella* model [43,44]. Further studies are required to confirm the expression level and activities of these compounds in *C. auris*.

We showed that *C. auris* secretes QS molecules that inhibit filamentation in *C. albicans*, but we were curious to know if they play any role in dual-species biofilm of *C. auris* with *S. aureus*. For this, *S. aureus* cultures were grown as biofilms in the presence of *C. auris* extract and analyzed for biofilm intensity. We noticed an increase in biofilm density of *S. aureus* treated with *C. auris* QS molecules as compared to untreated. This observation resembles with the QS molecule farnesol that in its nanomolar concentration, there was increased growth of *S. aureus* in biofilm [11].

In conclusion, we have shown that *C. auris* can grow along with *S. aureus* as biofilms in a skin mimicking environment. We have further shown that quorum sensing system of both microbes might have led to increased virulence. The acquisition of such basic concept along with knowledge of their virulence factors are important for developing therapeutics to cure *C. auris* and *S. aureus* dual biofilm related infection.

5.6 References

1. Krüger, W.; Vielreicher, S.; Kapitan, M.; Jacobsen, I.D.; Niemiec, M.J. Fungal-Bacterial Interactions in Health and Disease. *Pathogens* **2019**, *8*, 70, doi:10.3390/pathogens8020070.

2. Archer, N.K.; Mazaitis, M.J.; Costerton, J.W.; Leid, J.G.; Powers, M.E.; Shirtliff, M.E. *Staphylococcus aureus* Biofilms. *Virulence* **2011**, *2*, 445–459, doi:10.4161/viru.2.5.17724.

3. Calvo, B.; Melo, A.S.A.; Perozo-Mena, A.; Hernandez, M.; Francisco, E.C.; Hagen, F.; Meis, J.F.; Colombo, A.L. First Report of *Candida auris* in America: Clinical and Microbiological Aspects of 18 Episodes of Candidemia. *Journal of Infection* **2016**, *73*, 369–374, doi:10.1016/j.jinf.2016.07.008.

4. Singh, S.; Uppuluri, P.; Mamouei, Z.; Alqarihi, A.; Elhassan, H.; French, S.; Lockhart, S.R.; Chiller, T.; Edwards, J.E.; Ibrahim, A.S. The NDV-3A Vaccine Protects Mice from Multidrug Resistant *Candida auris* Infection. *PLoS Pathog* **2019**, *15*, e1007460, doi:10.1371/journal.ppat.1007460.

5. Chakrabarti, A.; Sood, P.; Rudramurthy, S.M.; Chen, S.; Kaur, H.; Capoor, M.; Chhina, D.; Rao, R.; Eshwara, V.K.; Xess, I.; et al. Incidence, Characteristics and Outcome of ICU-Acquired Candidemia in India. *Intensive Care Med* **2015**, *41*, 285–295, doi:10.1007/s00134-014-3603-2.

6. Horton, M.V.; Johnson, C.J.; Kernien, J.F.; Patel, T.D.; Lam, B.C.; Cheong, J.Z.A.; Meudt, J.J.; Shanmuganayagam, D.; Kalan, L.R.; Nett, J.E. *Candida auris* Forms High-Burden Biofilms in Skin Niche Conditions and on Porcine Skin. *mSphere* **2020**, *5*:e00910-19, doi: 10.1128/mSphere.00910-19..

7. Spivak, E.S.; Hanson, K.E. *Candida auris*: An Emerging Fungal Pathogen. *J Clin Microbiol* **2018**, *56*, e01588-17, doi:10.1128/JCM.01588-17.

8. Hornby, J.M.; Jensen, E.C.; Lisec, A.D.; Tasto, J.J.; Jahnke, B.; Shoemaker, R.; Dussault, P.; Nickerson, K.W. Quorum Sensing in the Dimorphic Fungus *Candida albicans* Is Mediated by Farnesol. *Appl Environ Microbiol* **2001**, *67*, 2982–2992, doi:10.1128/AEM.67.7.2982-2992.2001.

9. Weber, K.; Sohr, R.; Schulz, B.; Fleischhacker, M.; Ruhnke, M. Secretion of E,E-Farnesol and Biofilm Formation in Eight Different *Candida* Species. *Antimicrob Agents Chemother* **2008**, *52*, 1859–1861, doi:10.1128/AAC.01646-07.

10. Jabra-Rizk, M.A.; Meiller, T.F.; James, C.E.; Shirtliff, M.E. Effect of Farnesol on *Staphylococcus aureus* Biofilm Formation and Antimicrobial Susceptibility. *Antimicrob Agents Chemother* **2006**, *50*, 1463–1469, doi:10.1128/AAC.50.4.1463-1469.2006.

11. Krause, J.; Geginat, G.; Tammer, I. Prostaglandin E2 from *Candida albicans* Stimulates the Growth of *Staphylococcus aureus* in Mixed Biofilms. *PLOS ONE* **2015**, *10*, e0135404, doi:10.1371/journal.pone.0135404.

12. Daum, R.S. Skin and Soft-Tissue Infections Caused by Methicillin-Resistant *Staphylococcus aureus*. *New England Journal of Medicine* **2007**, *357*, 380–390, doi:10.1056/NEJMcp070747.

13. Abdalhamid, B.; Almaghrabi, R.; Althawadi, S.; Omrani, A. First Report of *Candida auris* Infections from Saudi Arabia. *Journal of Infection and Public Health* **2018**, *11*, 598–599, doi:10.1016/j.jiph.2018.05.010.

14. Kean, R.; Rajendran, R.; Haggarty, J.; Townsend, E.M.; Short, B.; Burgess, K.E.; Lang, S.; Millington, O.; Mackay, W.G.; Williams, C.; et al. *Candida albicans* Mycofilms Support *Staphylococcus aureus* Colonization and Enhances Miconazole Resistance in Dual-Species Interactions. *Front Microbiol* **2017**, *8*, 258, doi:10.3389/fmicb.2017.00258.

15. Merritt, J.H.; Kadouri, D.E.; O'Toole, G.A. Growing and Analyzing Static Biofilms. *Curr Protoc Microbiol* **2005**, *0 1*, Unit-1B.1, doi:10.1002/9780471729259.mc01b01s00.

16. Erlandsen, S.L.; Kristich, C.J.; Dunny, G.M.; Wells, C.L. High-Resolution Visualization of the Microbial Glycocalyx with Low-Voltage Scanning Electron Microscopy: Dependence on Cationic Dyes. *J Histochem Cytochem* **2004**, *52*, 1427–1435, doi:10.1369/jhc.4A6428.2004.

17. Veerapandian, R.; Vediyappan, G. Gymnemic Acids Inhibit Adhesive Nanofibrillar Mediated *Streptococcus gordonii–Candida albicans* Mono-Species and Dual-Species Biofilms. *Front Microbiol* **2019**, *10*, 2328, doi:10.3389/fmicb.2019.02328.

18. Todd, O.A.; Fidel, P.L.; Harro, J.M.; Hilliard, J.J.; Tkaczyk, C.; Sellman, B.R.; Noverr, M.C.; Peters, B.M. *Candida albicans* Augments *Staphylococcus aureus* Virulence by Engaging the Staphylococcal Agr Quorum Sensing System. *mBio* **2019**, *10*, e00910-19, doi:10.1128/mBio.00910-19.

19. Novick, R.P.; Geisinger, E. Quorum Sensing in *Staphylococci*. *Annu Rev Genet* **2008**, *42*, 541–564, doi:10.1146/annurev.genet.42.110807.091640.

20. Kavanaugh, J.S.; Horswill, A.R. Impact of Environmental Cues on Staphylococcal Quorum Sensing and Biofilm Development. *J Biol Chem* **2016**, *291*, 12556–12564, doi:10.1074/jbc.R116.722710.

21. Ben-Ami, R.; Berman, J.; Novikov, A.; Bash, E.; Shachor-Meyouhas, Y.; Zakin, S.; Maor, Y.; Tarabia, J.; Schechner, V.; Adler, A.; et al. Multidrug-Resistant *Candida haemulonii* and *C. auris*, Tel Aviv, Israel. *Emerg Infect Dis* **2017**, *23*, 195–203, doi:10.3201/eid2302.161486.

22. Borman, A.M.; Szekely, A.; Johnson, E.M. Comparative Pathogenicity of United Kingdom Isolates of the Emerging Pathogen *Candida auris* and Other Key Pathogenic *Candida* Species. *mSphere* **2016**, *1*, e00189-16, doi:10.1128/mSphere.00189-16.

23. James, G.A.; Swogger, E.; Wolcott, R.; Pulcini, E. deLancey; Secor, P.; Sestrich, J.; Costerton, J.W.; Stewart, P.S. Biofilms in Chronic Wounds. *Wound Repair and Regeneration* **2008**, *16*, 37–44, doi:10.1111/j.1524-475X.2007.00321.x.

24. Camarillo-Márquez, O.; Córdova-Alcántara, I.M.; Hernández-Rodríguez, C.H.; García-Pérez, B.E.; Martínez-Rivera, M.A.; Rodríguez-Tovar, A.V. Antagonistic Interaction of *Staphylococcus aureus* Toward *Candida glabrata* During in Vitro Biofilm Formation Is Caused by an Apoptotic Mechanism. *Front Microbiol* **2018**, *9*, 2031, doi:10.3389/fmicb.2018.02031.

25. Eyre, D.W.; Sheppard, A.E.; Madder, H.; Moir, I.; Moroney, R.; Quan, T.P.; Griffiths, D.; George, S.; Butcher, L.; Morgan, M.; et al. A *Candida auris* Outbreak and Its Control in an Intensive Care Setting. *New England Journal of Medicine* **2018**, *379*, 1322–1331, doi:10.1056/NEJMoa1714373.

26. Tajeddin, E.; Rashidan, M.; Razaghi, M.; Javadi, S.S.S.; Sherafat, S.J.; Alebouyeh, M.; Sarbazi, M.R.; Mansouri, N.; Zali, M.R. The Role of the Intensive Care Unit Environment and Health-Care Workers in the Transmission of Bacteria Associated with Hospital Acquired Infections. *J Infect Public Health* **2016**, *9*, 13–23, doi:10.1016/j.jiph.2015.05.010.

27. Götz, F. *Staphylococcus* and Biofilms. *Molecular Microbiology* **2002**, *43*, 1367–1378, doi:10.1046/j.1365-2958.2002.02827.x.

28. Silverman, R.J.; Nobbs, A.H.; Vickerman, M.M.; Barbour, M.E.; Jenkinson, H.F. Interaction of *Candida albicans* Cell Wall Als3 Protein with *Streptococcus gordonii* SspB Adhesin Promotes Development of Mixed-Species Communities. *Infect Immun* **2010**, *78*, 4644–4652, doi:10.1128/IAI.00685-10.

29. Nobbs, A.H.; Vickerman, M.M.; Jenkinson, H.F. Heterologous Expression of *Candida albicans* Cell Wall-Associated Adhesins in *Saccharomyces cerevisiae* Reveals Differential Specificities in Adherence and Biofilm Formation and in Binding Oral *Streptococcus gordonii*. *Eukaryot Cell* **2010**, *9*, 1622–1634, doi:10.1128/EC.00103-10.

30. Peters, B.M.; Ovchinnikova, E.S.; Krom, B.P.; Schlecht, L.M.; Zhou, H.; Hoyer, L.L.; Busscher, H.J.; van der Mei, H.C.; Jabra-Rizk, M.A.; Shirtliff, M.E. *Staphylococcus aureus* Adherence to *Candida albicans* Hyphae Is Mediated by the Hyphal Adhesin Als3p. *Microbiology (Reading)* **2012**, *158*, 2975–2986, doi:10.1099/mic.0.062109-0.

31. Kean, R.; Delaney, C.; Sherry, L.; Borman, A.; Johnson, E.M.; Richardson, M.D.; Rautemaa-Richardson, R.; Williams, C.; Ramage, G. Transcriptome Assembly and Profiling of *Candida auris* Reveals Novel Insights into Biofilm-Mediated Resistance. **2018**, *3*, 14.

32. Yue, H.; Bing, J.; Zheng, Q.; Zhang, Y.; Hu, T.; Du, H.; Wang, H.; Huang, G. Filamentation in *Candida auris*, an Emerging Fungal Pathogen of Humans: Passage through the Mammalian Body Induces a Heritable Phenotypic Switch. *Emerg Microbes Infect* **2018**, *7*, 188, doi:10.1038/s41426-018-0187-x.

33. Wang, X.; Bing, J.; Zheng, Q.; Zhang, F.; Liu, J.; Yue, H.; Tao, L.; Du, H.; Wang, Y.; Wang, H.; et al. The First Isolate of *Candida auris* in China: Clinical and Biological Aspects. *Emerg Microbes Infect* **2018**, *7*, 93, doi:10.1038/s41426-018-0095-0.

34. Kumar, D.; Banerjee, T.; Pratap, C.B.; Tilak, R. Itraconazole-Resistant *Candida auris* with Phospholipase, Proteinase and Hemolysin Activity from a Case of Vulvovaginitis. *J Infect Dev Ctries* **2015**, *9*, 435–437, doi:10.3855/jidc.4582.

35. Staib, P.; Morschhäuser, J. Differential Expression of the NRG1 Repressor Controls Species-Specific Regulation of Chlamydospore Development in *Candida albicans* and *Candida dubliniensis*. *Molecular Microbiology* **2005**, *55*, 637–652, doi:10.1111/j.1365-2958.2004.04414.x.

36. Abisado, R.G.; Benomar, S.; Klaus, J.R.; Dandekar, A.A.; Chandler, J.R. Bacterial Quorum Sensing and Microbial Community Interactions. *mBio* **2018**, *9*, e02331-17, doi:10.1128/mBio.02331-17.

37. Chen, H.; Fujita, M.; Feng, Q.; Clardy, J.; Fink, G.R. Tyrosol Is a Quorum-Sensing Molecule in *Candida albicans*. *Proc Natl Acad Sci U S A* **2004**, *101*, 5048–5052, doi:10.1073/pnas.0401416101.

38. HAZEN, K.C.; CUTLER, J.E. Isolation and Purification of Morphogenic Autoregulatory Substance Produced by *Candida albicans*. *The Journal of Biochemistry* **1983**, *94*, 777–783, doi:10.1093/oxfordjournals.jbchem.a134419.

39. Ghosh, S.; Kebaara, B.W.; Atkin, A.L.; Nickerson, K.W. Regulation of Aromatic Alcohol Production in *Candida albicans*. *Applied and Environmental Microbiology* **2008**, *74*, 7211–7218, doi:10.1128/AEM.01614-08.

40. Chauhan, N.M.; Raut, J.S.; Karuppayil, S.M. A Morphogenetic Regulatory Role for Ethyl Alcohol in *Candida albicans*. *Mycoses* **2011**, *54*, e697–e703, doi:10.1111/j.1439-0507.2010.02002.x.

41. Al-Ansari, M.M.; Dhasarathan, P.; Ranjitsingh, A.J.A.; Al-Humaid, L.A. *Ganoderma lucidum* Inspired Silver Nanoparticles and Its Biomedical Applications with Special Reference to Drug Resistant *Escherichia coli* Isolates from CAUTI. *Saudi J Biol Sci* **2020**, *27*, 2993–3002, doi:10.1016/j.sjbs.2020.09.008.

42. Noverr, M.C.; Huffnagle, G.B. Regulation of *Candida albicans* Morphogenesis by Fatty Acid Metabolites. *Infect Immun* **2004**, *72*, 6206–6210, doi:10.1128/IAI.72.11.6206-6210.2004.

43. Prasath, K.G.; Sethupathy, S.; Pandian, S.K. Proteomic Analysis Uncovers the Modulation of Ergosterol, Sphingolipid and Oxidative Stress Pathway by Myristic Acid Impeding Biofilm and Virulence in *Candida albicans*. *Journal of Proteomics* **2019**, *208*, 103503, doi:10.1016/j.jprot.2019.103503.

44. Honorato, L.; de Araujo, J.F.D.; Ellis, C.C.; Piffer, A.C.; Pereira, Y.; Frases, S.; de Sousa Araújo, G.R.; Pontes, B.; Mendes, M.T.; Pereira, M.D.; et al. Extracellular Vesicles Regulate Biofilm Formation and Yeast-to-Hypha Differentiation in *Candida albicans*. *mBio* **2022**, *13*, e00301-22, doi:10.1128/mbio.00301-22.

Chapter 6 - Conclusion

The findings presented in this dissertation have provided better understanding of yeast-hyphal switch and hyphal inhibition of *C. albicans* along with evaluating the expression of a major regulator of yeast-hyphal switch, Nrg1 in *C. auris*. This study has also highlighted interaction of *C. auris* with another skin resident microbe with augmented virulence.

Chapter 2 and 3 of this dissertation are focused on a known hyphal inhibitor, Gymnemic acid (GAs), to determine its efficacy and understand mechanisms involved. Previous work from our group showed that GAs inhibited hyphal growth of *C. albicans* both *in vitro* and in non-mammalian model [1]. However, its efficacy in mammalian model was not known. So, in **Chapter 2**, we have determined the hyphal inhibitory efficacy of GAs using the mouse model of disseminated candidiasis **(Figure 6.1)**. We showed that GAs successfully rescued mice infected with *C. albicans* and this survival of GAs treated mice corresponded with the clearance of fungal burden from kidney of GAs treated mice, based on histopathology results and CFU analyses. These are encouraging results based on disseminated mice model but more such *in vivo* studies are required for complete understanding. Since *C. albicans* commonly resides on several body parts and is able to cause different types of candidiasis, other models such as oropharyngeal candidiasis, mucocutaneous candidiasis on skin, wound, mucous membranes, and others should be tested in future.

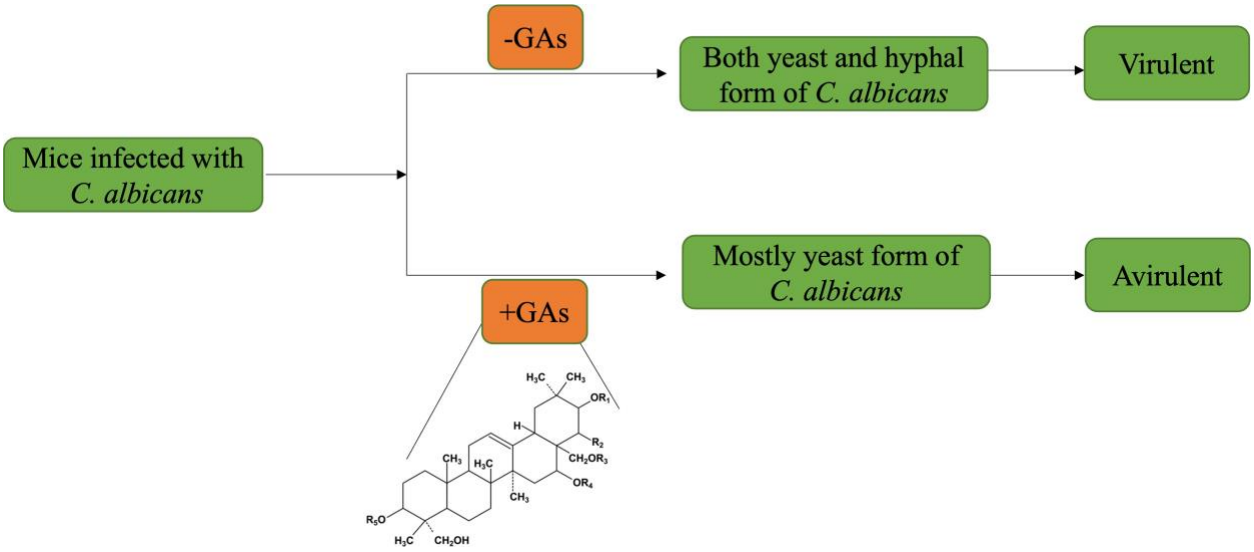

Figure 6.1. GAs rescues mice infected with *C. albicans*.

Mice were infected with *C. albicans* intravenously, directly into the bloodstream. Only mice treated with GAs survived whereas those without GAs treatment did not survive.

These results from chapter 2 supported the *in vitro* results of GAs mediated hyphal inhibition and led us to our next question which was to identify targets of GAs **(Chapter 3)**. Identifying targets of GAs would help us understand its mechanism of action. Using proteomics approaches such as affinity purification and mass spectrometry, we aimed for identifying proteins that co-purified with Nrg1 and Ume6p, negative and positive hyphal regulators respectively, in the presence and absence of GAs. Co-purified proteins included DNA binding proteins, RNA binding proteins, proteins having role in filamentation, and others. Among these proteins, we found several proteins involved in the Sln1 branch of the HOG pathway that were copurified only in GAs treated but not in control (-GAs). Null mutants of these genes were also insensitive to GAs. These results point towards the notion that GAs might be acting through HOG pathway where *C. albicans* cells respond to adopt osmotic stress by inhibiting the energy-expensive hyphal growth and initiating the budding **(Figure 6.2A)**.

Presence of several ribosomal proteins in GAs treated sample and their absence in control samples without GAs, hinted towards specificity of these proteins to GAs. Although a recent study claimed ribosomal proteins as target of GAs and showed decreased protein expression in GAs treated *C. albicans* [2], our result contradicted. We saw significantly more proteins in GAs treated *C. albicans* as compared to the control samples without GAs.

We further demonstrated upregulation of *NRG1* promoter and downregulation *UME6* promoter in the presence of GAs using reporter fusion assays. Tup1, a repressor that works together with Nrg1 to suppress hypha specific genes [3], was expressed more in the presence of GAs. All these findings corresponded to the yeast morphology of *C. albicans* in the presence of GAs. To understand if GAs directly affect binding of Nrg1 to promoter of hypha specific genes, we used promoter of *ALS3*, that contains two binding sites for Nrg1. We observed GAs disrupting the binding of Nrg1 to *AlS3* promoter **(Figure 6.2B)**. Failure of Nrg1 to bind on promoter of hypha specific gene should promote hypha which is not the case as GAs treated *C. albicans* are in yeast morphology. As yeast-hypha switch is regulated by multiple proteins and pathways, other hypha specific genes required for hypha formation might be repressed by GAs. Further studied are needed for complete understanding.

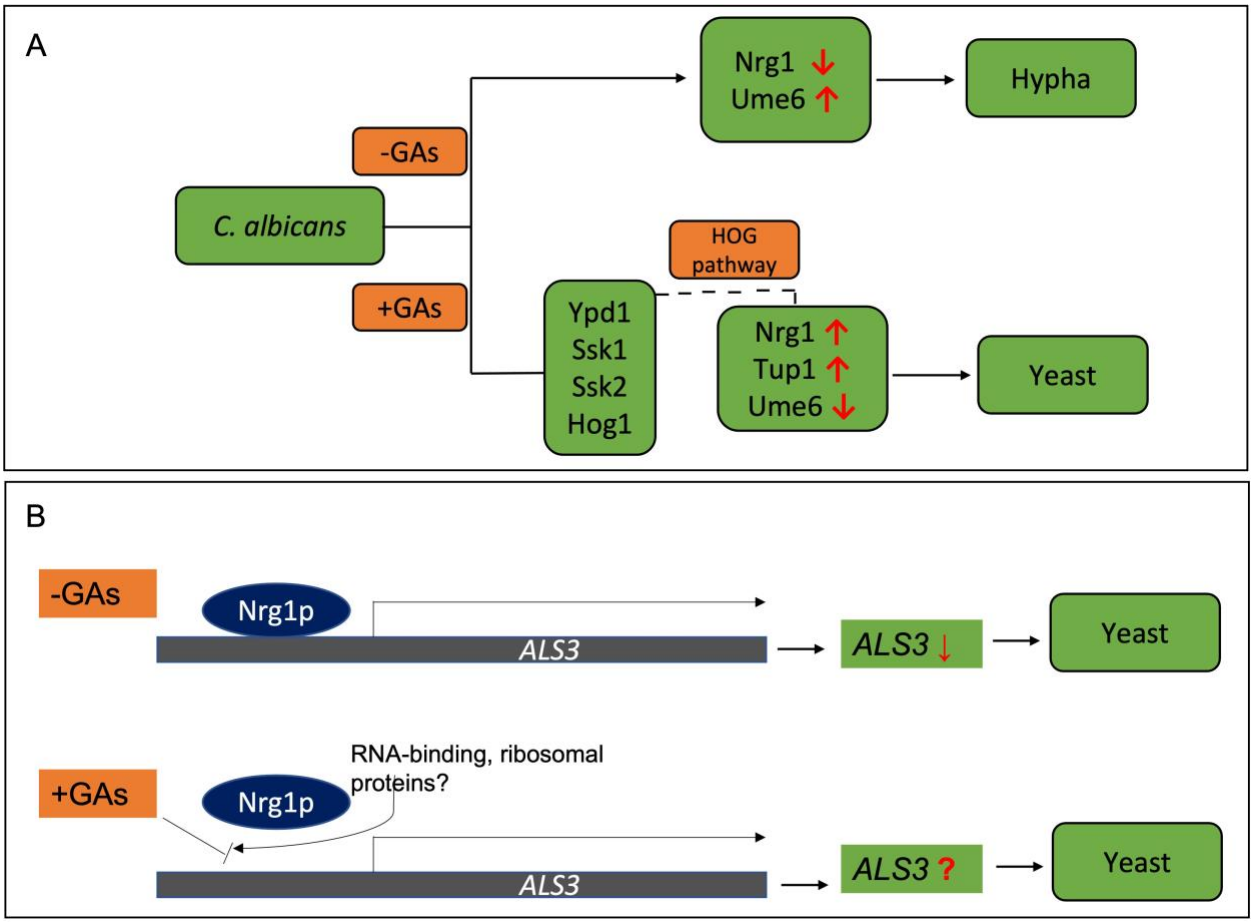

Figure 6.2. Models for GAs mediated hyphal inhibition in *C. albicans*.

(A) Predicted mode of action of GAs in *C. albicans*. Proteomics data suggested involvement of HOG1 pathway leading to the inhibition of hypha-specific gene expression. Upregulation of Nrg1 and downregulation of Ume6 expression resulted in the observed phenotype of *C. albicans* as yeast in the presence of GAs. **(B)** GAs inhibited the binding of Nrg1 to the promoter of hypha specific gene, *ALS3*. This observation is unclear but GAs targeting RNA-binding proteins or ribosomal proteins and blocking their access to the binding site in the promoter region might be a possibility.

Another emerging multi-drug resistant pathogen, *Candida auris*, is mostly found in yeast form but there have been reports where they switched to pseudohyphal forms [4,5]. As Nrg1 is a transcription factor that is known to repress hypha in *C. albicans* and has similar folding pattern with predicted structure of Nrg1 of *C. auris*, expression and role of Nrg1 was unknown in *C. auris*. So, our next study was to determine the expression of Nrg1 in *C. auris* **(Chapter 4) (Figure 6.3)**. *C. auris* easily forms biofilm on skin surface so we used synthetic sweat medium to

mimic our skin environment. Along with identifying biofilms-specific proteins, we showed Nrg1 expressing well in both cytosol and surface of the cell. By using 2D-electrophoreis, Western, and immunofluorescence assays, we verified the cell surface localization of Nrg1 in *C. auris*. The expression of Nrg1 protein was significantly more in synthetic medium as compared to the nutrient rich YPD medium, which suggests its expression in skin mimicking environment. Although we expected deletion of *NRG1* in *C. auris* would promote filamentation, it was not the case. In fact, mutants were larger in size and were clustered together as compared to the wild-type strain **(Figure S4.2 and S4.3).** These observations suggest that morphogenetic regulation in *C. auris* is different from that of *C. albicans.*

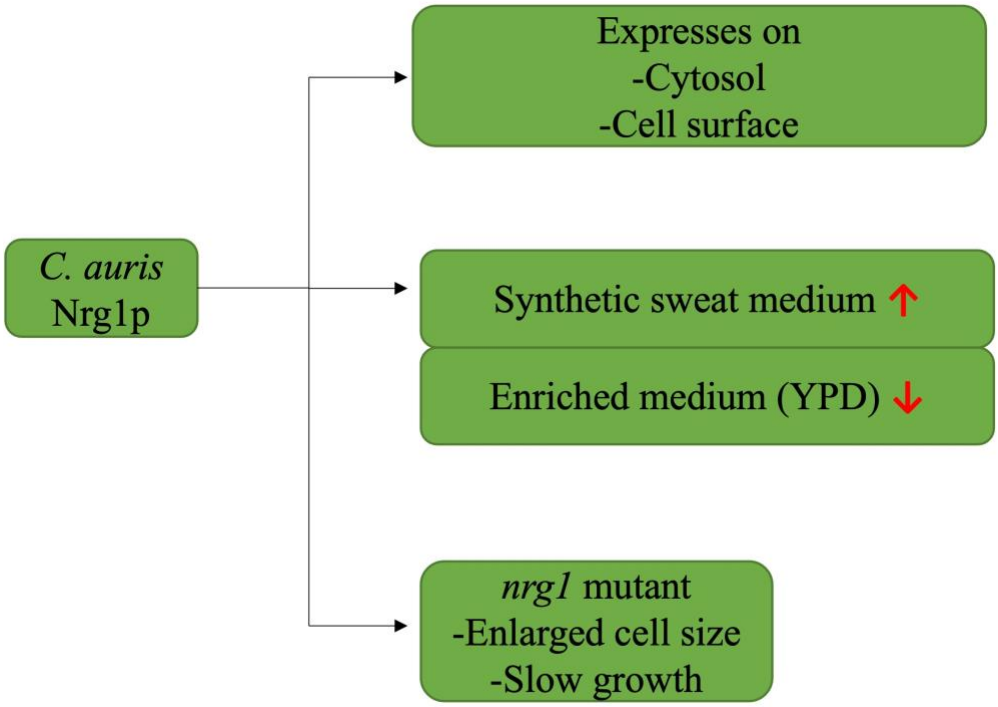

Figure 6.3. Expression of Nrg1 in *C. auris*.

Nrg1is expressed well in cytosol and localized on cell surface region of *C. auris*. Its expression was significantly more when grown in synthetic sweat medium mimicking our skin environment which might correlate with its biofilm forming ability in skin environment. *Nrg1* mutant exhibited larger sized cell with slow growth as compared to wild type strain.

As we saw *C. auris* easily formed biofilm in skin environment, we extended our study to evaluate possible interaction of *C. auris* with another skin resident bacterium, *Staphylococcus aureus* **(Chapter 5)**. Both microbes are salt tolerant and are capable of forming biofilms on their own but relationship between them was unknown. Using biofilm assays, we demonstrated that they formed increased biofilm when grown together in skin mimicking environment. Also, we observed increased hemolysis of *S. aureus* when grown together with *C. auris.* We also evaluated quorum sensing molecules secreted by *C. auris*. We used solvent extraction method, followed by thin layer chromatography and GC-MS. QS molecules from *C. auris* inhibited filamentation in *C. albicans* similar to known QS molecule from *C. albicans*, farnesol. However, we did not detect farnesol in *C. auris* extract. QS molecule identified by GC-MS, 9-cedrenone has been reported earlier as a fungal metabolite [6]. However, it is yet to be verified as it is not available commercially. We also noted an increase in biofilm forming ability of *S. aureus* in the presence of *C. auris* QS molecule containing extract. These results point toward possible crosstalk between these two microbes with increase virulence although *in vivo* or *ex vivo* studies using wound models would provide more precise understanding of their interaction. Schematics of chapter 5 is shown below **(Figure 6.4)**.

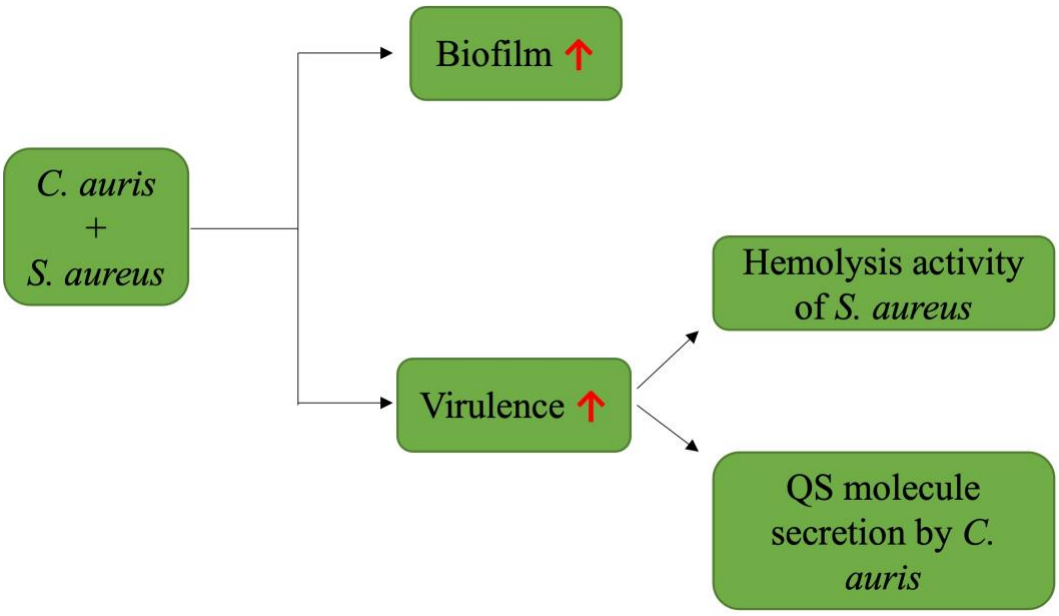

Figure 6.4. *C. auris* forms dual-species biofilms with *S. aureus* with increased virulence.

C. auris and *S. aureus* can grow together as a dual-species biofilms in skin mimicking environment with increased hemolytic activity. QS molecule secreted by *C. albicans* slightly increased biofilm forming ability of *S. aureus* hinting toward crosstalk between QS molecules of *C. auris* and *S. aureus*.

6.1 References

1. Vediyappan, G.; Dumontet, V.; Pelissier, F.; d'Enfert, C. Gymnemic Acids Inhibit Hyphal Growth and Virulence in *Candida albicans*. *PLoS One* **2013**, *8*, e74189, doi:10.1371/journal.pone.0074189.

2. Capolupo, A.; Esposito, R.; Zampella, A.; Festa, C.; Riccio, R.; Casapullo, A.; Tosco, A.; Monti, M.C. Determination of Gymnemic Acid I as a Protein Biosynthesis Inhibitor Using Chemical Proteomics. *J. Nat. Prod.* **2017**, *80*, 909–915, doi:10.1021/acs.jnatprod.6b00793.

3. Braun, B.R.; Johnson, A.D. Control of Filament Formation in *Candida albicans* by the Transcriptional Repressor TUP1. *Science* **1997**, *277*, 105–109, doi:10.1126/science.277.5322.105.

4. Yue, H.; Bing, J.; Zheng, Q.; Zhang, Y.; Hu, T.; Du, H.; Wang, H.; Huang, G. Filamentation in Candida auris, an emerging fungal pathogen of humans: Passage through the mammalian body induces a heritable phenotypic switch. *Emerg. Microbes Infect.* **2018**, *7*, 188.

5. Wang, X.; Bing, J.; Zheng, Q.; Zhang, F.; Liu, J.; Yue, H.; Tao, L.; Du, H.; Wang, Y.; Wang, H.; et al. The first isolate of *Candida auris* in China: Clinical and biological aspects. *Emerg. Microbes Infect.* **2018**, *7*, 93.

6. Al-Ansari, M.M.; Dhasarathan, P.; Ranjitsingh, A.J.A.; Al-Humaid, L.A. *Ganoderma lucidum* Inspired Silver Nanoparticles and Its Biomedical Applications with Special Reference to Drug Resistant *Escherichia coli* Isolates from CAUTI. *Saudi J Biol Sci* **2020**, *27*, 2993–3002, doi:10.1016/j.sjbs.2020.09.008.

Appendix A - Supplementary materials for chapter 3

Table S3. 1List of significantly different proteins obtained from MS in *C. albicans* Nrg1-TAP samples.

Protein IDs	Gene name	Mol. weight [kDa]	Q-value	Peptides	Sequence coverage [%]	Intensity
P46587	SSA2	70.07	0	42	68.1	3565000000
A0A1D8PE97	GCV2	109.88	0	37	52	697550000
P83779	PDC11	62.44	0	32	64.6	2.3406E+10
Q5A0N3	RNR1	96.253	0	33	46.3	502160000
Q9HGT6	SES1	52.99	0	32	70.8	474760000
Q5A5Q8	RPS4A	29.364	0	24	71.8	2664700000
A0A1D8PHR0	VAS1	127.55	0	40	44.1	299690000
Q59Q46	IMH3	56.239	0	21	51.2	365030000
A0A1D8PPG7	ILV5	44.848	0	19	46.5	3216900000
P0CH96	ADE12	47.888	0	20	40.2	302860000
A0A1D8PRQ1	ADE1	32.923	0	22	80.1	627040000
P40910	RPS1	28.986	0	22	68	2792900000
A0A1D8PRL4	MIS12	111.27	0	27	35.3	141240000
Q5APF2	GUA1	58.812	0	22	55.5	213670000
A0A1D8PJF9	ILV2	74.333	0	20	41.4	172040000
Q59UF7	DPS1-1	65.29	0	24	42.9	400800000
Q5ANA3	CDR1	169.98	0	29	27.7	92419000
A0A1D8PF11	RPL82	28.258	0	18	64.6	47934000
A0A1D8PNF5	TIF5	46.64	0	17	44.3	162310000
A0A1D8PQS0	RPP0	33.272	0	15	47.1	2367500000
A0A1D8PSC8	ARC1	40.931	0	18	66.4	279430000
O94038	ADH2	36.807	0	16	50	120210000
P79023	ARO4	40.291	0	19	52.4	348610000
Q5AGV4	PRT1	84.251	0	21	35.9	125420000
A0A1D8PLC9	RPL20B	20.338	0	14	65.1	2252900000
A0A1D8PN83	orf19.4149.1	17.6	0	14	58.7	2223100000
O59931	RPL13	23.053	0	14	55	3140200000
Q59S06	NOP58	57.114	0	16	41.3	84791000
A0A1D8PK40	RPL19A	21.884	0	14	48.4	1778900000
A0A1D8PQ54	orf19.5620	33.653	0	14	75.1	295820000
A0A1D8PCJ9	ARP8	121.35	0	27	34.9	118150000
A0A1D8PFL9	RPL14	14.721	0	12	56.5	2835000000
A0A1D8PHG1	orf19.6883	48.288	0	16	43.7	251760000

A0A1D8PRY3	ATP3	32.119	0	11	43.9	719390000
O43101	C1_10620W_A	54.321	0	13	37.4	52474000
Q3MNT0	SPT6	162.07	0	16	13.9	28806000
Q5A5V8	orf19.5293	57.817	0	18	44	70541000
Q5A863	TRM1	62.468	0	13	30.4	34389000
A0A1D8PCX8	RPL6	19.763	0	14	67	2663300000
A0A1D8PI17	RNR22	45.734	0	14	28.4	99470000
A0A1D8PI93	RPT6	44.962	0	11	40.1	78144000
A0A1D8PTK1	ARO2	44.804	0	13	42.9	230570000
Q5A2A0	RPT1	49.814	0	12	31.8	83859000
Q5AGZ9	RVB2	54.548	0	16	39.4	67647000
Q5AJF7	RPL12	17.762	0	9	60	3039400000
A0A1D8PD15	RPN3	54.908	0	14	31.4	54086000
A0A1D8PE37	ADE4	59.951	0	13	29.4	67670000
A0A1D8PJF0	orf19.1632	46.23	0	14	43.5	49868000
A0A1D8PMJ1	orf19.2917	58.546	0	14	28.1	30858000
A0A1D8PMQ4	RPT5	47.729	0	14	43.5	76175000
P46250	SEC14	34.709	0	15	50.8	121340000
Q59VR3	FPR3	47.667	0	11	25.4	88660000
Q5A0V9	NOP1	33.167	0	13	39.6	80857000
Q5A0W7	RVB1	49.989	0	14	36	75104000
A0A1D8PCD0	RPB11	14.233	0	7	63.7	32595000
A0A1D8PE78	orf19.1229	119.2	0	9	11.2	14996000
A0A1D8PEV5	SAC1	71.098	0	10	19.7	18436000
A0A1D8PLB7	ILV6	33.094	0	10	40.7	61902000
A0A1D8PPN6	RPL32	14.956	0	10	48.1	1498100000
A0A1D8PTV0	RPN7	46.249	0	9	29.8	59158000
Q5A7K0	RPS24	15.513	0	10	57.8	2122200000
Q5A8X9	ISN1	52.384	0	10	27.4	29282000
Q5AA47	ARC35	40.522	0	11	41.9	45477000
A0A1D8PDV1	orf19.6245	64.467	0	11	24	31203000
A0A1D8PGY0	RPL21A	18.013	0	10	55.6	1257700000
A0A1D8PK11	orf19.5917.3	24.022	0	9	37	109840000
A0A1D8PSM6	SEC63	76.585	0	8	15	22391000
A0A1D8PTS0	RPP2A	10.858	0	6	54.6	1381300000
A0A1D8PU67	PUP1	29.407	0	7	23.2	73998000
Q59LF9	MAP2	50.379	0	12	33	51861000
Q59LU0	DBP2	61.28	0	14	29.7	16503000
Q59MA9	CLU1	155.83	0	15	13.8	20988000
Q59N42	GLC7	37.824	0	7	25.8	71951000
Q59PR9	HMO1	24.815	0	7	39	95174000
Q59PZ4	NMD3	59.207	0	9	19.8	21087000
Q5A507	NAM7	114.64	0	7	9.1	12912000

Q5A5P8	TIF11	17.376	0	7	32.5	97463000
A0A1D8PCP8	orf19.3686	47.376	0	7	16.6	21489000
A0A1D8PGT3	TOM1	375.41	0	10	3.9	19742000
A0A1D8PH08	COX6	17.434	0	8	42.7	76529000
A0A1D8PH72	orf19.4492	48.804	0	11	30.9	35058000
A0A1D8PHF9	orf19.3583	43.097	0	9	42.3	21591000
A0A1D8PK30	RPL35	14.086	0	9	50	1287100000
A0A1D8PPX6	orf19.5525	37.748	0	8	36.8	147050000
A0A1D8PQ89	orf19.5747	52.065	0	8	25.2	28763000
Q59QT3	FUR1	24.475	0	8	39	44579000
Q5A0H8	orf19.5833	40.455	0	7	23.1	20822000
Q5A4X7	orf19.969	44.465	0	11	34.4	22708000
Q5A8H8	PBP2	58.405	0	6	19.8	13899000
Q5ADQ8	orf19.6783	75.849	0	12	22.7	35512000
Q5AG96	orf19.4283	37.253	0	11	43.9	43025000
Q5AI20	RLI1	69.545	0	11	22.2	27737000
Q5AJ90	FOX3	43.877	0	10	37.1	27090000
A0A1D8PH73	orf19.4488	109.3	0	9	13.4	13013000
A0A1D8PHD8	RPC40	37.98	0	7	23.2	43197000
A0A1D8PMT8	orf19.5698	30.216	0	6	21.6	16123000
A0A1D8PP14	RPL43A	10.115	0	5	40.2	344130000
A0A1D8PQN7	NOP15	30.498	0	6	27	44675000
A0A1D8PR42	YCF1	177.58	0	8	6.7	8287300
A0A1D8PRH3	UME1	55.307	0	12	29.1	20075000
Q5A061	PRP13	99.325	0	10	12.7	14428000
A0A1D8PT03	YCP4	29.783	0	5	37.8	72202000
Q59MN0	VAC8	63.406	0	5	11.5	12860000
Q59SK0	orf19.4172	36.121	0	7	31.5	15510000
Q59WE9	orf19.2352	36.604	0	6	22.2	12485000
Q5A2L2	PRS5	48.526	0	7	22.4	18932000
Q5A3N5	orf19.5235	27.739	0	5	25.9	23788000
Q5A462	orf19.1248	35.046	0	7	28	30687000
Q5A4X0	BRE1	78.521	0	16	27.8	18862000
Q5A6S0	MRPL40	38.914	0	8	29.6	18607000
Q5A7M9	RHR2	28.133	0	8	39.8	184110000
Q5A932	orf19.3302	78.181	0	8	16.6	8399700
Q5AD20	orf19.2047	23.976	0	6	31.2	23150000
Q5AD47	HGT6	61.514	0	8	18.9	293470000
Q5ADW3	TIP120	134.47	0	8	8.8	17565000
Q5ANH5	RPP2B	11.177	0	5	54.1	268310000
Q5APB5	orf19.4850	70.738	0	6	15.9	12696000
A0A1D8PDH5	REI1	44.867	0	12	31.4	65603000
A0A1D8PFE1	CSI2	33.952	0.0009760	3	9.2	14731000

A0A1D8PGR8	orf19.5828	81.945	0	10	17.7	9468500
A0A1D8PHC4	orf19.3547	75.47	0	5	8.7	11858000
A0A1D8PI15	RPS10	13.813	0	3	30.5	859320000
A0A1D8PMR2	TRP4	39.481	0	7	22.2	17582000
A0A1D8PNX4	orf19.3920	34.633	0	6	22.7	5813000
A0A1D8PRJ5	UTP18	62.299	0	8	22.5	4597500
Q59QC2	EAF6	23.209	0	4	21.8	5133600
Q59YD8	C2_09660W_A	25.654	0	5	32.6	8609100
Q59ZG1	orf19.3558	24.577	0	5	20.2	8597400
Q5ALV6	RPS26A	13.571	0	4	37	546720000
A0A1D8PCZ5	ARP7	43.043	0.0014252	3	6.6	5598800
A0A1D8PDG0	orf19.752	36.686	0	4	14.1	5041000
A0A1D8PF50	NEP1	29.503	0	3	17.2	8129700
A0A1D8PH53	CAK1	39.919	0	3	8.8	4176400
A0A1D8PH89	orf19.4127	47.071	0	5	17.2	8841800
A0A1D8PHU4	orf19.2257	42.51	0	7	22.3	13485000
A0A1D8PJB1	orf19.1662	39.957	0	3	16	8741600
A0A1D8PL01	STE24	50.669	0.0013799	4	9.9	8297200
A0A1D8PMN4	orf19.3128	72.254	0.001432	3	4.7	6069200
A0A1D8PMU8	orf19.5682	60.903	0	5	14.2	12410000
A0A1D8PNL1	MIG1	62.599	0.0005277	2	4.7	4747800
A0A1D8PPM1	orf19.3438	43.014	0	4	14.8	8841000
A0A1D8PS97	PAN6	35.324	0	9	39.2	15020000
Q59L13	TIF6	26.393	0	4	19.2	68077000
Q59M52	CR_05550C_A	129.33	0	5	6.6	7795500
Q59R28	MNN26	87.221	0	4	6.3	4402200
Q59X92	ERV46	46.683	0.0014045	3	7.5	5315400
Q59YF4	C2_09780C_A	25.961	0.001023	2	17.2	14415000
Q5ALJ2	FGR22	33.585	0	5	17.6	9880800
Q5A7Q9	SOF1	49.42	0	5	15.1	12293000
Q5A879	LAG1	48.635	0	2	8	5874600
Q5AAS9	MRPL19	15.124	0	3	32.2	14386000
Q5AFP8	KEX1	78.711	0	6	9.1	9251500
Q5AGD1	C5_02400W_A	25.34	0	5	28.1	14114000
Q5AH14	TOM40	42.309	0	6	18.7	30234000
Q5AMN5	orf19.4611	35.854	0	5	21.6	10593000
Q5ANP3	orf19.5857	39.743	0	2	7	2844300
Q5APD5	orf19.4830	12.279	0	2	22.7	21198000
A0A1D8PD30	orf19.71	38.744	0	4	20.3	9509200
A0A1D8PLW7	NUP84	96.342	0.0009727	5	7.9	3201300
A0A1D8PLY2	orf19.789.1	16.757	0	5	50.7	9832100
A0A1D8PM86	IMG2	14.26	0	4	44.7	7880200
A0A1D8PN49	orf19.1967	20.963	0	3	17.2	17186000

A0A1D8PS44	CR_02060W_A	35.904	0	3	11.1	2909500
Q59L25	C3_01170W_A	53.345	0	4	9.1	3067000
Q5AAG6	MKC1	59.035	0	3	8.4	3099600
Q5AD10	orf19.2057	95.603	0	12	17	12316000
A0A1D8PL36	orf19.4184	76.175	0.0005260	4	5.5	2825600
Q5A8Y7	RPB7	19.149	0	4	33.5	6792100
Q92207*	HOG1	42.946	0	8	24.9	23318000
Q59WC6*	YPD1	20.564	0.006364	1	6.5	5620400
Q5AKU6*	SSK1	73.559	0	2	4.2	1431300
A0A1D8PM87*	SSK2	168.05	0	2	1.8	416780
A0A1D8PKE2*	PBS2	59.35	0	3	9.9	1586600

*- Represents proteins having either *P*-value more that 0.05 or contained less than 3 peptides but are included in the table due to their significance in our data analysis. Q-value obtained from MS data was used as one of the criteria to identify proteins and is obtained by using minimum false discovery rate required for a hit to be considered correct. Intensity values indicate intensities of peptide peaks observed in HPLC. Gene names and protein IDs were obtained from Candida genome database and UniProt database respectively.

Table S3. 2 List of significantly different proteins obtained from MS in *C. albicans* Ume6-TAP samples.

Protein IDs	Gene name	Mol. weight [kDa]	Q-value	Peptides	Sequence coverage [%]	Intensity
P83779	PDC11	62.44	0	32	64.6	2.3406E+10
Q5AK53	PFK1	108.57	0	47	53.7	1959000000
Q5A397	SSB1	66.448	0	30	59.1	5915300000
Q5A6R2	ADE17	64.939	0	31	64.4	1328400000
Q59QD6	TEF2	50.011	0	26	60	7729800000
Q5AGZ8	PFK2	104.13	0	37	39.7	1316000000
A0A1D8PP43	ADH1	36.909	0	29	67.4	1.4974E+10
A0A1D8PPG7	ILV5	44.848	0	19	46.5	3216900000
Q59KZ1	APE2	104.38	0	50	52.4	775500000
A0A1D8PLY4	PYC2	129.7	0	49	46.5	681400000
Q59SM8	MIS11	102.18	0	42	49.8	1167500000
Q5AIB8	RPL10	25.189	0	17	48.6	1132500000
A0A1D8PF08	RPL2	27.311	0	16	61.8	2050600000
A0A1D8PHG1	orf19.6883	48.288	0	16	43.7	251760000
A0A1D8PK43	RPL18	20.77	0	11	47.3	1376800000

A0A1D8PSR2	CR_04300W_A	81.256	0	36	51.3	240120000
P25997	CEF3	116.92	0	44	55.8	1531500000
Q5A9D9	LYS12	40.668	0	20	51.6	872480000
A0A1D8PJ01	PMA1	97.537	0	28	30.1	1543100000
A0A1D8PKC3	CAM1	46.99	0	24	51.2	650850000
A0A1D8PKJ3	UBA1	114.27	0	38	50.2	465710000
A0A1D8PPN6	RPL32	14.956	0	10	48.1	1498100000
P79023	ARO4	40.291	0	19	52.4	348610000
Q59RI1	ILS1	125.27	0	51	49.9	637580000
Q5A389	RPS20	13.344	0	9	57.1	1648800000
Q5AB87	RPL16A	22.635	0	11	39.5	1752500000
Q5AIA2	HOM6	38.836	0	22	63.8	332860000
Q5ANP6	SBP1	31.962	0	21	56.7	543760000
A0A1D8PEY9	RPS17B	15.739	0	8	56.9	973310000
A0A1D8PL14	CAR2	47.349	0	23	68.1	641560000
A0A1D8PMM2	orf19.3141	97.802	0	23	32.3	152160000
A0A1D8PQC8	orf19.1086	67.084	0	16	40.2	99321000
A0A1D8PRQ1	ADE1	32.923	0	22	80.1	627040000
Q59ZE0	ATP4	25.828	0	13	48.9	738210000
A0A1D8PQ54	orf19.5620	33.653	0	14	75.1	295820000
A0A1D8PT02	PST3	21.174	0	10	77.9	793600000
A0A1D8PTZ1	CR_09330C_A	100.05	0	25	36.4	152100000
A0A1D8PU56	FAA4	77.319	0	28	46.7	305390000
O74198	ERG6	43.071	0	14	42.6	389170000
Q5A2A5	GRS1	73.713	0	24	39.3	441680000
Q5A8K2	ALA1	108.27	0	42	52.3	403880000
Q5AEN2	RPL9B	21.718	0	12	64.4	1456400000
A0A1D8PCT4	FRS2	56.481	0	19	43.3	308380000
A0A1D8PDZ1	orf19.6220.4	13.739	0	3	26.2	1098100000
A0A1D8PE67	ADE5	85.945	0	25	37.9	373680000
A0A1D8PG16	RPL38	8.8924	0	5	42.3	642100000
A0A1D8PGY0	RPL21A	18.013	0	10	55.6	1257700000
A0A1D8PHR0	VAS1	127.55	0	40	44.1	299690000
A0A1D8PMV9	THS1	81.698	0	31	47.3	369660000
A0A1D8PPW1	orf19.3480	54.696	0	11	27.5	70088000
A0A1D8PQ55	orf19.5627	40.626	0	12	41	82713000
A0A1D8PR11	orf19.6507	43.098	0	18	44.4	321810000
A0A1D8PTK1	ARO2	44.804	0	13	42.9	230570000
P30418	NMT1	51.862	0	6	16.4	30721000
Q59Q46	IMH3	56.239	0	21	51.2	365030000
Q59R18	DED81	62.247	0	23	48.7	269940000
Q59UF7	DPS1-1	65.29	0	24	42.9	400800000
Q59Z12	CCT5	59.835	0	24	45.3	120470000

Q5A1E3	CBF1	29.153	0	9	48.2	67452000
Q5AB84	orf19.6090	43.523	0	13	36	89655000
Q5ADR2	PRO2	49.12	0	16	40.4	59010000
Q5AF98	ZUO1	48.348	0	22	52	255670000
Q5ALV5	COX4	17.289	0	7	63.1	79964000
Q5AML1	NIP1	99.815	0	28	36.4	169770000
A0A1D8PC77	UBP6	54.118	0	10	27.6	27040000
A0A1D8PDL7	orf19.2489	122.2	0	19	21.5	132710000
A0A1D8PE97	GCV2	109.88	0	37	52	697550000
A0A1D8PFV0	FTR1	42.504	0	5	15.7	84798000
A0A1D8PFZ8	RPN11	34.955	0	10	31.7	53652000
A0A1D8PLA3	PWP1	67.937	0	17	33.1	99887000
A0A1D8PM39	ZDS1	185.86	0	18	15.4	19249000
A0A1D8PNN8	CAM1-1	47.466	0	18	44.5	126170000
A0A1D8PQN7	NOP15	30.498	0	6	27	44675000
A0A1D8PRR7	ACC1	253.42	0	56	32.7	265900000
A0A1D8PSC8	ARC1	40.931	0	18	66.4	279430000
A0A1D8PSU2	PDX3	31.275	0	12	68	93143000
A0A1D8PSW5	CR_04940W_A	38.374	0	3	13.2	7369500
A0A1D8PTX9	PHO88	20.955	0	8	51.8	73946000
P0CH96	ADE12	47.888	0	20	40.2	302860000
Q59MZ5	ADE6	150.81	0	35	35.9	246310000
Q59V93	CR_06070W_A	38.358	0	10	29.5	127040000
Q59YE8	SUP35	79.975	0	17	25.2	141570000
Q59YH4	CCT7	60.421	0	20	45.7	88403000
Q59Z11	ARP3	46.647	0	14	52.5	57446000
Q5A0L0	RNR21	47.436	0	18	37	527150000
Q5A3P4	WRS1	48.082	0	14	40.8	124940000
Q5A4E2	DED1	72.838	0	17	30.7	58347000
Q5A678	SSZ1	58.529	0	21	42.4	268930000
Q5A863	TRM1	62.468	0	13	30.4	34389000
Q5AAU7	SUI2	33.881	0	10	36.3	72224000
Q5AD47	HGT6	61.514	0	8	18.9	293470000
Q5AFB3	TYS1	44.985	0	22	53.5	176110000
Q5AJX0	HTS1	55.588	0	16	37.1	96163000
Q5AME2	ARO1	169.39	0	48	39.8	209890000
Q5APF2	GUA1	58.812	0	22	55.5	213670000
Q874I4	URA1	48.425	0	14	37.8	124630000
A0A1D8PC75	orf19.6079	34.718	0	10	38.3	48079000
A0A1D8PE53	SMI1	68.826	0	7	16.9	23584000
A0A1D8PEZ3	orf19.2328	31.256	0	6	29.1	9419800
A0A1D8PFL7	RPN1	109.88	0	31	38.6	199490000
A0A1D8PGF0	PLB4.5	77.036	0	10	19.2	63304000

A0A1D8PGN7	HPT1	24.247	0	12	69.5	104910000
A0A1D8PH72	orf19.4492	48.804	0	11	30.9	35058000
A0A1D8PH91	orf19.185	40.989	0	11	35.6	28723000
A0A1D8PH93	orf19.4503	25.081	0	5	29.3	28309000
A0A1D8PJ45	FLC1	90.597	0	4	5.4	4923900
A0A1D8PJD2	orf19.1626	41.633	0	10	33.2	48874000
Q59SS4	PHB1	30.839	0	10	41	53148000
A0A1D8PKW2	FBP1	35.932	0	7	27.8	27029000
A0A1D8PKY7	HIS4	91.899	0	25	34.8	132000000
A0A1D8PLW8	RPN6	49.384	0	15	39.3	58729000
A0A1D8PNP4	orf19.6658	60.518	0	17	41.1	100680000
A0A1D8PP94	VID27	84.91	0	10	16.4	27361000
A0A1D8PQ89	orf19.5747	52.065	0	8	25.2	28763000
A0A1D8PQL8	GUS1	82.587	0	27	37.5	258160000
A0A1D8PRH3	UME1	55.307	0	12	29.1	20075000
A0A1D8PRK7	orf19.7140	28.209	0	10	44.4	168180000
A0A1D8PS02	DOT6	64.841	0	6	10.7	6861400
A0A1D8PSN8	CR_04170W_A	69.361	0	10	20.1	26191000
A0A1D8PTX2	SCO1	33.781	0	5	23.9	24930000
A0A1D8PUA6	RPO21	192.04	0	35	24.7	147670000
O43101	C1_10620W_A	54.321	0	13	37.4	52474000
P0CB54	C1_02760W_A	39.604	0	4	11.4	42147000
P10613	ERG11	60.675	0	13	29.5	32670000
P46589	AAF1	68.793	0	4	9.5	6817000
Q59QB7	TCP1	60.066	0	15	31.9	66635000
Q59TM0	OSH3	95.281	0	11	24.4	32444000
Q59V85	RPL7	33.951	0	9	34.9	21607000
Q59VR3	FPR3	47.667	0	11	25.4	88660000
Q59Y31	YWP1	54.277	0.00144	2	4.5	487350000
Q59Z50	SPE3	33.899	0	11	31.3	80756000
Q59ZV5	tif35	30.685	0	9	40.5	52115000
Q5A1D5	CDC68	121.33	0	28	32.8	104000000
Q5A4J9	orf19.3442	47.009	0	15	42.4	99210000
Q5A798	MRPL3	44.988	0	12	34.7	31672000
Q5A7M9	RHR2	28.133	0	8	39.8	184110000
Q5A8A6	CPA2	127.09	0	22	22.2	77158000
Q5A8Y5	orf19.3349	139.85	0	36	32.6	137900000
Q5AGZ9	RVB2	54.548	0	16	39.4	67647000
Q5AI37	ARX1	62.232	0	9	18.6	30159000
Q5AI80	C1_02850W_A	74.744	0	7	16.6	6778900
Q5AJ85	C3_01430W_A	24.911	0	4	31.5	6986200
Q5APD2	MLS1	62.528	0	29	49	307440000
Q92207*	HOG1	42.946	0	8	24.9	1226360

*- Represents proteins having either *P*-value more that 0.05 or contained less than 3 peptides but are included in the table due to their significance in our data analysis. Q-value obtained from MS data was used as one of the criteria to identify proteins and is obtained by using minimum false discovery rate required for a hit to be considered correct. Intensity values indicate intensities of peptide peaks observed in HPLC. Gene names and protein IDs were obtained from Candida genome database and UniProt database respectively.

Appendix B - Supplementary materials for chapter 4

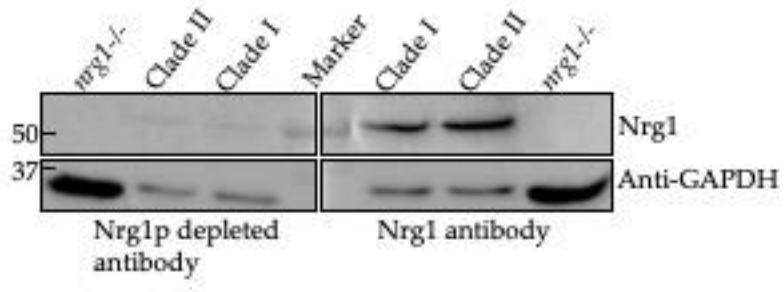

Figure S4. 1. Determination of specificity of the anti-*Cal*Nrg1 antibody

The *Cal*Nrg1 antibody was divided into two equal aliquots. One of the aliquots was incubated to a PVDF membrane containing the immobilized *C. albicans* purified Nrg1 protein overnight at 4 ^{o}C on a roller. To verify if the *C. albicans* Nrg1p depleted antibody can still detect *C. auris* Nrg1p, one set of cytosolic proteins from *C. auris* (clades I & II) was analyzed by Western blot (left panel). The second set of the identical blot was analyzed in parallel with the original (undepleted) anti-Nrg1 antibody (right panel). *C. albicans nrg1* null mutant was also included as a negative control. While the undepleted anti-Nrg1 antibody reacted to a single protein band of about 52 kDa, the depleted antibody failed to show a strong reaction to *C. auris* cellular proteins suggesting the anti-*Cal*Nrg1 antibody recognizes Nrg1p specifically. The anti-GAPDH HRP-conjugate (human) antibody was used as a loading control.

Markerless CRISPR-Cas9 gene knockout in *C. auris*

Genetic manipulation allows for the characterization of genes of interest and identification of valuable pathways. Being an efficient and speedy gene editing tool, CRISPR is widely used across a wide range of species. It consists of an enzyme that has endonuclease activity and a single guide RNA that guides CRISPR-Cas complex to make a cut on DNA. The break in the DNA is commonly repaired either by homology directed repair or non-homologous end joining. Required mutations on the DNA can be incorporated during these repair mechanisms [1,2]. CRISPR-Cas9 in *C. albicans* was first optimized from *S. cerevisiae* system not long ago [3]. As there are limited dominant selectable markers in *Candida*, methods such as LEUpOUT system and HIS-FLP system have been developed for *C. albicans* that allow for a markerless genome editing system [4]. Similar markerless CRISPR-cas9 based genome editing was optimized recently for *C. auris* using LEUpOUT system. This method involves integration of Cas9 temporarily and expression of guide RNA via homology directed repair at LEU2 locus of *C. auris*. DNA repair template will further integrate at the site of DNA break directed by Cas9. Markers from mutant are removed by growing the fungus in the medium lacking leucin, after verification of required gene edit [4,5]. We used this approach to generate nrg1 knockout mutant and looked for the phenotypes **(Figure S4.2 & S4.3)**.

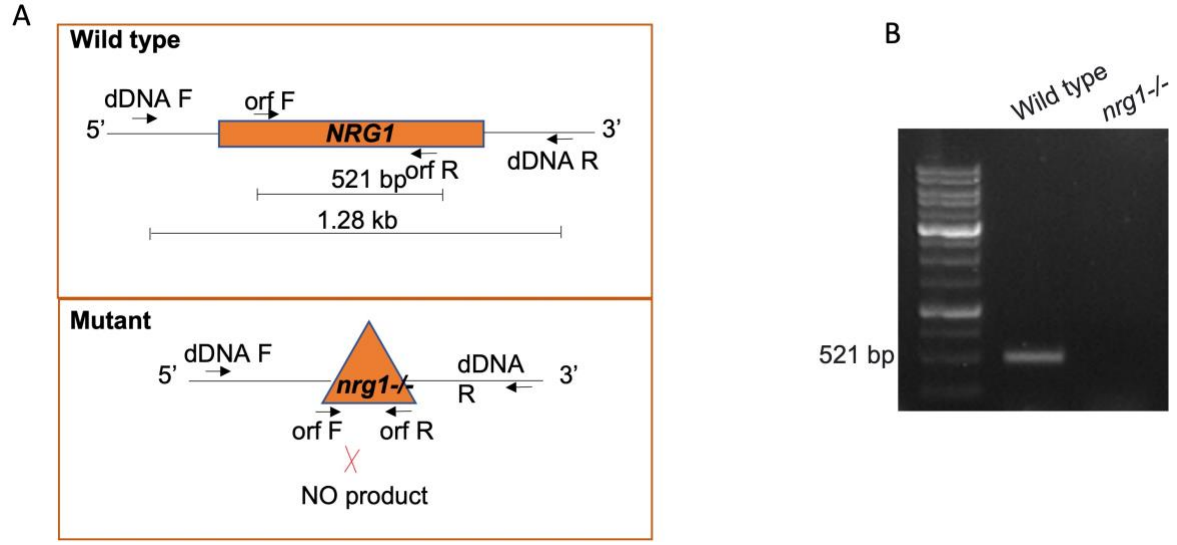

Figure S4. 2. CRISPR Cas9 mediated *NRG1* gene deletion in *C auris*.

(A) Schematics of CRISPR based gene deletion in *C. auris*. It is a markerless CRISPR-cas9 based genome editing tool for *C. auris* using LEUpOUT system [1]. It involves integration of Cas9 temporarily and expression of guide RNA via homology directed repair at *LEU2* locus of

C. auris. DNA repair template (dDNA) will further integrate at the site of DNA break directed by Cas9. After verifying mutant using gene-specific primers, marker is removed by growing mutant in the medium lacking leucine. The 1.28 kb bar represents dDNA fragment, and 521 bp bar represents the coding region of *C. auris NRG1* gene. **(B)** PCR verification of *C. auris nrg1-/-* mutant using *NRG1* specific primers. Absence of *nrg1* (521 bp) amplicon indicates absence of the gene.

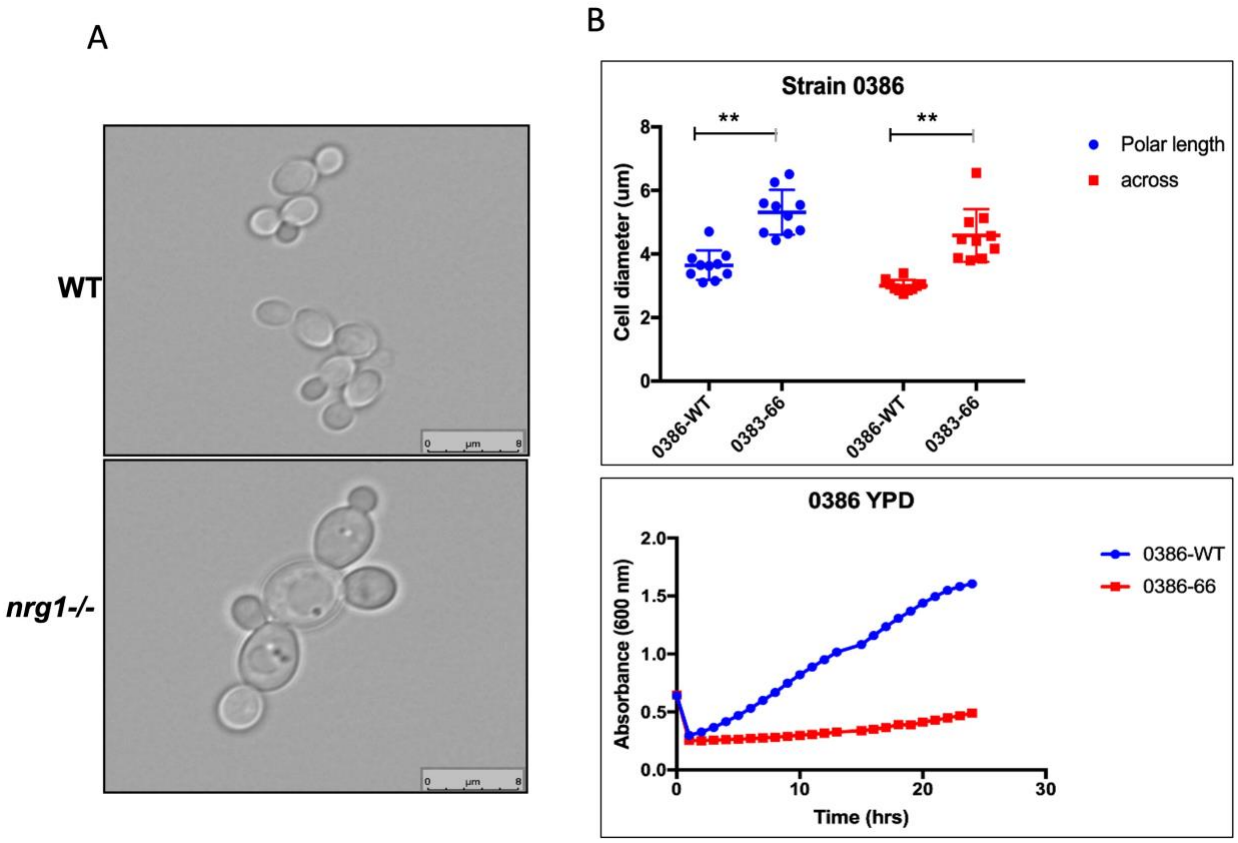

Figure S4. 3. *C. auris nrg1* mutant phenotype.

(A) Microscopic images of *C. auris* wild type and *nrg1-/-* mutant cells grown in YPD liquid media. **(B, top panel)** Cell diameters (both across and polar length) were compared between wild type and mutant. 50 cells per microscopic field were counted. Cell size of mutants were significantly larger than that of wild type. **(B, lower panel)** Growth rate of mutant and wild type *C. auris*. Mutants and wild type strains were grown in YPD for 24 hours and absorbance was measured for every one hour.

Reference

1. Dominguez, A.A.; Lim, W.A.; Qi, L.S. Beyond Editing: Repurposing CRISPR–Cas9 for Precision Genome Regulation and Interrogation. *Nat Rev Mol Cell Biol* **2016**, *17*, 5–15, doi:10.1038/nrm.2015.2.

2. Sander, J.D.; Joung, J.K. CRISPR-Cas Systems for Editing, Regulating and Targeting Genomes. *Nat Biotechnol* **2014**, *32*, 347–355, doi:10.1038/nbt.2842.

3. Vyas, V.K.; Barrasa, M.I.; Fink, G.R. A *Candida albicans* CRISPR System Permits Genetic Engineering of Essential Genes and Gene Families. *Science Advances* **2015**, *1*, e1500248, doi:10.1126/sciadv.1500248.

4. Nguyen, N.; Quail, M.M.F.; Hernday, A.D. An Efficient, Rapid, and Recyclable System for CRISPR-Mediated Genome Editing in *Candida albicans*. *mSphere* **2017**, *2*, e00149-17, doi:10.1128/mSphereDirect.00149-17.

5. Ennis, C.L.; Hernday, A.D.; Nobile, C.J. A Markerless CRISPR-Mediated System for Genome Editing in *Candida auris* Reveals a Conserved Role for Cas5 in the Caspofungin Response. *Microbiology Spectrum* **2021**, *9*, e01820-21, doi:10.1128/Spectrum.01820-21.

Appendix C - Supplementary materials for chapter 5

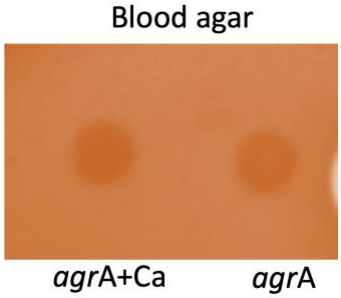

Figure S5. 1. Hemolytic assays of *agrA* mutant alone and in the presence of *C. auris*.

S. aureus quorum sensing mutant *agrA* along with *agrA+C. auris* scraped from wells and 2 uL cells were spotted on sheep blood agar plate and grown at 37 ^{o}C for 24 h. Hemolysis zones were noted.